Paleogeomorphic reconstruction of the Omokoroa Domain, Bay of Plenty, New Zealand

A thesis submitted in partial fulfilment

of the requirements for the degree

of

Masters of Science (Research) in Earth Sciences

at

The University of Waikato

by

Amy Jane Christophers

The University of Waikato

2015

THE UNIVERSITY OF
WAIKATO
Te Whare Wānanga o Waikato

Abstract

Omokoroa Peninsula, located on the shores of Tauranga Harbour, has undergone major land use changes with associated shoreline modifications; becoming increasingly urbanised since the 1950s. A low-lying area on the northeastern side of the peninsula, referred to loosely as the Omokoroa Domain, is important to the community for recreational use and as a location for a vehicular ferry service to Matakana Island. Sedimentation issues in the vicinity of the boat ramp have created problems regarding access to the boat ramp, as well as requiring protection works to deal with shoreline erosion. The primary aim of this research was to determine the geomorphic evolution of the Omokoroa Domain and assess the processes that contribute to the long-term stability and future evolution of the shoreline.

A range of different techniques were used to assess the prehistoric and historic geomorphic changes and interpret the driving processes; and also to quantify modern processes operating around the Omokoroa Peninsula. These have included analysis of historic photos, particularly aerial photographs; examination of LIDAR and mapped information, such as the underlying geology; field observations of the stratigraphic units in the cliffs and shore platforms around the peninsula; collection of sediment samples from potential sources, transport pathways and sinks, and associations lab analyses to characterise the sediments; shallow coring to determine the near surface stratigraphy of coastal sediments; and the deployment of a range of instruments, and subsequent analysis of the collected data to define the hydrodynamic processes around the Omokoroa Peninsula.

The various lines of evidence analysed indicate the Omokoroa Domain can be classified as a cuspate spit, which enclosed a tidal lagoon that was infilled with landfill during the construction of roads on the Peninsula. The spit has developed in an area of low sedimentation, with a low potential for sediment transport. The sediment comprising the shoreline around the Omokoroa Domain is primarily derived from local sources, specifically from mass-wasting from the peninsula and predominantly from debris from landslides in the immediate vicinity of the Domain.

There is evidence of both a tsunami event and rapid deposition of most of the sediment after 1,652 ± 20 BP. This appears to be associated with a local earthquake that also produced a tsunami deposit at Waihi Beach. It is possible that ground shaking and vertical movement triggered landslide events around Omokoroa Peninsula.

Continuous tidal action and episodic wind generated waves are the primary factors influencing sediment transport, redistributing sediment around the Peninsula, and forming the cuspate spit and tidal lagoon. More recently, landslides have mostly formed on the western side of the Omokoroa Peninsula, with the sandy debris being transported around the peninsula to accumulate on the northern flank of the modified cuspate spit. This sediment is a minor contribution to the sedimentation problems at the boat ramp; the major issue being settling of fine sediment within the turbid fringe that has been enhanced by the shape of the present boat and vehicular ferry ramps, and associated wharf.

Acknowledgements

Firstly, I would like to thank my chief supervisor Dr Willem de Lange, your vast knowledge and guidance throughout this experience has been amazing, you are now free from my never-ending queries. Special thanks to Dr Vicki Moon, my secondary supervisor, your input and advice is always appreciated.

I am extremely grateful for the funding from the Western Bay of Plenty District Council to enable this research. Special thanks to the Sir Edmund Hillary Scholarship for the continued support and belief throughout my university life and financial support from the University of Waikato Masters Research Scholarship.

Dirk Immenga, Christopher Morcom and Rex Fairweather for your assistance and hard work in the field. Thanks to all the staff in the Department of Earth and Ocean Sciences, particularly Kirsty Vincent, Annette Rodgers, Renat Radosinsky, Janine Ryburn, Glen Stichbury and Dean Sandwell, each providing helpful assistance for which I am grateful.

Thanks to the crew in F.1.02, Camillia Garae and Melissa Kleyburg. Friends don't let friends do silly things alone, and I am glad we went through the ordeal together, because "we're all mad here". Thanks to my fellow Earth Science MSc students, Megan and Billy, I could not have done it without your help during the final sprint to the finish.

My friends and family who are always there when I need you most. Dad, my number one field assistant, you have been my greatest motivator through your continued interest and encouragement, you deserve an honorary degree. Mum, although I have outgrown you, I will never outgrow home. I like to think of your continued love and support as a future investment.

Table of Contents

List of Figures

List of Tables

Chapter One

INTRODUCTION

The following chapter summarises the problem background that directed this study, establishes the objectives of the research, and outlines the layout of the thesis.

1.1 Background

Omokoroa Peninsula is located in the Tauranga Harbour on the north east coast of New Zealand (Figure 1.1). The low-lying feature on the eastern coast at Omokoroa is an important community asset, including the Omokoroa Beach Recreation Reserve, Omokoroa Boat Club Inc, boat ramps and associated wharves for recreational use and a vehicular ferry service to Matakana Island (Figure 1.2), collectively referred to as Omokoroa Domain in this thesis. There are issues with accumulation of fine sediment in the vicinity of the recreational boat ramp, causing difficulties regarding ramp access. Recent sedimentation has resulted in accumulation of sediment on the northern side of the ferry terminal and boat ramp with evidence of erosion on the southern flank of the Omokoroa Domain. The area has been subject to significant modification and has become increasingly urbanised. In order to establish potential management and/or infrastructural changes at Omokoroa, research into the evolution of the area and sedimentation patterns is essential in determining the future evolution of the Omokoroa Domain.

The low-lying area resembles the appearance of a cuspate foreland or cuspate spit, which indicates convergence of sediment transport and a significant wave driven sediment supply. The difference between these features is that a cuspate foreland has an approximately equal magnitude of opposing longshore transport whereas the formation of a cuspate spit results from a dominant transport direction with some opposing transport (Komar, 1998). If this is the case, in future the Omokoroa Domain is expected to accumulate sediment over time, posing further sedimentation issues. If it is not the case, there is a higher probability of a sediment deficit developing that would exacerbate existing sediment erosion problems. From the data available prior to this study, it was not possible to assess if the conditions

necessary to produce either a cuspate foreland or cuspate spit were present, or if completely different processes were involved, leading to the objectives of this study.

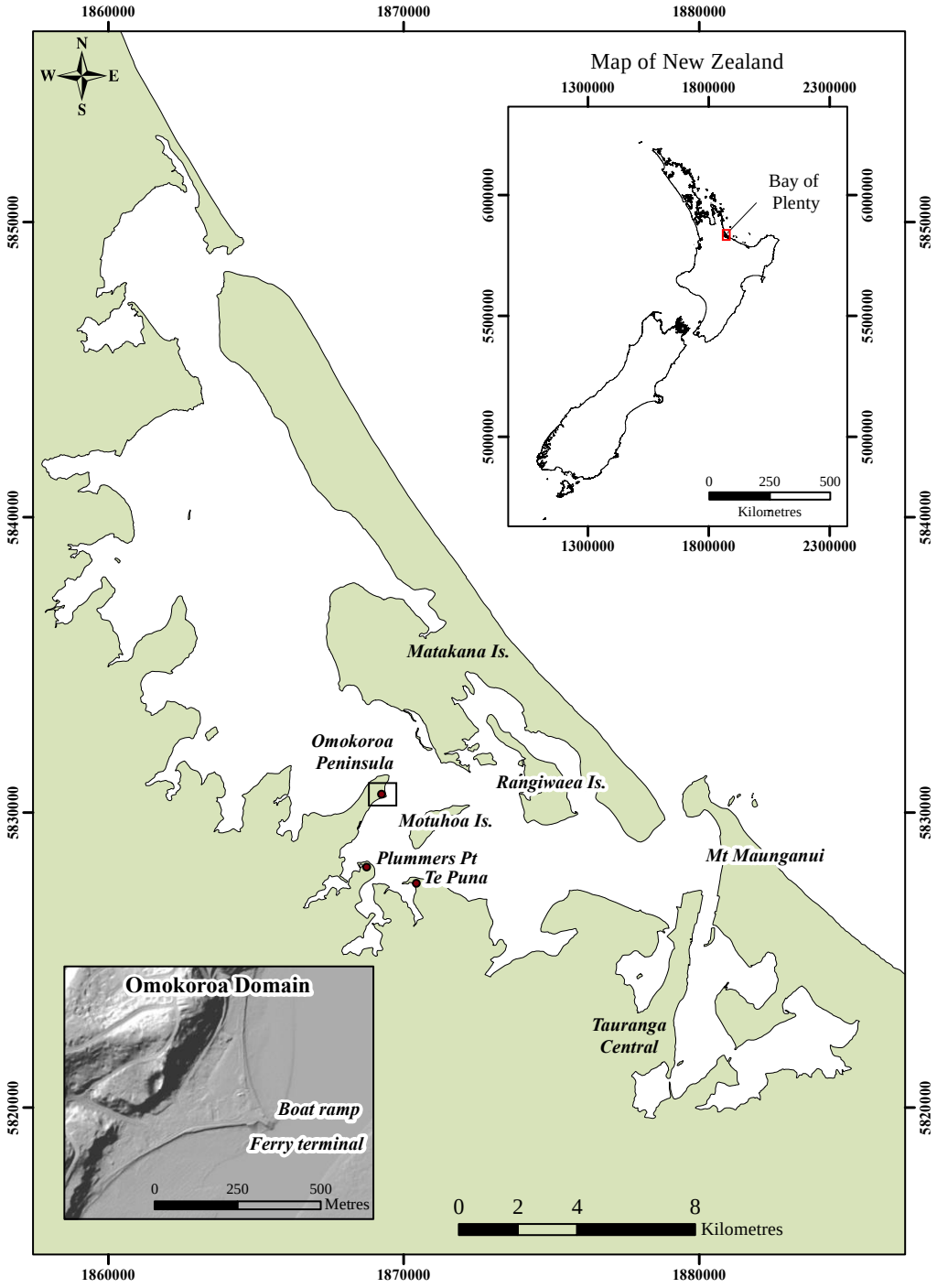

Figure 1.1: Location map of the Tauranga Harbour and position of the Omokoroa Domain.

Figure 1.2: Photograph facing east showing (a) Omokoroa Domain and (b) recreational facilities: ferry terminal (right) and boat ramp (left).

1.2 Thesis Objectives

The main aim of this proposed work is to determine the geomorphic evolution of the Omokoroa Domain and assess the processes that contribute to the long-term stability and future evolution of the shoreline. The specific objectives are:

1. Collate information on the historical shoreline positions for the area to assess impacts of historical modifications.
2. Establish the geological history and sedimentation patterns of the underlying sediments.
3. Examine the hydrodynamics, including tidal currents and waves in the vicinity of Omokoroa, used to evaluate sediment transport regime.
4. Identify potential sources of sediment and the pathways by which they contribute to sedimentation along Omokoroa Peninsula.
5. Develop a conceptual model for the geomorphic evolution of Omokoroa Domain.

1.3 Thesis Structure

Chapter Two: Literature review

This chapter reviews the background literature involving the Tauranga Harbour and Omokoroa Peninsula, including information regarding the history and development, geology, climate, hydrodynamics, sediment transport and potential future impacts on estuarine sedimentation.

Chapter Three: Methods

This chapter summarises the methods conducted and information examined for this study, including field experiments and laboratory analysis.

Chapter Four: Site Investigation

An initial investigation was carried out to determine historic evidence of changes over time based of photographs and site observations identifying sediment sources and processes, as well as the present geomorphology.

Chapter Five: Hydrodynamics

This chapter identifies the hydrodynamics surrounding Omokoroa Peninsula based on wave and current data obtained from field measurement, establishing the driving forces for sediment transport.

Chapter Six: Sediments

This chapter presents the underlying geology and surficial sediments surrounding the Omokoroa Peninsula, identifying historic sedimentation patters and present day sediment transport pathways.

Chapter Seven: Discussion

This chapter synthesises the results obtained, discussing the formation of the Tauranga region and the evolution of the Omokoroa Domain.

Chapter Eight: Conclusions

This chapter summarises the main findings from this study and outlines recommendations for further research.

Chapter Two

LITERATURE REVIEW

The following chapter provides a basis for discussing and identifying the various mechanisms of estuarine sedimentation and how they are affected by the varying hydrodynamics within estuaries. Firstly, the processes influencing estuarine morphology are described, followed by a review of the relevant literature in the Tauranga Harbour and Omokoroa Peninsula, including information regarding the history and development, geology, climate, hydrodynamics, sediment transport and potential future impacts on estuarine sedimentation. Findings from the literature review establish the framework for the investigation into the evolution of Omokoroa Domain.

2.1 Estuarine Morphology

Evolution of an estuarine environment is fundamentally governed by two processes: (1) the long-term sediment supply from both fluvial and marine sources and (2) the long-term residual sediment transport pattern (Dronkers, 1986). Estuarine characteristics are influenced by physical processes including freshwater influx, tidal currents, waves and wind driven circulation. Sediment supply (fluvial and marine) is largely dependent on physical features including catchment structure, topography and geology. Shoreline exposure and climate are dynamic controls, further influencing estuarine sedimentation (Hume & Herdendorf, 1988; Nordstrom & Roman, 1996). Additionally, anthropic activities can affect the evolution of estuaries as a result of altering the water level, sedimentation rates and through engineering works (Dronkers, 1986; Nordstrom & Roman, 1996).

2.1.1 Sediment supply

Estuaries are an interface between the land and sea and accumulate a large proportion of sediments. Estuarine sedimentation is a function of the erosion susceptibility of sediments and the physical processes acting on them. The input of sediment to estuarine shores is from various sources including catchment runoff,

erosion of cliffs, biological sources, aeolian transport, transport from ocean inlets and estuarine mouths (Nordstrom & Roman, 1996).

Erosional processes have a large effect on the way in which land use contributes to sedimentation. The degree of catchment sediment runoff is influenced by five interacting factors that affect the vulnerability of soil erosion. Factors include: topography, climate, geology, soil characteristics and the type and intensity of the land use (Walling, 2006).

2.1.2 Anthropic impacts

Anthropic activities have altered the rate of sedimentation in estuaries. In particular land use activities alter a large proportion of the Earth's surface through conversion of natural landscapes for anthropic activities or intensifying management practices. Anthropic actions have led to increasing rates of sediment transport from the land into coastal systems via fluvial networks (Walling, 2006). Alteration of land use leads to exposure of soils resulting in destabilisation, increasing erosion and sediment runoff (Carling *et al.*, 2001).

2.1.2.1 *Mass wasting processes*

Land use alterations lead to the destabilisation of soils resulting in mass wasting. Mass wasting processes are driven by the loss of root strength, increase in ground moisture, removal of toe support and destabilisation of hill slopes by disrupting natural drainage patterns (Syvitski, 2003). Main mechanisms leading to erosion include: landslides, sheet and gully erosion, channel-bank erosion and road-surface erosion. Erosion or mass wasting events occur as a result of slope stability in relation to the specific land use, of which the contribution of mass wasting has significantly increased subsequent to anthropic land use changes (Glade, 2003).

2.1.2.2 *Remedial measures*

Suspended sediment is a diffuse, rather than point source pollutant. To reduce sediment loading, the source and land use must be remediated. Each land use has fundamentally different surface characteristics, results of which produce clear

differences between the rates of sediment output from the respective land uses. Implementation of soil and water conservation can reduce the sediment erosion, runoff and river sediment loads. Conservation programmes are generally aimed at retaining water to reduce the effects of erosion, in turn reducing sediment mobilisation and sediment transfer to waterways and hence reducing the sediment load (Walling, 2006). Riparian Buffer Zones or engineering works improve water quality by reducing suspended sediment. Engineering works mitigate the impacts of suspended sediment through mesh fences or geotextile cloths that reduce sediment runoff. Engineering works alternatively remediate the potential of sediment runoff by reinforcing slopes and controlling drainage systems that reduce the occurrence of mass wasting processes (Boothroyd *et al.*, 2004).

2.1.3 Sediment transport

Natural morphological development of estuarine environments is driven by interactions between water motion, sediment transport and bed topography. Hydrodynamic regimes in estuaries are characterised by variations of flow and interactions between a number of processes including tides, freshwater input and ocean waves that propagate through inlets to combine with locally generated wind waves. Tidal currents and waves are the most important hydrodynamic processes influencing sediment transport patterns within tidal inlets (Komar, 1996).

Tidal asymmetry is an important factor controlling residual sediment transport and is driven by the difference in magnitude and duration during flood and ebb tides. Waves influence sediment transport through resuspension of sediment at high water, moving sediment transverse to the shoreline (Dronkers, 1986). Two modes of transport occur, either as bedload where coarse grains move along the bottom by traction or suspended load where fine sediments move as fluid mud. Net sediment transport results from interaction between both continuous tidal currents and intermittent waves (Green *et al.*, 1997). Waves effectively entrain sediment into suspension on the intertidal flats with further transportation being via currents, that are generally too weak to erode sediment (Brown *et al.*, 1999)

2.1.3.1 *Sediment movement by currents*

A boundary layer develops at the interface where water flow interacts with the sea-bed, creating a shear stress which reduces flow velocity. Flow dynamics within the boundary layer can be laminar or turbulent. The degree of sediment transport is a function of turbulence and the current shear, together determining shear stress. Sediment composition and bed roughness also influence shear stress. Furthermore, particle size, current speed, particle and water densities, viscosity of water and the laminar/turbulent flow collectively influence sediment transport and deposition. Initiation of sediment movement occurs when the shear stress at the bed overcomes frictional and gravitational forces, an effect defined as the critical shear stress. Sediment transport is controlled by sediment characteristics, primarily grain size, and is further influenced by cohesiveness of the sediments (Brown *et al.*, 1999). For non-cohesive sediments, the threshold of sediment entrainment is slightly greater than the depositional velocity and is defined by the settling velocity. For cohesive sediments the additional forces of clay materials means that the sediment threshold for entrainment is significantly greater than the depositional velocity. Sediment entrainment is defined by the ratio of fluid stress to immersed stress of the shields parameter (Brown *et al.*, 1999).

Deposition of the bedload occurs when the current speed is reduced to a point where the shear stress at the bed is slightly less than the critical shear stress. Deposition of the suspended load is a function of the sediment settling characteristics, resulting in a settling lag (Brown *et al.*, 1999).

2.1.3.2 *Sediment movement by waves*

In shallow-water waves, water particles follow orbital paths that become progressively flattened towards the sea-bed. In shallow water depths the shear stress at the bed and the maximum horizontal orbital velocity increase as wave height increases and water depth decreases. Sediment movement is determined based on wave height, wave period and water depth. The orbital velocity required to initiate sediment movement for given sediment characteristics increases as the wave period increases (Brown *et al.*, 1999).

Dolphin (2003) investigated the impact of waves on sediment behaviour in the Manakau Harbour. Results demonstrated that the suspended sediment transport was confined to a near-bed layer of approximately 10 cm thick and was defined by the turbid fringe, a narrow, highly turbid edge of the estuarine water body (Green *et al.*, 1997).

2.1.4 Sediment trend analysis

Sediment characteristics are specific to any given location however significant variability exists over a range of spatial scales. Sediment distribution depicts the mode of transport, energy conditions and nature of source material (Friedman, 1961; Larson *et al.*, 1997).

Sediment Trend Analysis (STA) is a method that recognises patterns of net sediment transport pathways based on relative changes in grain-size distributions of surficial sediments. The theory of STA describes the changes in grain size parameters (mean grain size, sorting and skewness) between neighbouring deposits in the direction of net sediment transport providing an understanding of sedimentary environments. Furthermore, STA can predict sediment behaviour in regards to erosion, accretion or dynamic equilibrium indicating sediment sources and sinks (McLaren *et al.*, 2007). Numerous models have been proposed based on the theory of STA.

2.1.4.1 *Sunamura and Horikawa (1972) Model*

Sunamura and Horikawa (1972) developed a model based on relative changes in sediment characteristics including mean grain size and sorting to determine the direction of longshore sediment transport. The model includes nine situations that reflect different trends, of which the direction of sediment transport is inferred based on the various relationships between mean grain size and sorting (Figure 2.1).

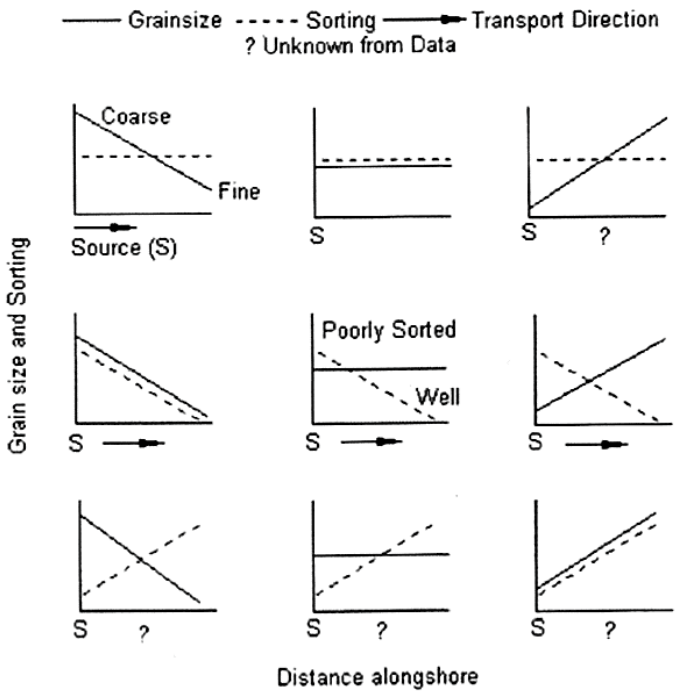

Figure 2.1: Criteria for the inference of sediment transport direction according to Sunamura and Hroikawa (1972). Combinations of grain size and sorting may indicate littoral drift direction (de Lange, 1988).

2.1.4.2 *One-dimensional model*

The McLaren (1981) model is a one-dimensional method that predicts sediment transport based on spatial trends between textural parameters of all possible pairs of samples along a given transect (Figure 2.2). McLaren (1981) originally described four sedimentological trends (Table 2-1).

A further study by McLaren and Bowles (1985) identified three cases that can be characterised by relative differences in textural parameters between two locations (assigned distributions *d1* and *d2)* that vary as a result of erosion, transportation and deposition (McLaren, 1981; McLaren & Bowles, 1985). Case IIIA described by McLaren (1981) was proven invalid, demonstrated by the use of transfer functions that determined when sediment becomes finer it must also become more negatively skewed. Additionally, Case II and Case IIIB are identical trends. Case II is a lag deposit which cannot determine sediment transport alone and was hence not considered. Therefore the McLaren and Bowles (1985) model only considers two of the sedimentological trends initially proposed by McLaren (1981): Case B and

Case C (McLaren & Bowles, 1985). A significance test (Z-Score) is calculated to determine the validity of the vector field. The sediment trend is confirmed by the qualitative evaluation of a multiple correlation coefficient between the textural parameters of each sample along the transect (McLaren *et al.*, 1993).

Table 2-1: Correlation of sedimentological trends identified by different methods.

Sedimentological Trend	**Code**	**McLaren (1981) Model**	**McLaren and Bowles (1985) Model**	**Gao and Collins**	**Le Roux and Rojas**
Finer grain size Better sorted Negatively skewed	CB-	Case I	Case B	Case 1	Type 1
Coarser grain size Better sorted Positively skewed	FB+	Case II	Case A *Cannot infer transport direction*	considered	Type 2
Finer grain size Better sorted Positively skewed	FB-	Case IIIA	Invalid	considered	Type 3
Coarser grain size Better sorted Positively skewed	CB+	Case IIIB	Case C	Case 2	Type 4

Case A: Lag deposit

A sediment lag deposit can be inferred if the deposited sediment (*d2)* has a coarser mean grain size, is better sorted and more positively skewed than its source (*d1).* In this case, the sediment transport direction cannot be determined without further information.

Case B: Fining sediments

In a situation where *d2* has a finer mean grain size, is better sorted and more negatively skewed than *d1*, the transport direction can be inferred from sample *d1* to *d2*. In this case the coarser sediments are not transported as far as finer sediments as the energy regime controlling sediment transport is decreasing from *d1* to *d2.*

Case C: Coarsening sediments

If the mean grain size is coarser, better sorted, and more positively skewed at distribution *d2* than *d1*, the sediment transport direction can be inferred from sample *d1* to *d2*. As with Case B, the energy regime is decreasing from *d1* to *d2*. A trend indicating an increase of coarse sediments can be explained by the effect of "armouring" at *d1*. Coarser material shields underlying layers of finer sediment, hence the sample contains a higher percentage of fine material. The energy regime is enough that the coarser material can be transported and deposited at *d2* as the energy regime decreases. Any fine suspended sediment will be further transported past the location of *d2*.

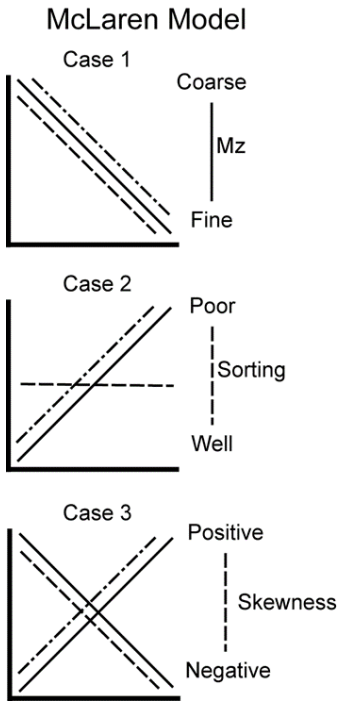

Figure 2.2: Summary of the trends applied to a sediment trend analysis. Note that Case 1 shows the changes along the coast in the direction of transport (spatial pattern). Cases 2 & 3 are the changes over time at a specific location (temporal pattern) (de Lange, 1988).

2.1.4.3 *Gao and Collins (1991, 1992) Model*

Gao and Collins (1991, 1992) developed a 2D model based on the relationship of textural trends between neighbouring sample sites. Neighbouring sites are determined on the basis of a 'characteristic distance' that considers the spatial scale of the sampling area. A single vector is calculated at each site if a textural trend is

recognised and displayed as a dimensionless trend vector of unit length indicating the direction of transport based on the relationship of the two sampling sites. The final outcome is filtered by averaging the value of each site and its nearest neighbours to produce transport vectors that indicate net transport pathways. Similar to the McLaren model, a final statistical test (the L test) is used to validate the vector field (Gao & Collins, 1992).

Gao and Collins (1992) retitled Cases B and C proposed by McLaren and Bowles (1985) as Case 1 and Case 2, respectively. A combination of the cases CB+ and FB − was also considered as well as the possibility of FB+ occurring in a beach environment. A further study by Gao et al. (1994) identified four sedimentological trends (CB+, FB−, CB− and FB+) that should be considered out of the fourteen initial theoretical trends analysed.

2.1.4.4 *The Asselman method*

Asselman (1999) proposed a modified approach of the Gao-Collins method, applied in a Geographic Information System analysed using geostatistical tools. Data interpolation of each textural parameter is achieved using block kriging to create separate raster maps. Vectors are defined if a type 1 or 2 trend is apparent by comparison with neighbouring cells. The trend vectors of each textural parameter are compared cell by cell within an optimum range and averaged to produce a single vector. Monte Carlo is a simulation carried out as a statistical test on the trend vectors which indicate sediment transport directions (Asselman, 1999).

2.1.4.5 *Le Roux (1994) Model*

The Le Roux (1994) method reflects sediment transport driven by wide unidirectional flows, rather than point to point comparison which other models are based on. Five sample sites are used to calculate the mean vector direction and vector strength of the sediment transport paths. Sites include one central and four located on the principal radius at an equal distance from the centre. Irregularly spaced sites are resituated based on an iterative trigonometric technique. The textural parameters are combined into dimensionless numbers, followed by vector

analysis to produce proportional frequencies of sediment transport directions. To statistically evaluate the validation of the resulting vectors the Watson (1966) non-parametric test was used. The Le Roux (1994) method considers possible sediment trends; CB+, CB−, FB+ and FB−.

2.1.4.6 *The Rojas methods*

Along with mean grain size, sorting and skewness, the Rojas method also considers kurtosis. The combined grain size parameters are denoted as a facies function on the basis of depositional environments and transport processes which form a digital facies map. The digital facies map is constructed on a regular grid where the nearest neighbour is used to calculate each pixel within the surrounding four quadrants. Facies functions are weighted based on the distance to the central pixel. Vectors are calculated by one of either of two methods: (1) triangle method or (2) gradient method. The triangle method (Le Roux & Rojas, 2007) calculates vectors using dip and dip direction of all potential surfaces between the central pixel and two neighbouring pixels located within a defined radius. The gradient method (Le Roux & Rojas, 2007) uses points between central pixel and neighbouring pixels to measure the gradient, designating magnitudes of horizontal vectors that have the same directions. Both methods compare the generated vectors to observed sedimentary structures in order to calculate an angular error. False negatives are assigned where no sedimentary structures are observed and true positives are points that have both observed and generated vector data. The mean global error is calculated incorporating false negatives and true positives to indicate the validity of the results.

2.2 Tauranga Region

2.2.1 Tauranga Harbour

The Tauranga Harbour is a shallow meso-tidal estuarine lagoon extending 35 km along the northeast coast of New Zealand with an average width of 5 km (Healy & Kirk; de Lange & Healy, 1990b; Briggs *et al.*, 1996). The area of the Tauranga Harbour is 851 km^2 of which 70% is tidally exposed (de Lange & Healy, 1990a; Spiers *et al.*, 2009). The estuarine lagoon is enclosed by a Holocene barrier island,

Matakana Island, extending 24 km and connected to the mainland by tombolos, including Mt Maunganui in the Tauranga Basin (southeast) and Bowentown in the Katikati Basin (northwest) (Davies-Colley, 1976; Healy & Kirk). The two basins can be considered hydrodynamically independent, separated by extensive intertidal flats. Although the basins are connected, there is limited exchange of water between them (Barnett, 1985).

2.2.2 Geological setting

Tauranga Basin formed following eruption of the Waiteariki Ignimbrite which resulted in rapid subsidence with high amounts of infill comprised predominately of fluvial/estuarine sediments. Volcanic and sedimentary sequences unconformably overlie Waiteariki Ignimbrite as it was infilled subsequent to the eruption (Briggs *et al.*, 1996).

Tauranga Basin comprises late Pliocene to Holocene deposits consisting of amalgamated sedimentary, pyroclastic and volcanic sediments originating from both primary and secondary volcanics. Volcanic rocks and volcanogenic sediments are intercalated with terrestrial and estuarine sedimentary deposits of late Pliocene to Pleistocene age from the Tauranga area, overlain by late Pleistocene and Holocene tephra deposits (Briggs *et al.*, 1996) (Figure 2.3). Primary sediments are sourced from the Tauranga region, southern Coromandel Volcanic Zone and Taupo Volcanic Zone. Secondary deposits are reworked via fluvial, lacustrine and estuarine processes and redeposit in sequences interbedded with primary volcanic deposits. With the exception of the older materials found in the Tauranga region (including the Otawa Volcanics and Matakana Basalt), the more recent primary and secondary volcanic material comprising Tauranga Basin is predominantly rhyolitic in composition (Briggs *et al.*, 1996; 2005).

Davis and Healy (1993) reconstructed the depositional setting of the southeastern Tauranga Harbour during the Quaternary. Three lithofacies were identified in ascending order: pumiceous sand and gravel, shelly mud and shelly sand. The interpreted depositional environments suggest fluvial and fan deposits of Pleistocene to early Holocene dating 9420 ± 100 yr BP were overlain by shelly mud

as the sea level rose, representing a low-energy estuarine environment in a valley-like setting (8100 ± 80 yr BP). Continued sea level rise resulted in accumulation of overlying shelly sand, deposited in a wave-dominated shoreface similar to the present nearshore environment. The post-glacial marine transgression, or stillstand, of c. 6500 years ago led to formation of the barrier island complex including Matakana Island and a system of progradational dune ridges joining Bownetown and Mount Maunganui to the mainland. Recent low lying terraces accumulated from river and stream alluvium and peat deposits (Briggs *et al.*, 1996).

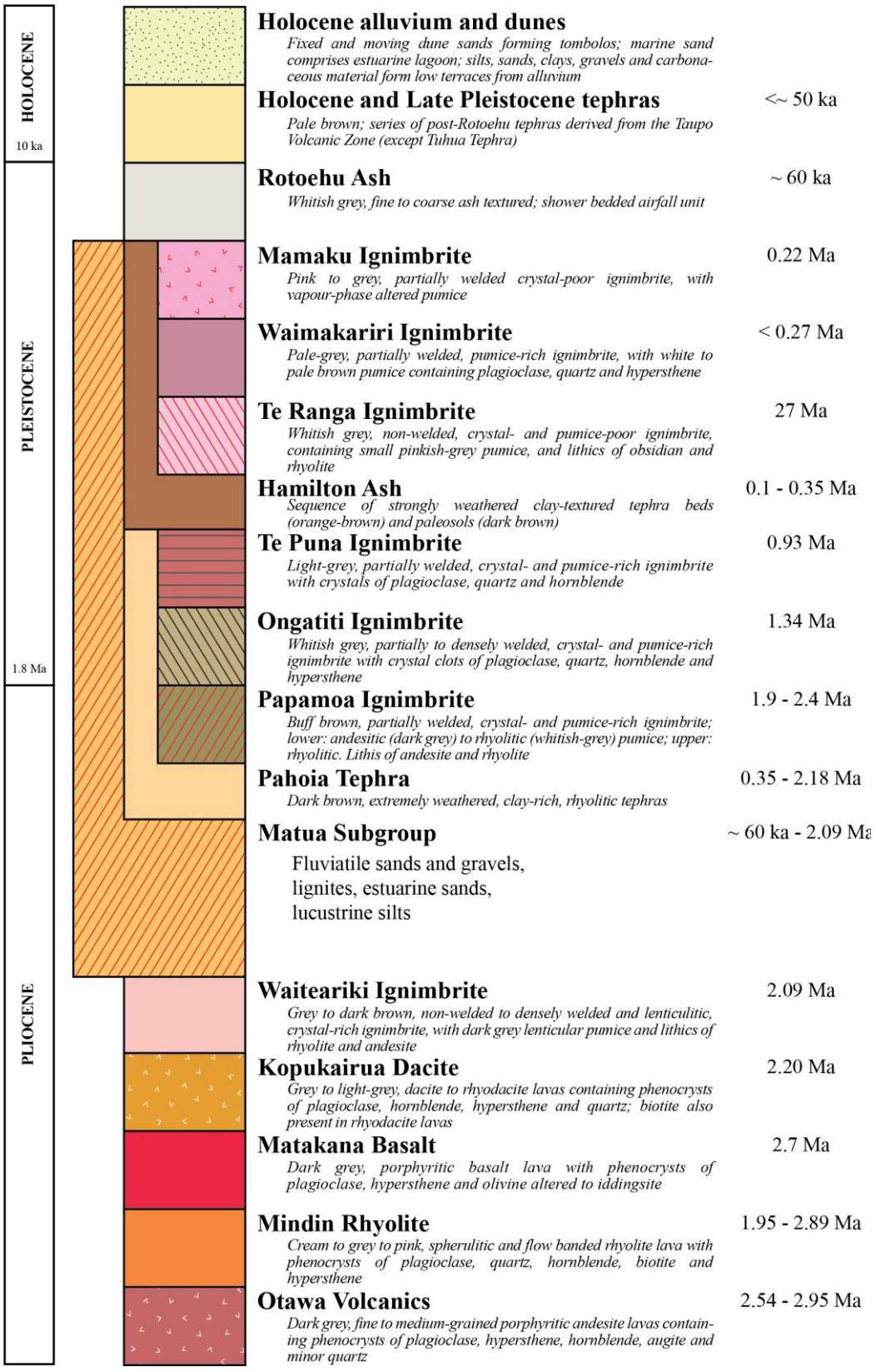

Figure 2.3: Generalised stratigraphy of the Tauranga region (compiled from Briggs and Leonard *et al.* (2010)

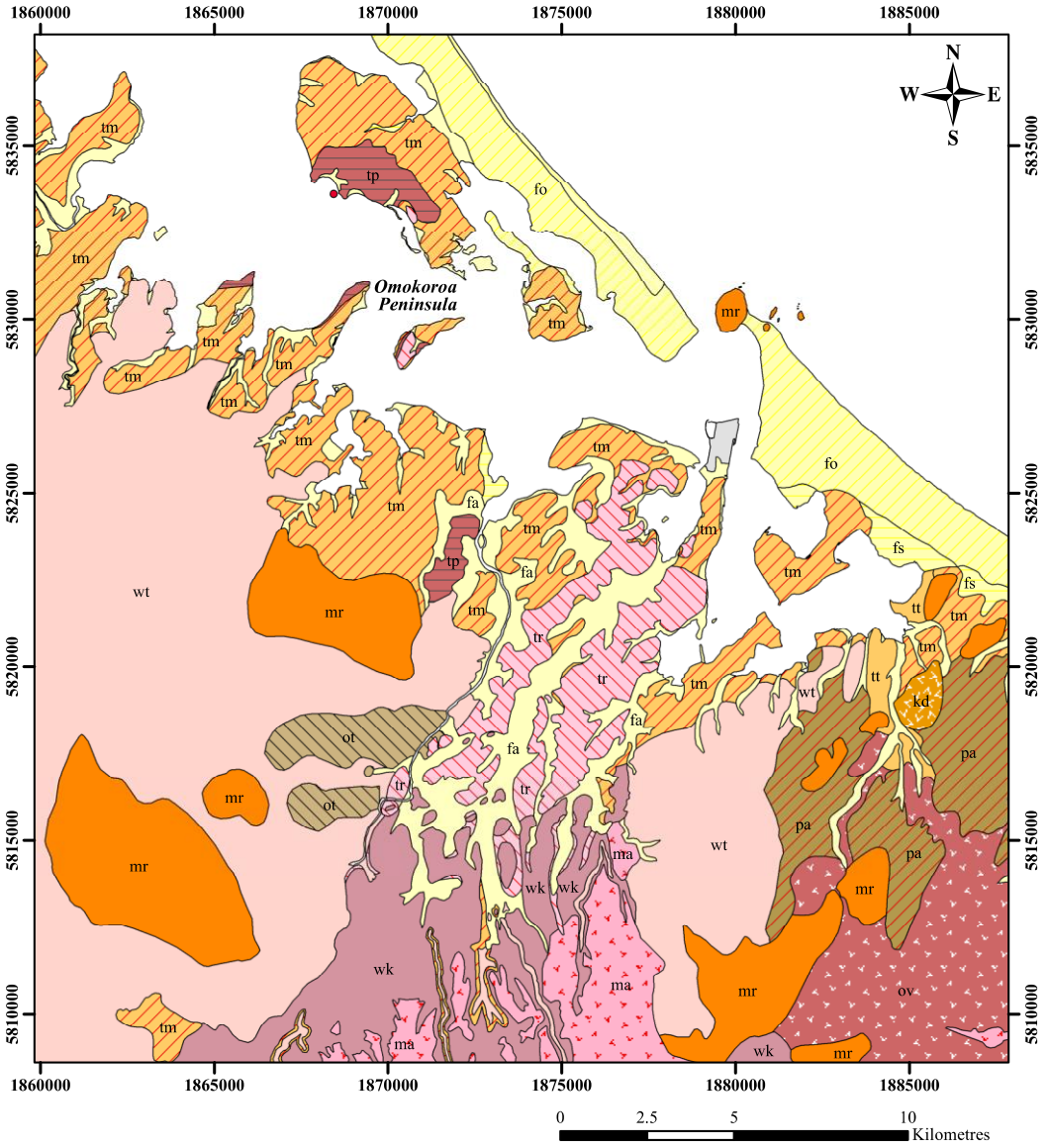

Figure 2.4: Geology of the Tauranga Region (after Briggs *et al.*, 1996).

2.2.3 Omokoroa geology

Omokoroa is one of a series of terraces that extends as a peninsula north east into the Tauranga Harbour. Omokoroa Peninsula is constructed of the Matua Subgroup intercalated with Pahoia Tephra and Te Puna Ignimbrite and subsequently overlain by Hamilton Ash, Rotoehu Ash and post Rotoehu Ash (Briggs *et al.*, 1996).

2.2.3.1 *Matua Subgroup*

Matua Subgroup is a complex unit formed subsequent to the Waiteariki Ignimbrite, comprising reworked volcanic deposits that range between 80 and 150 m thick (Harmsworth, 1983; Briggs *et al.*, 1996). The Matua Subgroup, aged between 2.09 Ma and 0.35 Ma, includes all terrestrial and estuarine sediments that post-date the Waiteariki Ignimbrite and pre-date the Hamilton Ash. The process of erosion, transportation and re-deposition of volcanic debris has resulted in a wide variety of lithologies characterised by the Matua Subgroup that vary laterally and vertically. Lithologies include fluvial pumiceous and rhyolitic silts, sands and gravels, lacustrine and estuarine muds, lignites, peats and airfall tephra. Various sedimentary structures are observed in the Matua Subgroup including cross-bedding, planar stratified and massive units, as well as post depositional slump and water escape structures (Briggs *et al.*, 1996; 2005).

2.2.3.2 *Pahoia Tephras*

The Pahoia Tephras are a sequence of severely weathered ashes of rhyolitic composition, being older than the Hamilton Ash (2.18 – 0.35 Ma) (Harmsworth, 1983; Briggs *et al.*, 1996). Sediments of fluvial origin (Matua Subgroup) and distal ignimbrites are incorporated within the Pahoia Tephra sequence (Briggs *et al.*, 1996).

2.2.3.3 *Te Puna Ignimbrite*

Te Puna Ignimbrite (0.93 Ma) is described as a crystal-rich ignimbrite with pumice fragments. Te Puna Ignimbrite differs in character from a non-welded weak rock to partially welded rock with medium-strong strength, which weathers to a firm clay.

The distribution of the Te Puna Ignimbrite varies and is recorded in coastal sections at Omokoroa up to 3 m thick (Briggs *et al.*, 1996).

2.2.3.4 *Hamilton Ash*

The Hamilton Ash (0.35 – 0.1 Ma) comprises a sequence strongly weathered, clay-textured tephra beds and paleosols. The sequence is divided into eight units (H1-H8) however erosion has obscured some units so that not all divisions are observed at each site (Briggs *et al.*, 1996; Lowe *et al.*, 2001). McCraw (2011) classifies seven members in the Hamilton Ash and believes the sequence originated from rhyolitic caldera eruptions north of Taupo. At Omokoroa, Briggs *et al.* (1996) identified the Hamilton Ash by the well-developed brown paleosol on the upper surface to be approximately 2.5 m thick with an orangey-brown base.

2.2.3.5 *Rotoehu Ash*

Rotoehu Ash derives from the Taupo Volcanic Zone and is characterised as a widespread shower bedded airfall deposit that varies in thickness from 0.3 m to 2.4 m within the Tauranga region. Rotoehu Ash is described as a whitish-grey, fine to coarse textured ash (Briggs *et al.*, 1996; Wilson *et al.*, 2007) and is aged between 44.8 ± 0.3 and 47.5 ± 2.1 ka cal BP (Danišík *et al.*, 2012).

2.2.3.6 *Post Rotoehu Ash Tephras*

A series of younger tephras overlie the Rotoehu Ash, forming the parent material of much of the soils in the Tauranga region. A number of tephras have been identified including: Mangaone, Kawakawa, Te Rere, Okareka, Rotorua, Mamaku, Tuhua, Waimihia, Taupo and Kaharoa tephras. The tephras identified above are all sourced from the Taupo Volcanic Zone, with the exception of the Tuhua Tephra which derived from Mayor Island (Briggs *et al.*, 1996).

2.2.3.7 *Holocene sediments*

Progradational dune ridges formed during the post-glacial sea level rise and comprise dune sands. Recent alluvial and peat deposits are composed of silts, sands, clays, gravels and carbonaceous material (Briggs *et al.*, 1996). Tauranga Harbour

is a shallow estuarine lagoon with well-developed ebb-tide and flood-tidal deltas at both the north and south entrances. The exposed intertidal area of the estuarine lagoon is largely composed of marine sand (Davies & Healy, 1993).

2.2.4 Climate

Climate in the Bay of Plenty is modified by the local topography, as high country shelters the region to the west, south and east resulting in a sunny climate with light winds and variable rainfall (Chappell, 2013). Chappell (2013) identified five meteorological situations affecting climate within the Bay of Plenty region: (1) north to northeast airstreams, (2) disturbed west to southwest airflows, (3) south to southeast airstreams, (4) west to northwest flows and (5) cyclones of tropical origin. North to northeast airstreams approaching the Bay of Plenty region produce widespread rain as a result of long trajectories over the warm ocean north of New Zealand. Wind associated with the north to northeast airstreams is light to moderate with wind speeds <10.5 $m.s^{-1}$. Disturbed west to southwest airflows are frequent, driven by cold fronts travelling east-north-east bringing light showers and moderate to strong winds >8.5 $m.s^{-1}$. South to southeast airstreams produce fine dry weather in the Bay of Plenty with warmer temperatures due to foehn warming. West to northwest flows results in high cloud cover and intermittent rain associated with fronts. Tropical cyclones are infrequent in the Bay of Plenty region, however produce heavy rain and strong winds between November and April (Chappell, 2013).

2.2.4.1 *Wind*

West and southwest prevailing winds are strong and frequent at the Tauranga Aerodrome Automatic Weather Station (Aero AWS), followed by northerlies and south easterlies (Figure 2.5). Strong wind speeds between 10.5 and 22.5 $m.s^{-1}$ are predominately from the southwest, west and north. Most common winds in Tauranga prevail from the west and southwest and are driven by the north to northeast airstreams and disturbed west to southwest airflows.

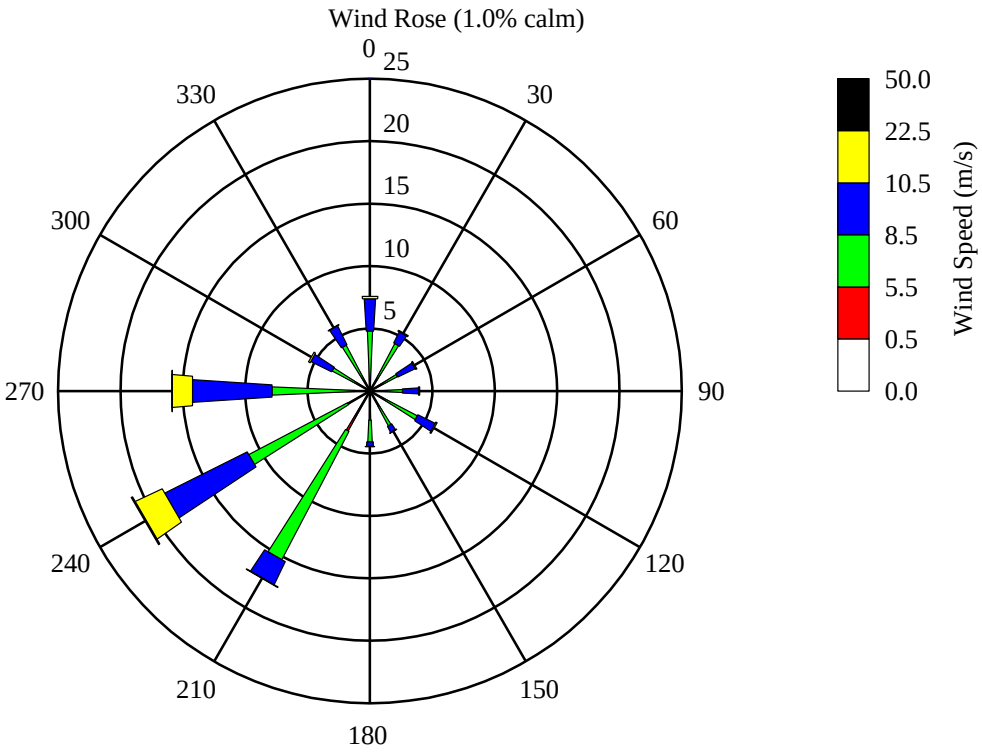

Figure 2.5: Wind Rose at Tauranga Aero AWS between 1995 and 2012.

Seasonal variations in wind speed are apparent as spring has the windiest days whereas summer and autumn have the largest number of light wind days. Gale force winds, although infrequent and can occur throughout the year, most commonly in the winter months (Chappell, 2013).

The diurnal variation is apparent in Tauranga as the greatest wind speeds are recorded during the early afternoon. Diurnal variation is a result of surface heating, resulting in turbulent mixing with the stronger winds causing increased wind speeds at the surface. Overnight, as the effect of surface heating reduces, a lighter wind regime is restored. Diurnal variation is much more pronounced in summer than in winter. Furthermore, Tauranga is subject to northerly sea breezes ranging from 20 to 30 km/hr during the mid-late afternoon over summer, when pressure gradients are weak. Uneven surface heating creates a pressure gradient as the land heats up faster than the ocean. Cooler air from over the ocean replaces rising warm air over land, resulting in a sea breeze. At night, coastal areas are subject to light southerly winds caused by cool air draining from inland (Chappell, 2013).

2.2.4.2 *Rain*

Spatial variability of rainfall over the Bay of Plenty region reflects topography, with high rainfall recorded at high elevations, decreasing towards the coast. Rainfall in the Bay of Plenty is driven by the northerly airstreams where the highest rainfall is recorded during the winter months (Figure 2.6). Seasonal fluctuations in rainfall are apparent particularly in summer and autumn where long periods of dry spells or heavy rain is experienced (Chappell, 2013). Rainfall records at Omokoroa weather station from July 2013 until June 2014 generally lie within the range recorded at the Tauranga Aerodrome AWS (data shows total monthly rainfall, averaged over an 18 year period from 1995 to 2012) (Figure 2.6).

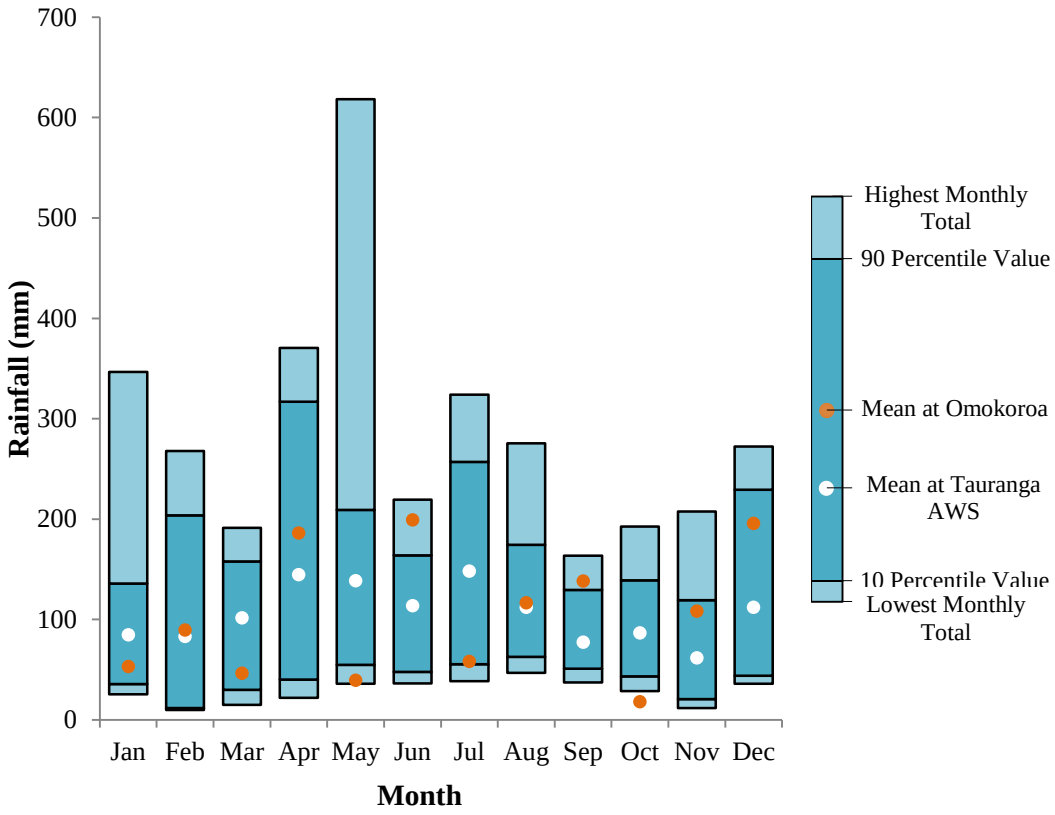

Figure 2.6: Average monthly rainfall at Tauranga Aero AWS between 1995 and 2012 and at Omokoroa WS between June 2013 and June 2014.

2.2.5 Climate change

Bell *et al.,* (2006) identifies that changes in climate may impact erosion and accretion patterns along the Bay of Plenty coastline due to changes in the wave climate. The Bay of Plenty wave climate is moderately influenced by the El Niño Southern Oscillation. During La Niña periods, more stormy conditions are associated with an increase in northeasterlies. During El Niño periods, a higher occurrence of southwesterlies occurs, reducing wave conditions, however episodic extra-tropical cyclones still occur. Currently La Niña phase dominates, hence the Bay of Plenty region may experience increased rates of erosion associated with northeasterlies.

Future changes in the climate will have a significant influence on sediment transport. Changes in climate will have a direct effect on local wind forcing parameters (wind speed and direction) and indirectly through parameters (significant wave height, period and direction) representing swells generated by wind over wide expanses of the Pacific Ocean. Hence climate change must be considered at a range of geographic scales (Bell *et al.*, 2006). Hume *et al.,* (2009) predicts that climate change will have the greatest increase in sediment accumulation rates as a result of increased runoff.

2.2.6 Sea level

Sea levels are the principal control on the degree of coastal inundation and limit the ability to transport sediment. Sea level is altered by the tidal height, storm surge and wave conditions. Variations in sea level are caused by a number of events over different timescales by a wide range of physical forces and processes (Pugh & Woodworth, 2014). Historic rates of relative sea level rise in the Bay of Plenty are 1.40 mm/yr (without considering subsidence/uplift) on historic and projected sea level rise in the Bay of Plenty (Bell *et al.*, 2006). Clement *et al.,* (2010) illustrates that historic sea levels during the Holocene have oscillated between 2 m above and below the current sea level (Figure 2.7).

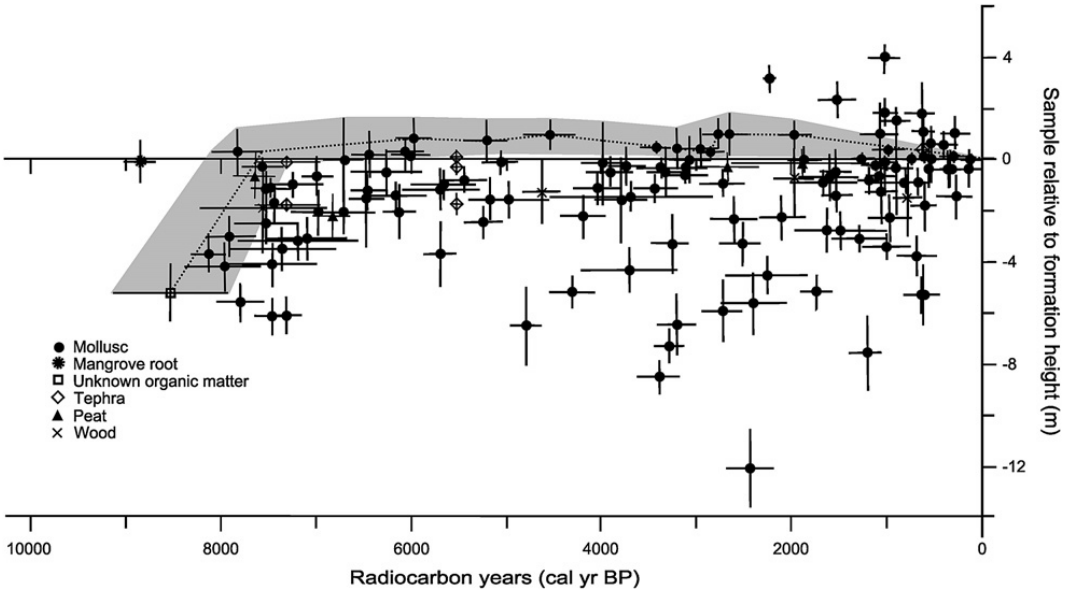

Figure 2.7: Holocene sea level curve for New Zealand (Clement *et al.*, 2010).

2.2.7 Land use changes in New Zealand

Land use changes have modified the sediment runoff rate and patterns in New Zealand. Historic sedimentation rates within New Zealand are determined through analysis of cores from numerous estuaries that indicate past land use changes by fluctuations in sedimentation rates. Sediment grain size varies as the land use alters the rate of erosion, therefore the rate and nature of the sediment transported to the estuary fluctuates (Hume *et al.*, 2001; Mead & Moores, 2005; Swales *et al.*, 2005). Results illustrate a clear correlation between European settlement and an increase in sedimentation rate, furthermore the impact of urbanisation is recognised. It is now widely accepted that the enhanced sedimentation of estuarine environments is not attributed to natural depositional processes but the modification to land use.

Hancock *et al.*, (2009) determined the sediment accumulation rate of cores within the southern Tauranga Harbour. Results range between 0.75 and 1.57 mm/yr over periods of 23 to 90 years. Sediment accumulation rates determined in Tauranga Harbour are low in comparison to other studies conducted in the North Island, indicating that long-term accumulation rate of fine terrigenous material on the intertidal flats is negligible.

2.2.8 Hydrodynamics

Numerous studies have been undertaken in the Tauranga Harbour, largely associated with the tidal inlet and development of the Port of Tauranga for engineering purposes (Nordstrom & Roman, 1996).

The initial investigation of the hydrodynamics and sediment transport within the Tauranga Harbour was completed in the Tauranga Harbour Study (Black, 1984). The Tauranga Harbour Study provided a basis for further research. The dominant hydrodynamic processes in the Tauranga Harbour are tidal currents and wind generated waves (Davies-Colley & Healy, 1978; Pritchard *et al.*, 2009). Furthermore, Davis-Colley (1976) observed that the freshwater input was small compared to the tidal flow.

2.2.8.1 *Wave climate*

de Lange and Healy (1990a) demonstrated that the harbour entrance filters out a large proportion of offshore wave energy, where high frequency, wind generated waves contribute to a significant amount of wave energy in the Tauranga Harbour. Based on the findings by de Lange and Healy (1990), the wave climate at Omokoroa will be dominated by locally generated wind waves.

2.2.8.2 *Tidal range*

Astronomical tidal regimes for Tauranga Harbour are semidiurnal and the mean spring and neap tidal range is 1.79 m and 1.21 m, respectively, considered to be micro-tidal. The highest astronomical tide is 0.9 m RL and the maximum range is 2.19 m RL. The spring tidal prism of the Tauranga inlet is 165x106 m^3 (Hicks & Hume, 1996).

Tidal forcing dictates the water level in the Tauranga Harbour and degree of coastal erosion due to interaction with the coastline. Erosion driven by coastal processes at Omokoroa is limited to high water levels and enhanced by spring tides and storm surges (Tonkin & Taylor, 2010). The tidal station in Tauranga Harbour is located ~12 km east of Omokoroa at the Port of Tauranga (Tug Berth).

Table 2-2: Tidal Level in the Tauranga Harbour (LINZ, 2014).

Tidal Level	Level (m, CD)	RL (m, above MSL)
Mean High Water Springs (MHWS)	1.94	0.90
Mean Low Water Springs (MLWS)	0.15	-0.89
Mean High Water Neaps (MHWN)	1.66	0.62
Mean Low Water Neaps (MLWN)	0.45	-0.59
Spring Range	1.79	1.79
Neaps Range	1.21	1.21
Mean Sea Level (MSL)	1.07	0.03
Highest Astronomical Tide (HAT)	2.11	1.07
Lowest Astronomical Tide (LAT)	-0.08	-1.12

Chart Datum source: New Zealand Nautical Almanac (LINZ, 2014).

As the primary tides propagate into the harbour, the shape of the tidal wave changes as the flooding tide becomes shorter and faster whereas the ebbing tide is longer and slower (Bell *et al.*, 2006). Peak velocities of ebb and flood flow are asymmetric in both direction and magnitude, and lag behind mid tide (Davies-Colley, 1976). McKenzie (2014) identified the major tidal constituents as M2 followed by N2, S2, K1 and O1 (Table 2-3).

Table 2-3: Main tidal constituents in the Tauranga Harbour (McKenzie, 2014).

Constituent	Location	Frequency	Period (hours)	Amplitude (m)	Phase (˚GMT)
M2	A Beacon	0.0805	12.42	0.719	188.97
	Tug Berth			0.690	198.68
	Sulphur Pt			0.713	199.91
	Omokoroa			0.709	220.75
S2	A Beacon	0.0833	12.00	0.120	267.77
	Tug Berth			0.107	281.89
	Sulphur Pt			0.111	281.79
	Omokoroa			0.098	313.70
N2	A Beacon	0.0790	12.66	0.180	158.28
	Tug Berth			0.169	169.57
	Sulphur Pt			0.176	171.59
	Omokoroa			0.162	194.66
K1	A Beacon	0.0418	23.93	0.035	181.92
	Tug Berth			0.035	189.57
	Sulphur Pt			0.035	179.08
	Omokoroa			0.034	206.40
O1	A Beacon	0.0387	25.82	0.014	150.74
	Tug Berth			0.013	141.87
	Sulphur Pt			0.015	139.81
	Omokoroa			0.012	144.71

2.2.8.3 *Storm effects*

Goring (1995) examined sea level data around New Zealand, including Moturiki Island, located off the Bay of Plenty coast. Results show there is a time difference between the recorded barometric pressure and recorded storm surge. Furthermore, the inverse barometric pressure is greater than the recorded storm surge with only 53% of the overall variation in sea level justified by barometric pressure. Correlating the local wind data shows no significant influence. This suggests that sea level in the Bay of Plenty is altered by waves propagating into the region, in addition to the sea level response to barometric pressure. Within the Tauranga Harbour it is likely that the wind set up has a larger influence on the water level.

Within Tauranga Harbour storm-tide levels differ from Moturiki Island due to damping of open-coast storm surge through the entrance (Tonkin & Taylor, 1999; Bell *et al.*, 2006).

A study by de Lange (1996) calculated maximum storm surge elevations above Mean High Water Springs (MHWS) of 0.6 m 0.8 m and 1.0 m for events with return periods of 1-in-10 years, 1-in-100 years and 1-in-1000 years, respectively. Furthermore, the study concluded that Bay of Plenty is subject to increased storm events during La Niña periods. Further research by de Lange and Gibb (2000) analysed storm surge events within the south-eastern Tauranga Harbour between 1960 and 1998. Events were classified as greater than 10 cm increase from the predicted high tide level. The results showed variations in the magnitude and frequency of storm surge events, correlating to Inter-Decadal Pacific Oscillations (IPO). A greater number of storm surge events were recorded during the La Niña phase between 1960 and 1976 than the El Niño phase from 1976 to 1998. Bell *et al.*, (2006) reports that during the current IPO beginning around 1998, of which predicted to have an increased occurrence of storm surge event relative to the previous period, does not show an increase in storm surge events.

Within Tauranga Harbour, Gibb (1997) reviews the minimum sea flood levels, including at the Omokoroa Golf Course. Historic records indicate maximum storm surge heights of ~70-90 cm have occurred since 1840. Heights of storm surge events are subject to local factors including exposure of the physiography of the coastline. Furthermore, Gibb (1997) identified that the pattern of storm surge levels was not uniform, as coasts facing NW-NE experienced higher storm surges compared to S-SW facing coasts in the order of 20 cm. Furthermore, variability in storm surge height was recorded either side of Omokoroa, relative to the prevailing wind direction.

Hay *et al.* (1991) complied a storm data base for the Western Bay of Plenty between 1873 and 1990. For a storm to qualify as having the ability to impact the coastal environment, the onshore wind velocity must exceed 63 – 74 km/hr (Force 8 on the Beaufort Scale) which could be expected every 14 years. Winds between 52 – 61

km/hr (Force 7) associated with storm events occur at a frequency of 0.71% per year. Annual storm fluctuations evident within the database indicate storm events were most frequent during May and July whereas November recorded the lowest number of storm events. The duration of storms varied between 6 and 36 hours.

Future predictions of storm systems suggest there is no clear evidence to indicate whether there will be an increase or decrease in storm surge magnitudes in the next 50 to 100 years and hence the changes in storm tide. It is assumed that storm tide elevations will rise at the same rates as mean sea level rise (Bell *et al.*, 2006).

2.2.8.4 *Sediment transport*

In southeastern Tauranga Harbour, wind generated wave heights exceed 45 cm only 2% of the time. Analysing sediment transport by waves suggests that orbital velocity at the bed significantly reduces with depth, therefore sediment will be affected in depths shallower than 1.0 – 1.5 m. The impact of wind generated wave action is a function of water depth and dependant on the tidal phase, hence influences intertidal areas with negligible impact in subtidal areas (Davis-Colley & Healy, 1978). Davis-Colley and Healy (1978) conclude that within the Tauranga Harbour, waves are an important process in aiding sediment entrainment in shallow water however the primary mode of sediment transport is tidal currents. Sediment transport is episodic and relates to the magnitude and frequency of storms (surges) as well as the timing of high tides (Bell *et al.*, 2006).

The Tauranga Harbour Sediment Study (THSS) conducted by NIWA in 2009 attempts to quantify fine sediment transport in the Tauranga Harbour by coupling a catchment model with a hydrodynamic model of the Tauranga Harbour. The results suggest that the suspended sediment derived from catchment runoff, primarily sourced from the Wairoa River, is transported up the harbour. The primary source of sediment accumulating east of Omokoroa is predicted to derive from the Wairoa subcatchment, some 6 km southeast of Omokoroa (Hume *et al.*, 2009). Secondary sources of fine sediment are derived from subcatchments extending from Matahui point to Tauranga City and from Matakana Island, receiving sediments from a wide range of sources. Elliot *et al.* (2009) demonstrated the sediment load from the various subcatchments in the Tauranga Harbour, where that Waipapa, west of the

Omokoroa Peninsula and Mangawhai, east of Omokoroa, deliver 4722 and 1251 tonnes per year, respectively. Results from the Elliot *et al.* (2009) contradict other research such as Tay (2011) who illustrate that fine sediment is transported out of the harbour entrance. The THSS is not a reliable indicator of sediment transport in Tauranga Harbour as sedimentation is based on catchment runoff, and does not consider cliffs as a direct sediment source, which are recognised as a primary contributor to sediment. Additionally, the hydrodynamic model controlling the processes that determine sediment transport has not been accurately calibrated and verified.

2.2.8.5 *STA in the Bay of Plenty*

STA concepts have been applied in a number of studies in the Bay of Plenty (de Lange, 1988; Perano, 2000; Bear, 2009). Bear (2009) applied the Sunamura and Horikawa (1972) model and McLaren (1981) model to beach sediments at Waihi Beach along the Bay of Plenty coast. Overall, the results were questionable as the inferred trends did not correlate well to geomorphic evidence. The "Waihi" model, a model proposed by Phizackela (1993) which considers the effects of grain shape and variation in mineralogy, was applied to Waihi Beach and improved the results. Within Tauranga Harbour, de Lange (1988) successfully applied the Sunamura and Horikawa (1972) model to beach sediments at Pilot Bay. Results suggest sediment transport directions corresponded to the residual tidal flows at Pilot Bay. Perano (2000) used the McLaren (1981) model to determine sediment transport patterns in the Wairoa Estuary, Tauranga Harbour. To obtain viable results, given estuaries are complex systems and are subject to numerous processes of which the model does not consider, samples were categorised based on morphodynamic units and dynamic patterns (eg. multiple sediment sources and bi-directional flow). The results, based on pre-determined transport environments, are comparable with field observations.

Little and Bullimore (2015) evaluates the reliability of the STA method, concluding that multiple lines of evidence support the methods and conclusions obtained from applying a STA. Further, Little and Bullimore (2015) supports the technique as a pilot study, background investigation for environmental monitoring and managing

in combination with interdisciplinary studies. The use of sediment textural parameters to determine sediment transport pathways have been successfully implemented in some New Zealand studies. Application of the method has been applied to a number of different environments. Those studies which reported a successful correlation with hydrodynamic driving forces or geomorphic indicators appear to derive from tidally driven environments (de Lange, 1988; McLaren & Teear, 2013). Alternatively, in a wave dominated environment (Saunders, 1999; Bear, 2009) the method does not appear to produce comparable results.

2.3 Omokoroa Peninsula

2.3.1 Land use and history of subdivision

Urban development of Omokoroa Peninsula began in 1943 and is expected to continue to expand in the future (Tonkin & Taylor, 1980). Land use prior to development was predominantly pastoral farming, primarily dairy, or original plantings of radiata pine (Western Bay of Plenty District Council, 2010b). Initial subdivision began on the northern sector in 1943 with an interval of significant subdivision between 1952 and 1974. Development of the Bramley Drive subdivision on the western margin of the peninsula was approved in 1967 which involved the removal of mature pine trees followed by construction of dwellings between 1974 and 1979. Further expansion initiated the development of two major subdivisions that commenced in 1979 (Tonkin & Taylor, 1980). The current land use of the northern portion of the Omokoroa Peninsula has been subdivided for residential living, where the southern area consists of horticulture and lifestyle blocks, with continued development of subdivisions (Western Bay of Plenty District Council, 2010b).

2.3.2 Instability

Omokoroa Peninsula is subject to erosion and is recognised as unstable as a result of several sizable landslides, the largest being the Bramley Drive landslide in August 1979. The Bramley Drive landslide involved the failure of a 34 metre high cliff extending 60 metres wide and 20 metres deep, generating a flat-lying run out that extended over 150 metres (Tonkin & Taylor, 1980). Numerous investigations

were undertaken to determine the stability and potential hazards of the Omokoroa Peninsula subsequent to the Bramley Drive landslide.

Tonkin and Taylor (1980) examined the coastline and identified that erosion resulting from landslides has occurred along the Omokoroa Peninsula for a long period of time. In recent years the northern and western margin has been subject to erosion from landslides. Tonkin and Taylor (1980) documents over 50 sites where significant landslides have occurred along the western side of the Omokoroa Peninsula, of which 17 can be classed as 'deep seated failures', similar to the Bramley Drive landslide. The remaining failures are considered to be a result of 'active shallow instability'. Other recent large scale landslides identified by Tonkin and Taylor (1980) include the occurrence of three landslides in 1962, on the western margin removing a 60 by 20 metre section of cliff generating a flat lying tongue similar to the Bramley Drive failure. Significant landslides along the western side have been recorded in 1968 (Tonkin & Taylor, 1980, 1981; Shrimpton & Lipinski Ltd, 1998; Tonkin & Taylor, 2011), 1995 (Walnut Grove) and 1998 (21 landslides over 2-3 weeks).

The primary factors contributing to the failures encountered along the cliffs of the Omokoroa Peninsula result from increased of pore water pressures that originate from high intensity rainfall following a prolonged wet period. These conditions saturate a layer of sensitive weathered volcanic ash, that, when overstressed is prone to failure (Shrimpton & Lipinski Ltd, 1998). Additional factors act in conjunction influencing the stability of the cliff including: subdivision that alters the groundwater system through the use of soakpits, drainage, waste water disposal and the long-term impact of marine erosion (Tonkin & Taylor, 1980, 1981; Shrimpton & Lipinski Ltd, 1998; Tonkin & Taylor, 2010; Taylor, 2014). Tonkin and Taylor (1980) states that the risk of further major failures along the western coast of the Omokoroa Peninsula is high. On May 11, 2011, the Bramley Drive failure of 1979 was reactivated where the upper 20 metres of the slope re-inundated the initial failure deposit (Tonkin & Taylor, 2011). A factor that has not been considered in consultancy reports is the available fetch and exposure to westerly winds. The long fetch west of the Omokoroa Peninsula leads to increased wave height affecting on the coastal margin, reducing the strength at the base of the cliff.

Tonkin and Taylor (1981) assessed the coastal cliffs along the eastern flank of the Omokoroa Peninsula. Past slope failures have been identified along a majority of the eastern margin, however these are much older than the landslides documented on the western side. Tonkin and Taylor (1981) concludes that the coastal cliffs, excluding a 100 metre section at the northern end of the peninsula, are relic and coastal erosion is no longer eroding the base of the cliffs. However, Garae (2015) identified cliff retreat between 1942 and 2011 on both the eastern and western side of the peninsula. Failures on the eastern margin have been stabilised by a number of retaining walls and dense vegetation, reducing the appearance of cliff erosion.

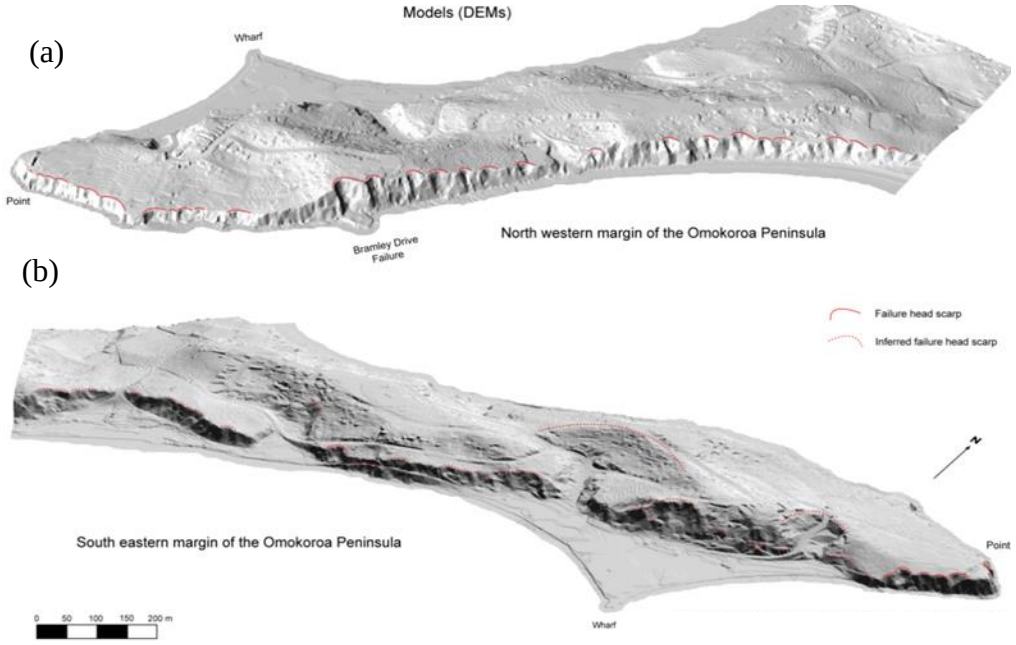

Figure 2.8: DEM processed from LIDAR showing identified failure head scarps (a) on the north west margin and (b) on the south eastern margin of the Omokoroa Peninsula (VE:1.4) (Keam, 2008).

2.3.3 Remedial measures

Numerous types of protection works have been implemented along the Omokoroa Peninsula in order to reduce erosional processes acting on the shoreline.

Hard engineering structures line the eastern margin of the peninsula, constructed between 1968 and 1985, covering approximately 650 metres. Concrete, grouted rock and timber seawalls protect The Esplanade, toilet block and Omokoroa Beach Domain. North of the boat ramp, the accretion of sediment has increased the beach

width by ~10 m in front of the seawall. South of the wharf, grouted seawalls were constructed which show signs of collapse and erosion of backfill. Additionally, the timber seawall lining The Esplanade is subject to overtopping and collapse requiring frequent repair. Further south, various materials have been used to protect private properties, including rock and concrete blocks and rubble. Concrete block groynes were constructed at Cooney Reserve to reduce littoral drift, creating a small pocket beach, however, this caused down drift erosion and the groynes have now been removed (OPUS, 2000).

Along the western side, private property owners have built structures made from timber posts and rails, stacked tree trunks, tyres, wire fences and stonework (grouted and ungrouted) with the purpose of reducing coastal erosion (Shrimpton & Lipinski Ltd, 1998; OPUS, 2000). Rock revetment structures were built between 2003 and 2010 subsequent to ongoing slope failures of the coastal escarpments, under the management of the Western Bay of Plenty District Council. The structures cover a total length of 300 metres in three sections along the north western margin of Omokoroa Peninsula (OPUS, 2009). Soft engineering solutions, such as planting vegetation have been applied along the north western margin in order to improve slope stability and reduce erosion.

In the past, the stormwater system has been a major cause of slope failure along Omokoroa Peninsula (OPUS, 2000). Stormwater and domestic waste water drainage and disposal systems have been improved and future updates are planned to reduce water entering the groundwater system to improve slope stability (Western Bay of Plenty District Council, 2014). Furthermore, a pipe network has been installed and stormwater ponds added to reduce overland flow (Western Bay of Plenty District Council, 2010a).

2.3.4 Impact of hard engineering structures on sedimentation

Hard engineering structures border a large proportion of Omokoroa Peninsula which can alter the sediment supply and therefore sediment transport regime. Shrimpton & Lipinski Ltd. (1998) describe the structures as reflective, causing scouring and/or overtopping resulting in continual regression and collapse of the

seawall. Studies carried out by Herbst et al., (2002) indicate that vertical structures have a lower bed level and, in higher wave energy regimes, the structures develop scour holes seaward of the wall as a result of reflected wave energy. In order to reduce adverse effects of the seawalls, construction of the more recent rock revetment will dissipate wave energy rather than create a reflective environment.

Herbst et al., (2002) identify that cliffs provide a source of sediment to littoral drift, therefore the protection of cliffs reduces the sediment supply and is a likely factor relating to the degradation of beaches. Assessments at Omokoroa indicate conflicting results in regards to the supply of sediment. OPUS (2000) identifies that cliff erosion is likely to be a source of sediment supply for the beaches and cliff bases around the peninsula and if protection structures are used to reduce erosion, it is likely that beaches will erode and will not be replenished by material derived from the surrounding cliffs. Furthermore, a sediment deflect effect will be created and adjacent unprotected shorelines may erode faster in order to meet the sediment demand. A conflicting report on the coastal processes states that the rock revetments constructed at the toe of landslides will have a minor effect on sediment transport. Furthermore, that the potential erosion of debris from the landslides will not enter the Tauranga Harbour sediment system (Abbiss, 2002).

2.3.5 Potential sources and erosion mechanisms

OPUS (2000) identifies that cliff erosion is likely to be a sediment source for the surrounding beaches. Briggs *et al.* (2006) recognise that in wet conditions, the Matua Subgroup is susceptible to marine cliff erosion and landslides. The intercalated sequence of Te Puna Ignimbrite, Matua Subgroup and Pahoia Tephras encountered at Omokoroa are prone to both shallow and deep landslide events (Briggs *et al.*, 1996). It is likely that the erosion and failure of these units are the primary contributors of sediment to the surrounding estuarine beaches. Tonkin and Taylor (1980) note that marine erosion over the last 60 years has not had much impact on the retreat of the cliffs and is not a major factor contributing to cliff failure. Although marine erosion is not considered to be a main cause for the initial failure, Shrimpton & Lipinski Ltd. (1998) documents active erosion along the peninsula. Marine erosion by wave action subsequent to failure affects the stability

through constant toe erosion of the debris which would typically provide a buttress, forming an oversteepened slope, vulnerable to further failure. Additionally, marine erosion acts on the run out debris and provides a large source of sediment. Herbst *et al.*, (2002) concludes that the combination of shoreline exposure and wave energy is the dominant control on erosion. Erosional processes of secondary importance include splash, earth-slip, rill and gully and earth-creep (Nautilis Contracting Ltd, 2011). Additionally, exposed cliff materials are subject to wetting and drying within the slash zone leading to accelerated erosion (OPUS, 2000). Green (2009) predicted that land use change will alter the sedimentation patterns. Fine sediment accumulation rates under the influence of land use change will reduce slightly, being driven by urbanisation, and the expected land use will change, which has a lower sediment runoff yield.

2.3.6 Boat ramp

A design report for the Omokoroa boat ramp identifies the potential effects on the coastal zone, recognising that the dominant sediment movement is west (south in terms of terminology discussed in this research) and that the boat ramp acts as a barrier to sediment movement, illustrated by the accumulation of sediment on the east (northern) side of the boat ramp. The report further states that the lower section of the boat ramp is below the existing bed level. As a consequent, the report identifies there is potential for sediment to accumulate, requiring regular maintenance which was accepted by the Council and local community at the time (Harrison Grierson Consultants Limited, 1997). Construction plans for the Omokoroa boat ramp are attached in Appendix 4.

2.4 Summary

Processes influencing estuarine sedimentation within the Tauranga Harbour have been reviewed. Estuarine evolution is governed by the long-term sediment supply and residual sediment transport pattern. Mechanisms affecting the development and evolution of estuaries are well understood however the complex interaction between processes depicts the local environment. While several studies have attempted to model the hydrodynamics and sediment transport within the Tauranga

Harbour, they are largely focused on the tidal inlet or the development of the Port of Tauranga. Studies of the wider Tauranga Harbour display no clear understanding of the sedimentation patterns observed at Omokoroa. Tidal action and wind generated waves have been identified as the primary factors influencing sediment transport in the Tauranga Harbour. The Omokoroa Peninsula is bound by coastal cliffs that have been identified as unstable and provide a sediment source. In recent history, more and larger landslides have occurred on the western margin compared to the eastern side, however the long-term pattern of erosion is uncertain. Other studies have suggested catchment runoff as a primary source of sediment.

Following the review of the relevant literature, it is apparent that there is little understanding of the processes occurring at Omokoroa. Identifying the sediment supply and assessing the processes and mechanisms influencing the residual sediment transport is therefore important in understanding the morphological development of Omokoroa Domain.

Chapter Three

METHODS

Multiple lines of evidence were interpreted in order to establish the evolution of the Omokoroa Domain. Evidence supporting this study involves data obtained from historic images, field observations, sediment samples and hydrodynamic tracer experiments, along with archived weather data. Results were analysed using a combination of laboratory techniques computed for data visualisation and analysis. The following chapter provides detailed information of the methods conducted and information examined for this study. Generally, each method follows existing standards or guidelines with any deviations detailed below.

3.1 Introduction

A multidisciplinary approach was adopted involving initial site investigations, studies of available sediments and analyses of hydrodynamics. The different methodologies used and their outcomes are listed below:

- Analysis of aerial photos enables recognition of shoreline changes over time.
- Field observations enable identification of present landforms and processes.
- Documentation of local geology based on cliff exposures and sediment cores retrieved from the intertidal flats.
- Particle size analysis and AMS dating of the cores demonstrates changes in sedimentation and age depth relationships, respectively, to calculate sediment accumulation rates.
- Varying sediment thicknesses on the boat ramp depict responses to storm events.
- X-ray Diffraction analysis (XRD) of cliff and surficial sediments quantifies the source of sediments and dominant geological unit contributing sediment accumulation.
- Sediment trend analysis (STA) establishes sediment transport pathways based on textural parameters that were calculated from particle size results

of surficial sediments at Omokoroa. STA was completed at Plummers Point (Huhurua Harbour Park) following field observations to correlate different stages of sedimentation of a similar depositional feature.

- Records of the hydrodynamics and archived weather data indicate the processes driving sediment transport.

Evidence obtained from this research identifies historic changes, hydrodynamic forcings on the available sediment and the present processes and environments, which together, reveal the evolution of the Omokoroa Domain.

3.2 Site Investigation

3.2.1 Field observations

A number of site visits were made over the study period in order to observe and document the present day features and processes. Observations included; geomorphology, geomorphic indicators, potential sediment sources, sediment behaviour, influence of the ferry and the impact of different weather patterns. Observations were recorded and photographed where appropriate.

3.2.2 Aerial photograph analysis

Historic photographs are a primary source of evidence that provide document into past events and changes over time. A series of aerial photographs of the Omokoroa Peninsula, dated 1943, 1982, 1996 and 2011, were utilised to identify shoreline changes and influences on sedimentation patterns. Two georectified and georeferenced aerial photographs from 1943 and 2011 were obtained from New Zealand Aerial Mapping. An additional two aerial photographs from 1982 and 1996 were scanned and georeferenced using ArcMap 10.2, a Geographic Information System (GIS) (Table 3-1). ArcMap was used to digitise and correlate the identified changes influencing the evolution of the Omokoroa Peninsula.

Table 3-1: Reference details of aerial photographs at Omokoroa, used to identify changes over time.

Date	Scale	Serial Number	Source	Application
2011	0.25 m	50932D	New Zealand Aerial Mapping*/Crown copyright©	Georeferenced and georectified digital image supplied.
21/03/1996	1:15,000		Air Maps	Image scanned and georeferenced using ArcMap 10.2.
22/07/1982	1:30,000	15190	Air Maps	Image scanned and georeferenced using ArcMap 10.2.
1943	1:16,000	229	New Zealand Aerial Mapping*/Crown copyright©	Georeferenced and georectified digital image supplied.

*company now liquidated

3.3 Sediment Analysis

Surficial sediments were collected to enable analysis of sediment textural parameters and determine sediment transport pathways. Sediment cores were obtained to determine thicknesses of accumulated deposits and/or erodible sediments. Ogeechee Sampler (see 3.3.1.3) and Vibrocores (see 3.3.1.4) respective measurements of intertidal flats and beach sediments were taken across six cross shore transects outlined in Figure 3.1.

3.3.1 Field methods

3.3.1.1 *Surficial sediments*

Surficial sediment samples were collected from the intertidal flats surrounding the Omokoroa Peninsula. Samples were initially collected between the 14th and 17th of November, 2013. Sample sites were selected based on changes in geomorphology along the coastline, presence of constructed protection works or infrastructure, potential sources (streams, cliffs and landslides), or observed changes in grain size.

Cross shore transects of samples were obtained, where appropriate, from potential sources, backshore sediments, and at high, middle and low tide. Further sampling was undertaken on December 11, 2014, to remove the bias of predetermined sediment sources and possible pathways by collecting samples between chosen sites to create a grid. Samples encompassed the upper 5-10 cm of the surface sediment.

Analysis of preliminary results prompted a further set of samples to be collected surrounding Omokoroa from 17-19 January, 2015, and Plummers Point on January 25, 2015. Samples of the upper 2-5 cm were collected at approximately 50 m spacing at high tide and 100 m spacing at mid/low tide. A total of 113 samples were collected from Omokoroa and 35 from Plummers Point (Figure 3.1).

3.3.1.2 *Cliff sediments*

Geological descriptions of exposed cliffs at four locations along the Omokoroa Peninsula were taken according to the standard methodology outlined by the New Zealand Geotechnical Society (2005). Sedimentary features, boundaries and contacts were also identified. Additionally, geological units described by Briggs *et al.* (1996) were identified.

Bulk sediment samples of exposed cliffs were obtained on 26 January 2015. Samples of approximately 0.5 kg were extracted at four locations along the Omokoroa Peninsula, covering the major geological units including Te Puna Ignimbrite, Matua Subgroup, Pahoia Tephras and Hamilton Ash (Figure 3.1).

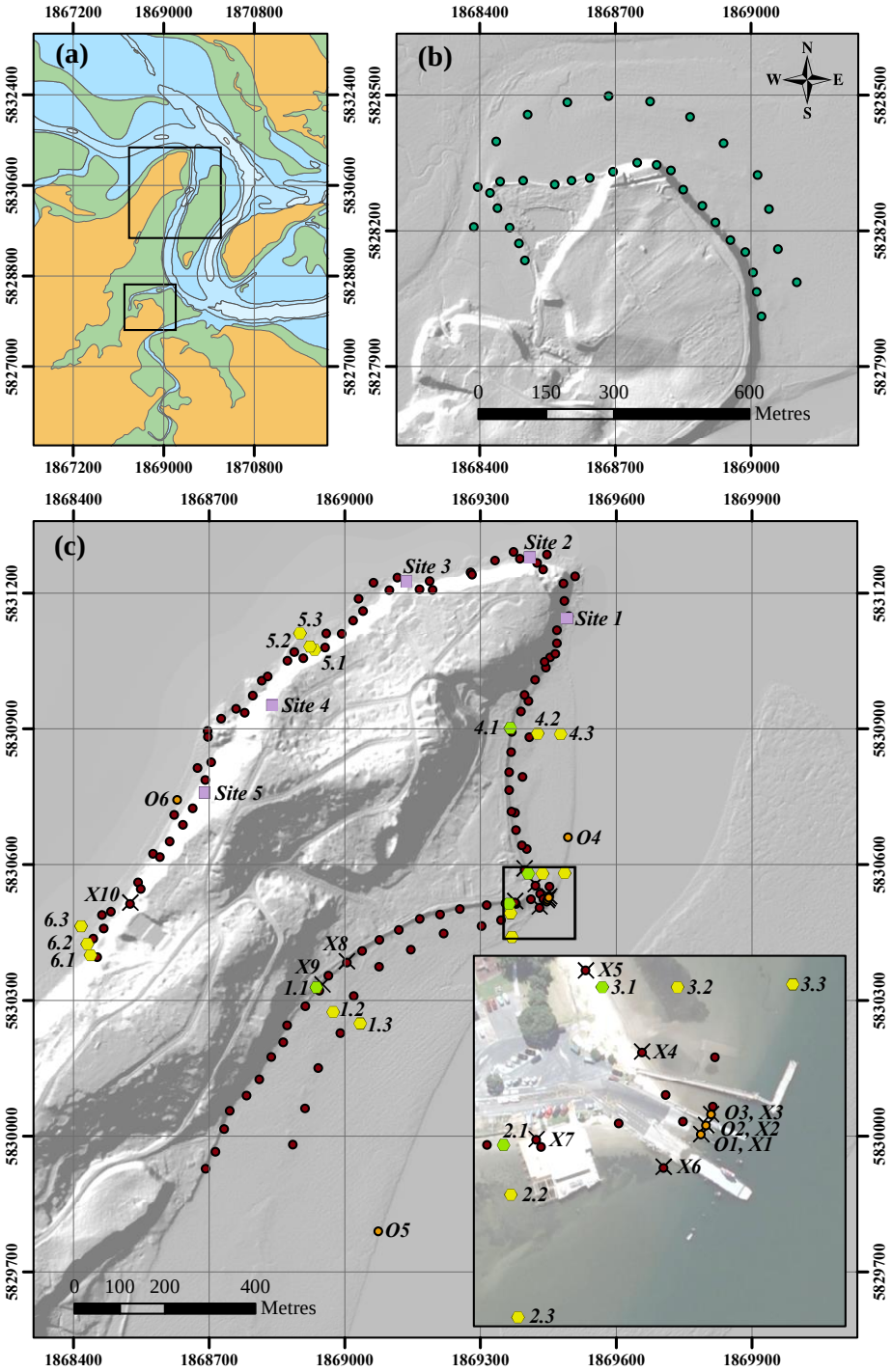

Figure 3.1: Location map (a) overview showing location extent. Sample locations for sediment analysis at (b) Plummers Point and (c) Omokoroa.

3.3.1.3 *Ogeechee Sampler*

The Ogeechee Sampler is a hand corer that was utilised to sample the intertidal flats. The corer consists of a core head with a manual valve, a stainless steel core body fitted with a plastic liner, and a core catcher secured by a driving tip (Figure 3.2a). The Ogeechee Sampler is driven into the sediment by repeated lifting and impacting of the weighted drive hammer, with an open valve (Figure 3.2b). The corer is retrieved by interchanging the drive hammer for the handle, and closing the valve, before pulling the core out from the sediment. Liners were removed from the core body, cut to the length of the sediment obtained and both ends were sealed by tape (Figure 3.2a). A total of 14 sites surrounding the Omokoroa Peninsula were cored between 24 and 28 November 2014. To prepare for laboratory analysis, lengthways incisions were made on either side of the plastic liners and the sediment was sliced in half.

Figure 3.2: Ogeechee Sampler (a) equipment and (b) field demonstration.

3.3.1.4 *Vibrocoring*

Beach sediments were retrieved by vibrocoring carried out on December 11, 2014 in which four cores were obtained. Corers were driven into sediment by a motor that transfers a high frequency, low amplitude vibration via a drive head clamped to the upper part of the aluminium core barrels (Figure 3.3a). A core cutter and sediment catcher were attached to the base of 2.5 m aluminium core barrels and driven to a maximum depth of 2 m, or until resistance prevented further penetration. Once the vibrocorer stopped progressing, the surrounding sediment was dug out to reduce the friction which enabled the corer to penetrate deeper. In addition, water was poured around the core allowing minor additional displacement of sediment grains by reducing friction, enabling further penetration into the substrate. The core was retrieved after these measures were applied, and no further penetration occurred. A block and tackle attached to a tripod was used to retrieve the core barrel (Figure 3.3b). The core barrels were cut to the length of the sediment retrieved and the ends were capped and taped. Core barrels were cut in half for laboratory analysis using the same technique used for the Ogeechee Sampler.

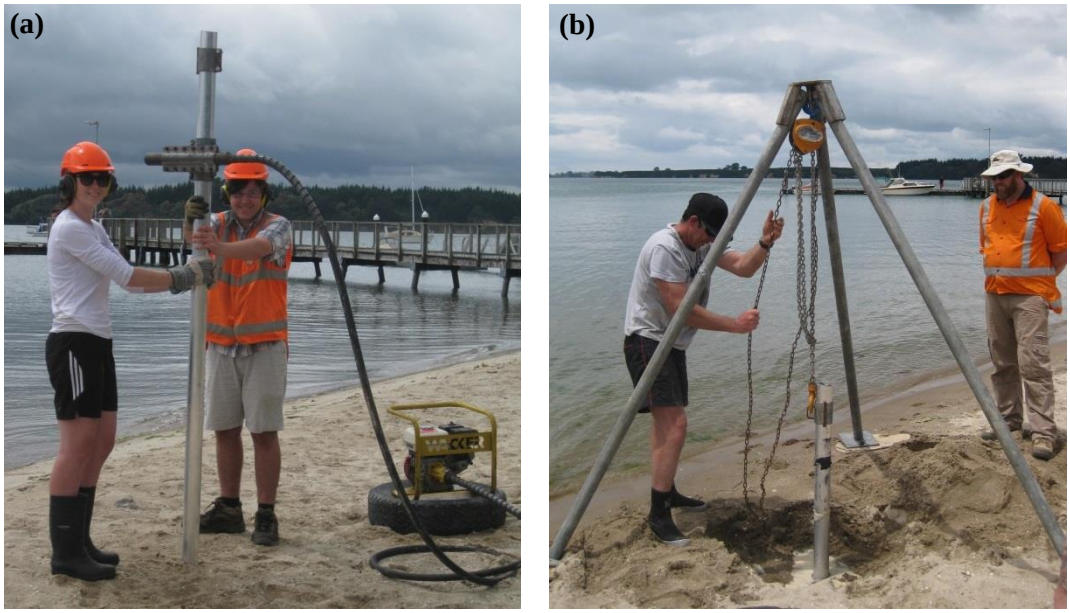

Figure 3.3: Vibrocoring (a) obtaining core driven by motor and (b) removal using block and tackle.

3.3.2 Laboratory Methods

3.3.2.1 *Loss on Ignition*

Organic matter content of six surficial sediment samples surrounding the Omokoroa Peninsula was determined by loss-on-ignition. Sample locations included four intertidal samples and two samples on the boat ramp (Figure 3.1). In this study, sub-samples of 2 – 4 g were used and the temperature setting of the muffle furnace for combustion was 550˚C and heated for 4 hours. Three sub-samples at each site were tested, the final recorded result being an average of these. Methods to determine loss-on-ignition followed standard operating procedures outlined by Wang *et al*. (2011).

3.3.2.2 *Sediment descriptions*

The cores were photographed and the sediments were described in accordance with standard methodology outlined by the New Zealand Geotechnical Society (2005). Characteristics considered to establish sediment descriptions included soil group, minor components, grading, particle shape, strength, other material, colour, plasticity, presence of coarse material, strength, weathering and sensitivity. Sedimentary features, boundaries and contacts were also identified. Refer to Appendix 1 for core logs.

3.3.2.3 *Accelerator Mass Spectrometry Dating*

Age estimates using Accelerator Mass Spectrometry (AMS) radiocarbon dating were performed on four samples from the cores retrieved along the eastern shoreline of the Omokoroa Peninsula, the depositional analyses of which enable the calculation of sedimentation rates. The four samples were taken from different depths in the cores of which two samples were shell and two were soil organic samples.

AMS combustion and graphitisation sample preparation was undertaken at the University of Waikato Radiocarbon Dating Laboratory. Pre-treatment of the humin fraction involved removing visible contaminants followed by repeated acid-base-acid wash using HCl (acid) and NaOH (base). Between washes the insoluble fraction was filtered, rinsed and dried. Physical pre-treatment of shells required

cleaning the surfaces, washing in an ultrasonic bath and testing for recrystallisation of aragonite, followed by a chemical pre-treatment of 0.1N HCl acid wash, shells were then rinsed and dried. The CO_2 purification process of the humin fraction is achieved through the conversion by oxidation at 800^oC using CuO and purified in the presence of silver wire. For shell samples, CO_2 is extracted by reaction with phosphoric acid (H_3PO_4). Purified CO_2 is reduced to graphite using H_2 and an iron catalyst heated to 550^oC. The prepared sample of pressed graphite was analysed at the Keck Radiocarbon Dating Laboratory at the University of California, and at the Center for Applied Isotope Studies, University of Georgia. Results were calibrated based on OxCal v.4.2.4 (Bronk Ramsey, 2001) and presented as a calibrated radiocarbon age (C^{14} yr BP).

3.3.2.4 *Particle size*

The particle size of the surficial sediments, cliff sediments and sediments obtained from cores were analysed using a Malvern Particle Laser Sizer (Mastersizer 2000) at the University of Waikato.

Depth integrated subsamples were taken from the analysed surficial sediment samples (see section 3.3.1.1.). Sediment samples from cores were taken at 10 cm intervals along the length of the core with smaller intervals sampled to include all units. Sampling started at 5 cm from the top of the core, representative of surficial sediment. Samples <1 g were passed through a 2 mm sieve and analysed using the Malvern Particle Laser Sizer (Mastersizer 2000).

Surficial sediments indicated low levels of organic material that, being volume weighted, would not significantly alter particle size results. However, samples collected from the boat ramp contained increased organic material, hence organic material was removed. Pre-treatment preparation of samples involved hydrogen peroxide soaking (10% H_2O_2) to remove organic material, which was added twice daily until no reaction occurred. This was followed by chemical deflocculation using sodium hexametaphosphate (10% Calgon) over heat to separate fine particles and remove remaining residual carbonaceous material (Konert & Vandenberghe, 1997).

Mean grain size was classified according to the Udden-Wentworth size scale (Udden, 1914; Wentworth, 1922). The reported sediment textural parameters, including mean grain size, sorting, skewness and kurtosis, were calculated from the laser sizer results, see Appendix 2.2 for raw data, using the graphical method of Folk and Ward (1957), and classified based on Folk (1968).

3.3.2.5 *X-Ray Diffraction*

X-Ray Diffraction (XRD) was used to determine the mineralogical assemblages of the major geological units obtained from cliff samples (Te Puna Ignimbrite, Matua Subgroup, Pahoia Tephras and Hamilton Ash) and surficial sediments retrieved from the boat ramp, beach and intertidal flats (Figure 3.1).

Sample preparation involved oven drying sediments to remove moisture. A subsample of approximately 15 g was milled down to a fine powder using the ring mill. A further subsample of 2 - 3 g was packed into a sample holder. The PANalytical Empyrean X-ray diffractometer was used to identify crystalline compounds present in the bulk samples between a scanning range of 2˚ and 80˚ 2-theta. XRD is based on the principle that each mineral has a unique pattern of diffraction directions that returns peaks of which crystalline substances are distinguished. Identification of minerals is achieved by correlating observed patterns obtained from the unknown sample to known patterns of crystalline substances (Whitton & Churchman, 1987). Results were analysed using Highscore software and records can be found in Appendix 2.3.

3.3.3 Sediment thickness

Sediment accumulation thickness on the boat ramp were measured before and after extra-tropical storm Pam (ETS Pam). Three transects were measured along the length of the boat ramp: one 50 cm from the north side, another 30 cm from the southern edge and a third along the centre. A measuring tape with sinkers was placed on the ramp to mark the transect. A ruler was vertically pushed into the sediment, recording the thickness at 20 cm increments. Sediment thickness was also measured relative to the lip that boarders the lower section of the boat ramp.

Locations include: on top of the lip, the outer edge of the lip and at the base of the boat ramp.

3.3.4 Sediment trend analysis

Analysis of spatial changes in grain size parameters (including mean size, sorting, skewness and kurtosis) is one method that enables inference of sediment transport pathways.

GiSedTrend is a QGIS application applied to compute vector fields based on the sediment textural parameters calculated from particle size results of surficial sediments surrounding the Omokoroa Peninsula and Huhurua Harbour Park. GiSedTrend enables a two-dimensional Grain Size Trend Analysis (GSTA) to be performed to deriving residual sediment transport patterns. Vector computation for GiSedTrend uses a buffer defined by a characteristic distance, a parameter of samples considered neighbouring. Samples located within the buffer are statistically compared based on defined trend(s). The weighting of the vector components for the surrounding samples is inversely proportional to the distance from the centre station. Obstacles such as land boundaries and engineering structures can be included. During vector computation if obstacles intersect a virtual line between points within the buffer the station is excluded. An XOR (exclusive or) function can be used to identify a single trend, alternatively a vectorial sum of the specified trends will be considered for the final vector. For further details regarding vector computation refer to Poizot and Méar (2010).

A number of different models were computed specifying different textural trend(s), characteristic distance and environmental boundaries. The results indicate sediment textural trends, and are used to infer sediment transport pathways surrounding the Omokoroa Peninsula and at Huhurua Harbour Park.

3.4 Hydrodynamics

Tracer experiments were conducted to enable a hydrodynamic analysis and include wave and current measurements surrounding the Omokoroa Peninsula over a complete spring-neap cycle (Figure 3.4). Instrument deployment involved *in situ* measurements of tides, storm surges, waves and currents which were analysed to assess potential sediment transport via available wave energy, storm surge and dominance of tidal and wind driven currents.

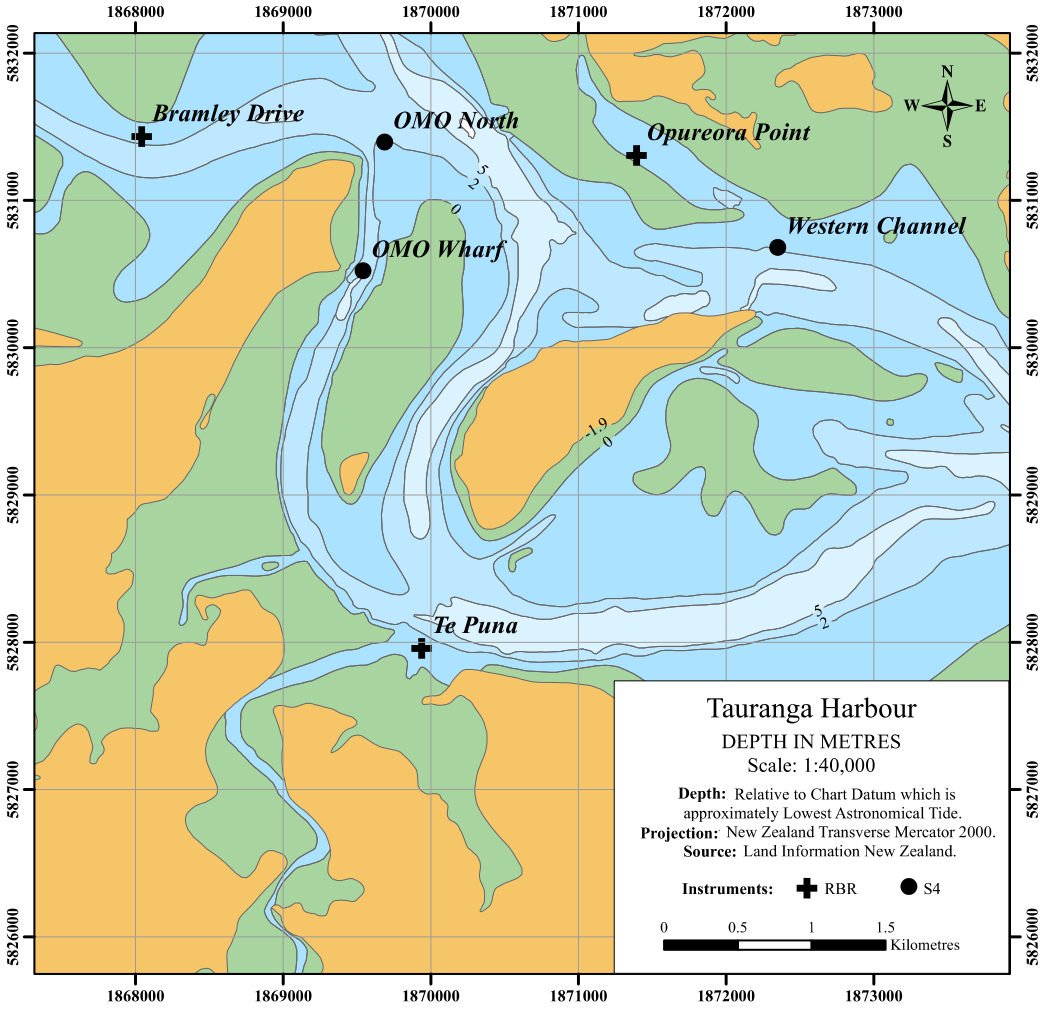

Figure 3.4: Location map of S4 and RBR instruments.

3.4.1 RBR Tide Gauge

The RBR tide gauge records tide and wave measurements by averaging pressure data (RBR Ltd, 2007). Three RBR tide gauges were deployed between 19 February and 19 March 2014 (Figure 3.4). The RBRs were attached to channel markers surrounding the Omokoroa Peninsula in approximately 3 – 6 m water depth at high tide. RBRs located at Te Puna and Opureora Point were programmed to record water level continuously and post processed to 10 minute bursts. The RBR positioned at Bramley Drive recorded bursts of 4 minutes and 20 seconds every 20 minutes (Table 3-2). Measurements recorded by the RBRs were processed using Ruskin software. Results were passed through a low pass wavelet filter (W.de Lange, pers. comm, 2014) and a MATLAB application, T_TIDE, was computed, which performs a tidal harmonic analysis (Pawlowicz *et al.*, 2010).

3.4.2 InterOcean S4 Current Meter

The InterOcean S4 current meter measured the voltage of water flow velocity as a result of the motion of a conductor through a magnetic field and was recorded according to Faraday's law of electromagnetic induction (InterOcean Systems, 1994). Three InterOcean S4 current meters were deployed in the channels surrounding the Omokoroa Peninsula in approximately 4 – 6 m water depth at high tide (Figure 3.4). The deployment period was between 19 February and 12 March 2014. The S4s were mounted on a steel frame located one metre above the seabed and anchored to the seafloor. The S4s were programmed to collect averages of north and east currents every 15 minutes (Table 3-2). The recorded burst measurements were processed using APPIBM and WAVE for Windows software. The S4s were located too deep to measure the small waves present at Omokoroa and no data were recorded at this location.

Table 3-2: Hydrodynamic instrument settings.

File ID	Instrument	Measurements recorded	Settings				Logging Time		Location (NZTM)	
			Sample Rate	Burst Duration	Burst Time	Burst Count	Deployed	Retrieved	Easting	Northing
Bramley Drive	TWR-2050 logger	Pressure Temperature	4 Hz	00:04:27	00:20:00	1024	19/02/2014 11:55	19/03/2014 13:15	5831432	1868041
Te Puna	RBRSolo D*	Pressure Temperature	2 Hz	00:10:00	00:10:00	1200	19/02/2014 12:30	19/03/2014 12:45	5827958	1869937
Opureora Point	RBRSolo D*	Pressure Temperature	2 Hz	00:10:00	00:10:00	1200	19/02/2014 12:05	19/03/2014 12:20	5831304	1871392
OMO North	S4AWD	Flow velocity (U,V) Pressure Temperature	2 Hz	00:00:05	00:15:00	600	19/02/2014 11:45	12/03/2014 12:00	5831398	1869687
OMO Wharf	S4AWD	Flow velocity (U,V) Pressure Temperature	2 Hz	00:00:05	00:15:00	600	19/02/2014 11:20	12/03/2014 11:45	5830523	1869541
Western Channel	S4AWD	Flow velocity (U,V) Pressure Temperature	2 Hz	00:00:05	00:15:00	600	19/02/2014 12:20	12/03/2014 12:30	5830681	1872350

*Continuous recording, post processed into 10 minute bursts

Chapter Four

SITE INVESTIGATION

The following chapter is an initial investigation into the evolution of the Omokoroa Peninsula. The chapter includes two sections: (1) analysis of a series of historic aerial images and photographic evidence that identifies changes over time and (2) site observations identifying sediment sources and processes, as well as the present geomorphology.

4.1 Historic Photographs

4.1.1 Georeferenced aerial photographs

The series of aerial photographs in Figure 4.1 illustrates the changes to the Omokoroa Peninsula between 1943 and 2011. Significant development along the Peninsula occurred between 1943 and 1982, continuing until 2011. From the 1982 photograph, the extent of the runout from the Bramley Drive failure in 1979 is evident. The runout debris, initially ~160 m, reduced significantly by 2011 as the debris was subjected to marine erosion.

4.1.1.1 Shoreline changes

Figure 4.2 illustrates the shoreline changes adjacent to the boat ramp, also highlighted in Figure 4.3. The shape of the shoreline at Omokoroa Domain changed significantly between 1943 and 1982 due to land reclamation at the domain. Between 1943 and 1982, the jetty was relocated and the ferry terminal was constructed. A seawall was built south of the ferry terminal and significant land reclamations occurred at the domain. By 1996, accumulation of sediment north and depletion of sediment south of the ferry terminal was evident, indicating net sediment transport south. This sediment accumulation suggests the ferry terminal is acting as a groin, trapping sediment towards the north and depleting sediment south of the ferry terminal. Construction of the public boat ramp north of the ferry terminal was completed in 2011. The boat ramp is currently located in the sediment transport pathway within the zone of sediment accumulation caused by the ferry

terminal. Sediment accumulation north of the ferry terminal and boat ramp, now acting as a groin, continued through until 2011.

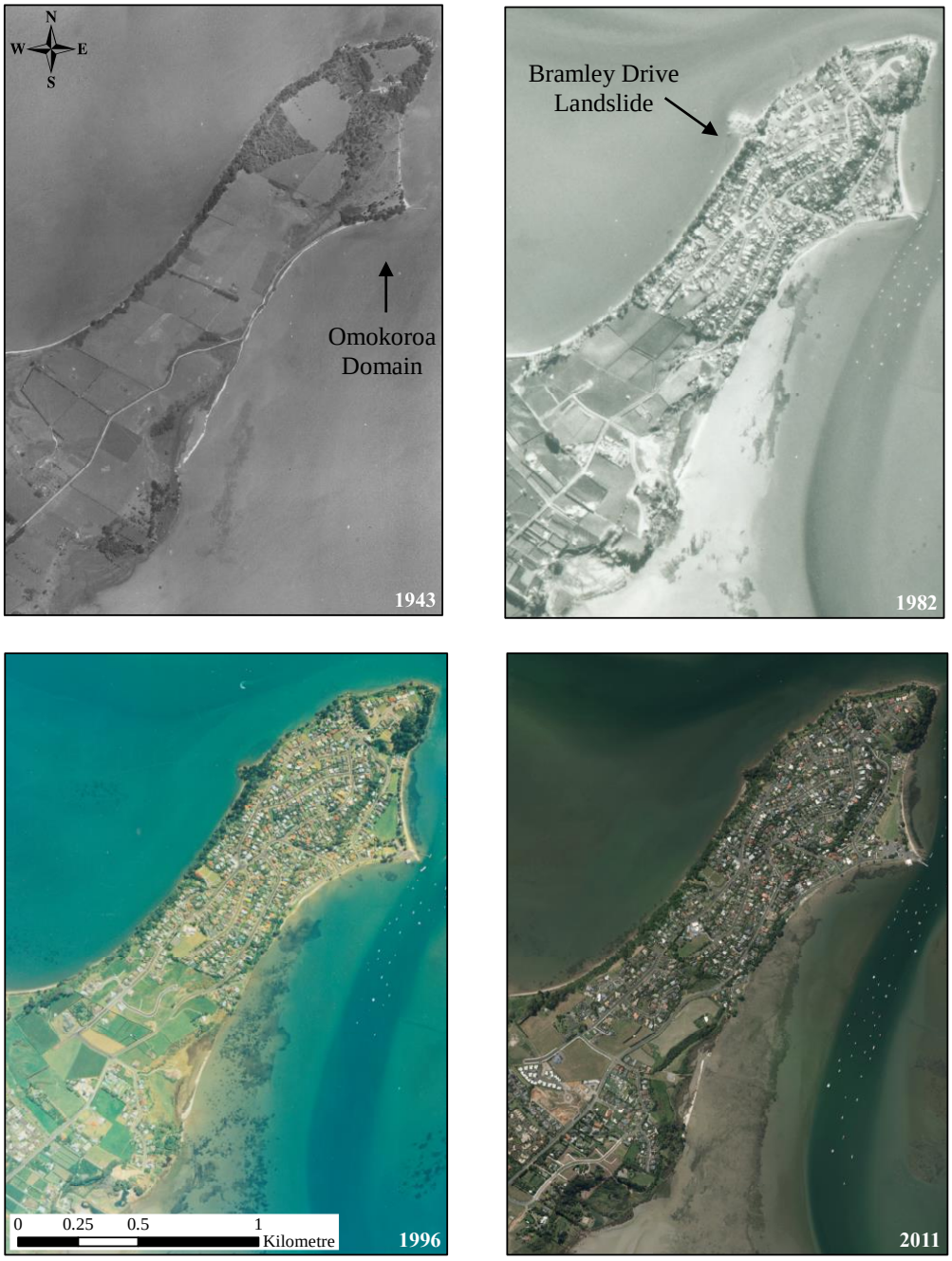

Figure 4.1: Aerial photographs of the Omokoroa Peninsula taken from 1943, 1982, 1996 and 2011.

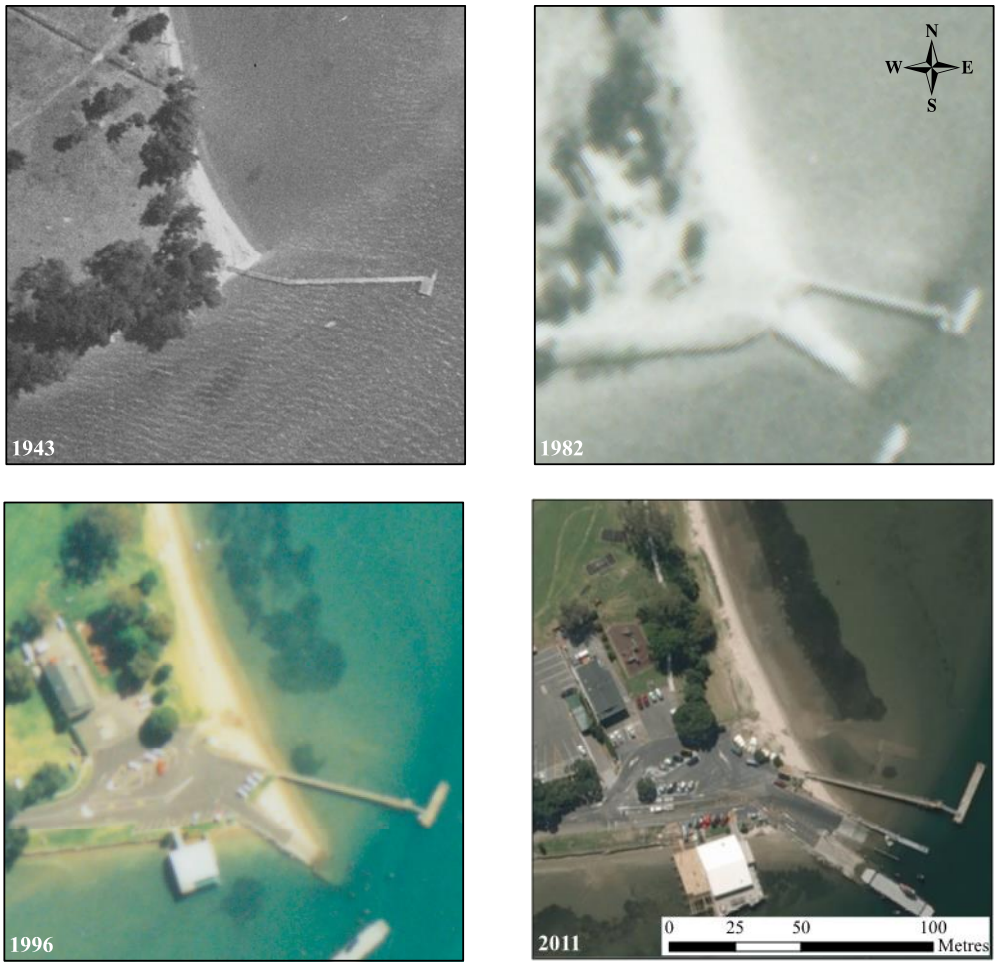

Figure 4.2: Aerial photographs of the current boat ramp area from 1943, 1982, 1996 and 2011.

4.1.1.2 Geomorphic indicators

Inferred directions of sediment transport were based on geomorphic indicators surrounding the Omokoroa Peninsula and are illustrated in Figure 4.4. A recurved spit is evident at Te Puna suggesting sediment transport occurred towards the east. At Cooney Reserve the formation of a spit, while breached in its northern end, indicates northward sediment transport. The sandbank east of Omokoroa shoals north-west, indicating minor sediment accumulation that occurs on the intertidal flats. Spit growth at the golf course on the western side of the peninsula suggests sediment transport towards the east.

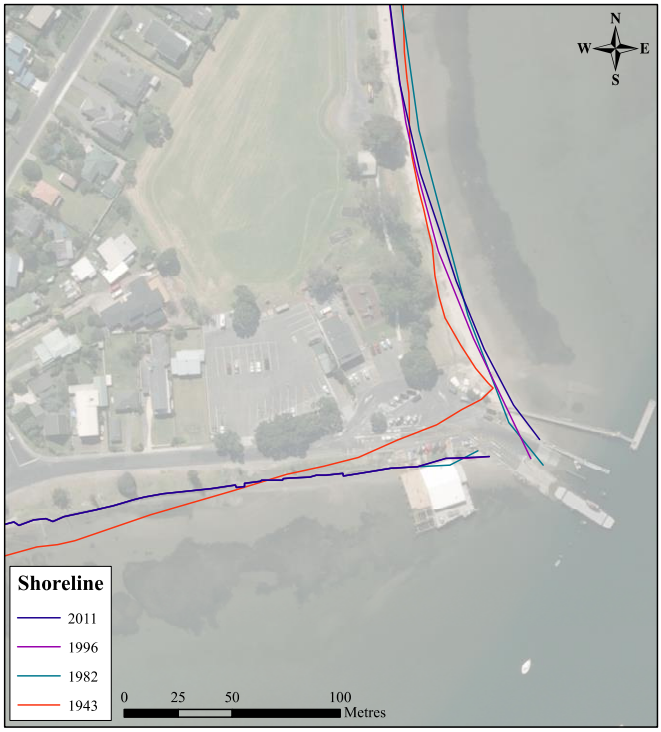

Figure 4.3: Omokoroa Peninsula shoreline changes based on aerial photographs between 1943 and 2011.

Figure 4.4: Inferred sediment transport pathways (white arrows) based on geomorphic indicators.

4.1.1.3 Seagrass cover

Seagrass extent surrounding Omokoroa Peninsula was mapped based on aerial photographs. Figure 4.5 indicates that seagrass cover increased markedly between 1982 and 2011, having a significant growth period between 1996 and 2011. The sandbank east of Omokoroa was the largest area of increased seagrass growth, occurring between 1996 and 2011. Areas north and south of the Omokoroa Domain had minimal seagrass in 1982. By 1996, coverage had markedly increased, particularly on the northern side of the Omokoroa Domain. Seagrass cover then increased predominately south of Omokoroa Domain by 2011.

Park (1999) reported decreased in seagrass cover between 1959 and 1996 within the Tauranga Harbour, suggesting sedimentation and eutrophication had a major impact on the pattern of distribution of seagrass within the harbour. Decline in water quality was generated by anthropogenic activities, other human impacts also reducing seagrass growth via reduced light penetration.

Prior to 1982, considerable loss of seagrass was likely, being driven by intense development that occurred between 1943 and 1980 (Tonkin & Taylor, 1980). The increase in seagrass reported in this study reflects improved environmental practices including reduced runoff (associated nutrients and suspended sediment from the surrounding catchment) and removal of point nutrient sources (Park, 1999). The significant increase in seagrass since 1982 suggests that stabilisation of bottom sediments prevented erosion of the intertidal flats and thus reduced sediment transport.

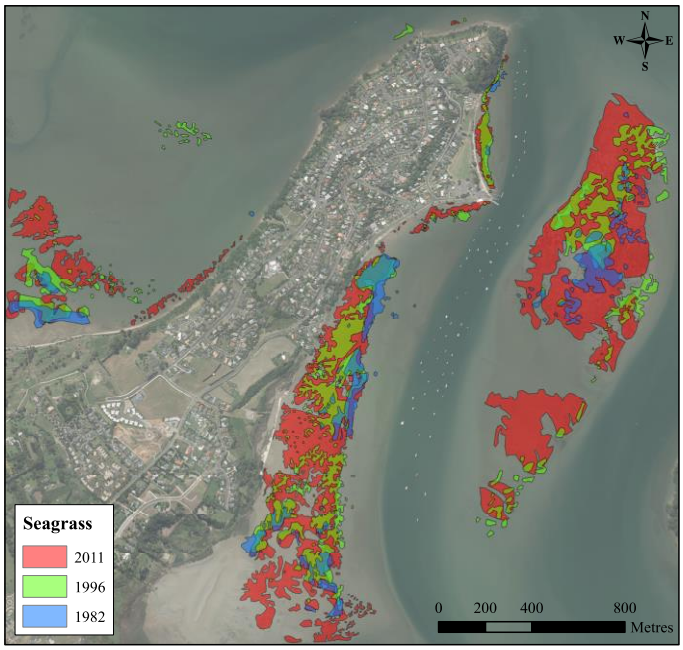

Figure 4.5: Variation in the distribution of seagrass based on aerial photographs taken between 1982 and 2011.

4.1.2 Historic photographic evidence

Historic photographic evidence at Omokoroa dates back to 1919 showing evidence and the location of the original jetty. A subsequent photograph from the 1950s illustrates the domain was previously subjected to tidal influences suggesting an estuarine lagoon environment (Figure 4.6a). It is unclear from the photograph as to what end of the domain was breached. It is also likely based on that the area was subject to tidal flooding via groundwater. There is no obvious evidence of a lagoon entrance in the images presented in Figure 4.7, taken in 1954, as the shoreline appears continuous, however a small ditch is located at the northern end of the Omokoroa Domain that looks as if it once discharged into the harbour. The straight nature of the ditch suggests it was manmade in order to assist drainage, indicating the area has been subject to significant human modification. Form examination of a late 1960s image (Figure 4.6b) there is evidence of a sandy beach preceding construction of the boat ramp/ferry terminal and seawall.

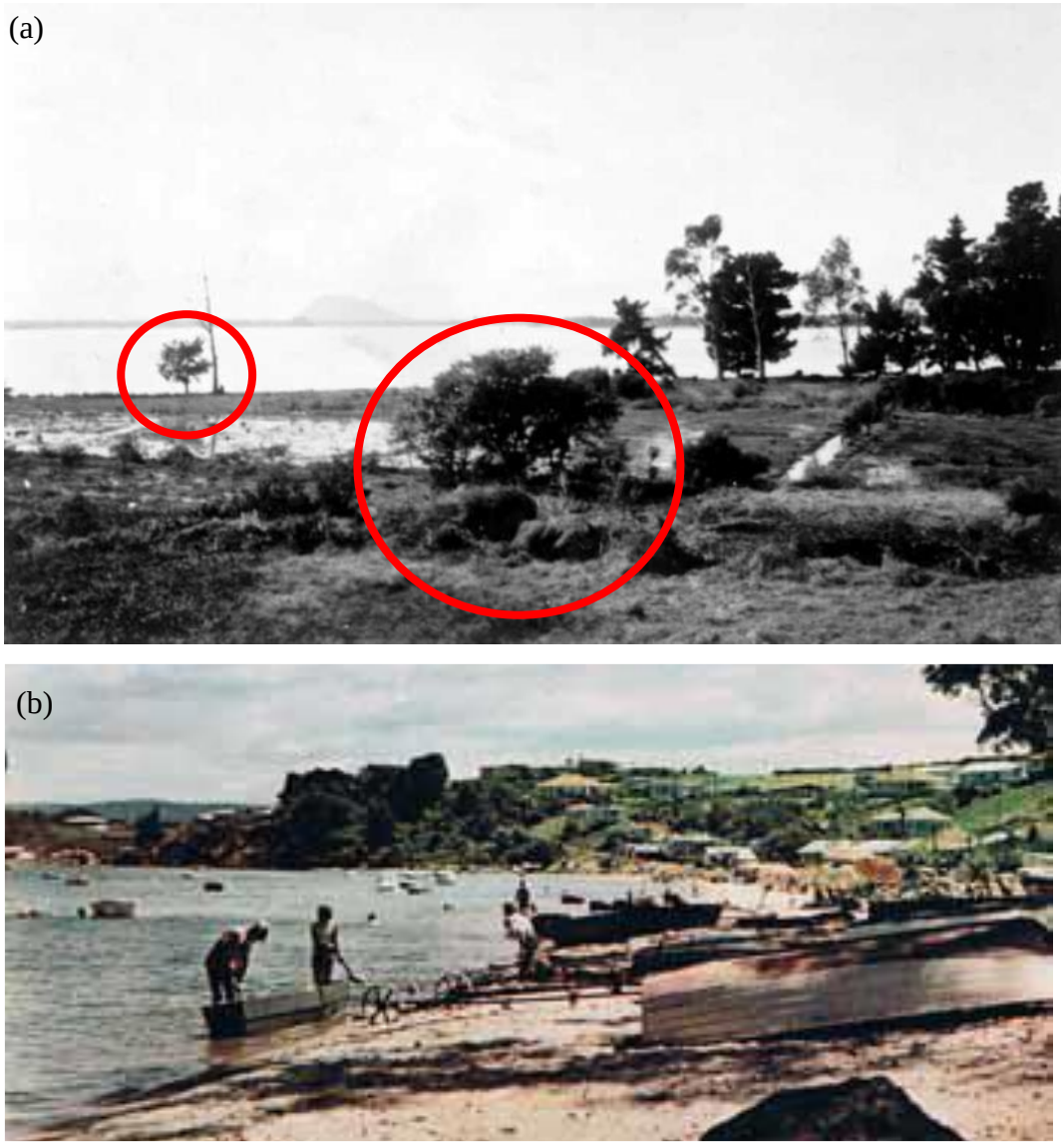

Figure 4.6: (a) Photograph of the domain in the 1950s, illustrating evidence of tidal influence. Shrubs (circled) correlate to those identified in Figure 4.7, indicating the location of tidal influence on the northern section. (b) The Esplanade, south of the current boat ramp and ferry terminal in the late 1960s (Neil, 2012).

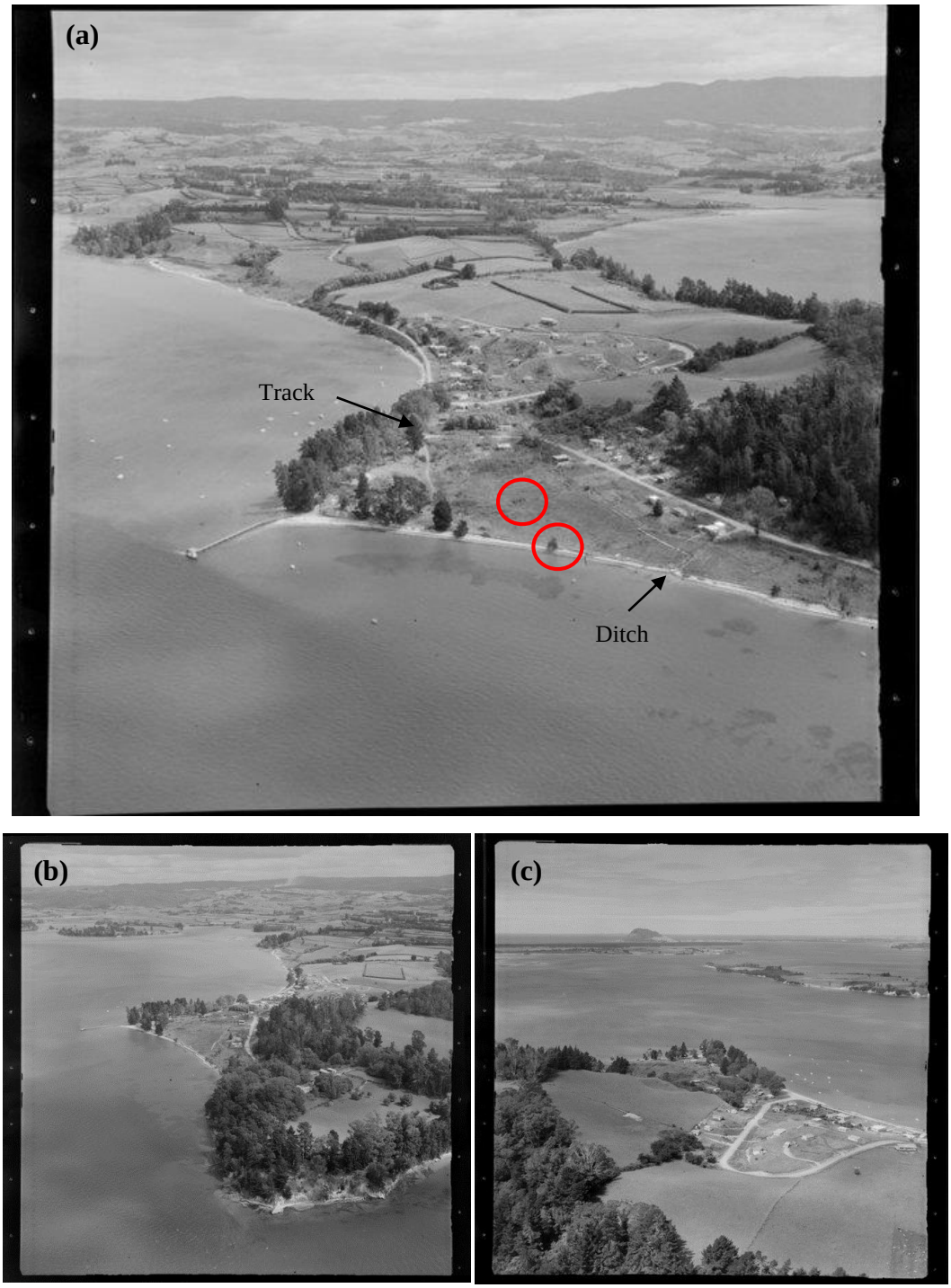

Figure 4.7: Photographs of the Omokoroa Peninsula in 1954: (a) facing south west at the Omokoroa Domain (Whites Aviation Ltd :Photographs, 1954b), (b) facing south at the point (Whites Aviation Ltd :Photographs, 1954a) and (c) facing east north-east over the Omokoroa Domain (Whites Aviation Ltd :Photographs, 1954c). Circled shrubs in (a) correlate to those identified in Figure 4.6.

4.1.3 Geomorphic indicators

Google Earth archives of Omokoroa Peninsula aerial and satellite imagery between 2002 and 2015 were studied in order to identify sediment movement based on geomorphic indicators. Two sites in particular indicated variations in the direction of sediment transport.

4.1.3.1 Stormwater drains

A series of stormwater drains are located on The Esplanade (south of the ferry terminal) and protrude onto the intertidal flats acting as groins and impounding sediment. The stormwater drains provide an indication of sediment transport by trapping sediment on the updrift side and causing downdrift erosion.

Records indicate sediment transport occurred north in 2002 and 2007 and is noticeable in Google Earth images (Figure 4.8a). By 2011 there is no significant indication of net sediment transport based on sediment impoundment from the stormwater drains. Evidence from August 2012 shows minor sediment impoundment on the northern side, suggesting a change in net sediment transport to the south along The Esplanade. However, in December of 2012 sediment impoundment suggests northward sediment transport. In 2013, sediment transport is south. Based on aerial images sediment transport is negligible by 2014. At present (January 2015), the direction of sediment transport is south (Figure 4.8b).

The boat ramp and ferry terminal acts as a large groin, indicating the dominant sediment transport south past the structure. The variation in sediment transport direction suggests that accumulation of sediment south of the boat ramp is not from bypassing but from occasional sediment transport north.

Figure 4.8: Sediment impoundment by storm water drains (a) 2007 indicating northeast sediment transport (Google Earth) and (b) indicates southward sediment transport in January 2015 (black arrows indicate direction of sediment transport. Red circle in (a) marks storm water drain featured in (b)).

4.1.3.2 Cooney Reserve

A spit enclosing a tidal lagoon is located at Cooney Reserve, Omokoroa, indicating the net sediment transport direction is north, as the spit grows and the stream migrates in the direction of sediment transport. However, photographic evidence between 2002 and 2015 indicates significant variation in the migration of the spit.

Images between 2002 and 2007 indicate accretion of the spit representative of northward sediment transport (Figure 4.9a). From 2007 until 2010, evidence of erosion suggests sediment transport occurred towards the south. Minor accretion

occurred in 2011, followed by erosion in 2012 and the formation of a small recurved spit on the northern side of the inlet, indicating sediment transport south. Between September and December of 2012 there is a period of accretion driven by sediment transport north. Significant erosion is evident at the beginning of 2013, yet, accretion is observed from July 2013 until January 2014. Continued erosion and growth of the recurved spit (north of the inlet) is evident from 2014, suggesting sediment transport south at present (Figure 4.9b).

Figure 4.9: Cooney Reserve spit showing (a) accretion in 2012, driven by northward sediment transport and (b) 2015 image showing erosion of the spit and growth of the recurved spit, north of the inlet, when dominant sediment transport is south (Google Earth).

Impoundment of sediment by stormwater drains and erosion, migration and accretion of the spit suggest that the sediment transport patterns on the eastern side of the Omokoroa Peninsula vary over different time scales and are thus poor indicators of long-term sediment transport.

4.2 Field Observations

4.2.1 Geomorphology

The geomorphology of the northern Omokoroa Peninsula is illustrated in Figure 4.10. Margins of the north east trending peninsula are lined by steep cliffs. Exposed coastal cliffs line the western and northern margins of the peninsula. A number of recent landslides have occurred on the western side of Omokoroa Peninsula, of which debris from the Bramley Drive and Ruamoana landslides remain inundating the coastal platform. On the eastern side of the peninsula, a low lying triangle formation (Omokoroa Domain) is located at the base of steep cliffs and borders the shoreline. Topographic evidence of the northern sector of the Omokoroa Domain shows a circular depression with two troughs leading to the shore. This evidence correlates to that identified in the historic photographs, supporting the presence of a lagoon. On the eastern side of Omokoroa Peninsula two large-scale relic landslides were identified. The circular nature of the head scarps suggests rotational failures. The northern most landslide is likely comparable to the Bramley Drive landslide. A number of retaining walls have been built to help stabilise the slope which is reflected by the stepped slope profile (Figure 4.11d). The southern, sizeable landslide shows evidence of a slumped block and may have occurred as multiple regressive failures. Figure 4.11c illustrates the slumped block with a steep cliff at the base. The valley down the centre of the landslide indicates an erosion pathway discharging to the shore. Figure 4.11b shows the shallow slope down the middle of the landslide where a road has been built. The failed block and erosion at the base of the head scarp are evident in Figure 4.11a. Significant erosion and human modification has altered the modern land surface.

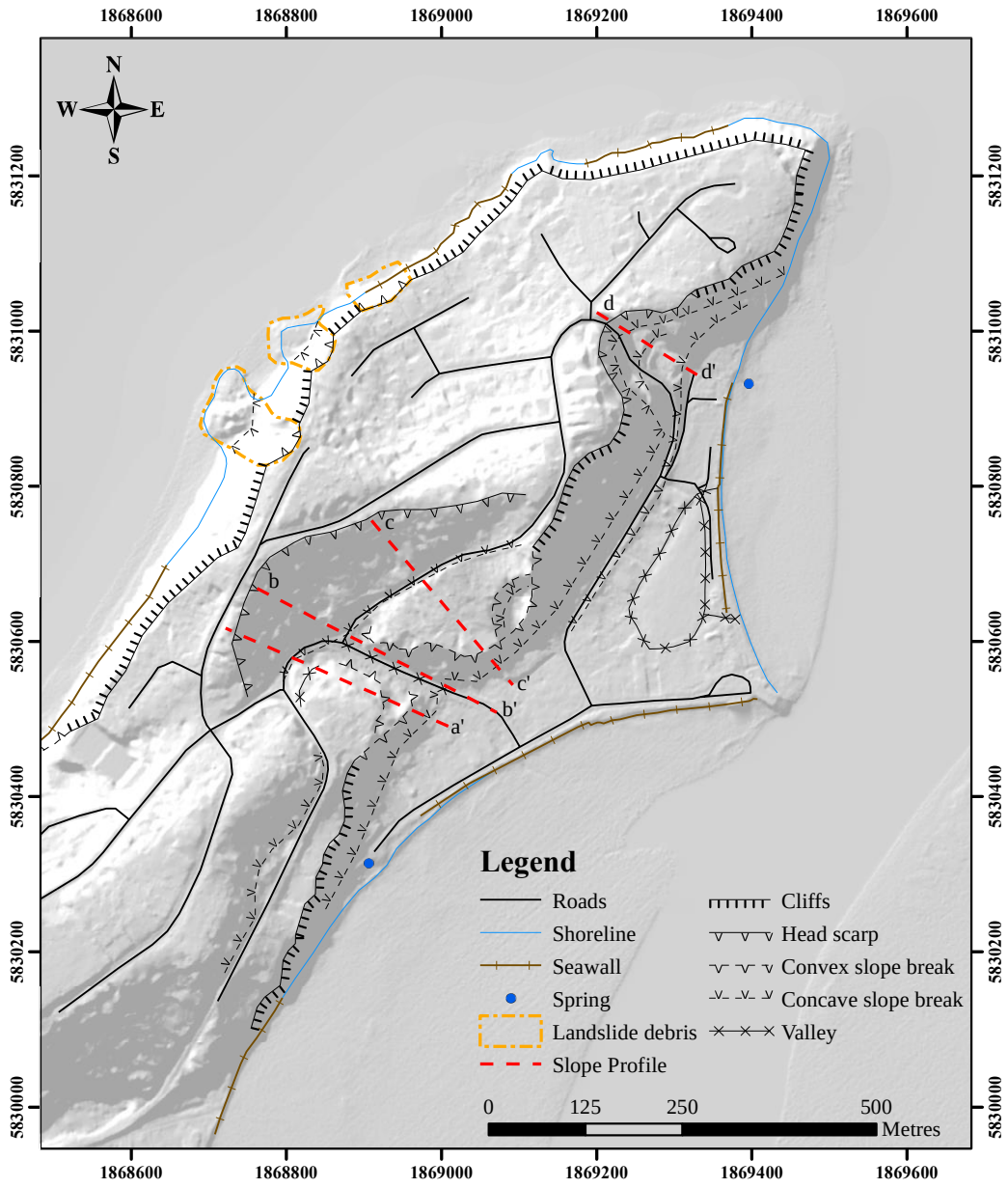

Figure 4.10: Geomorphic Map of the northern Omokoroa Peninsula. Slope profiles of the cross sections are illustrated in Figure 4.11.

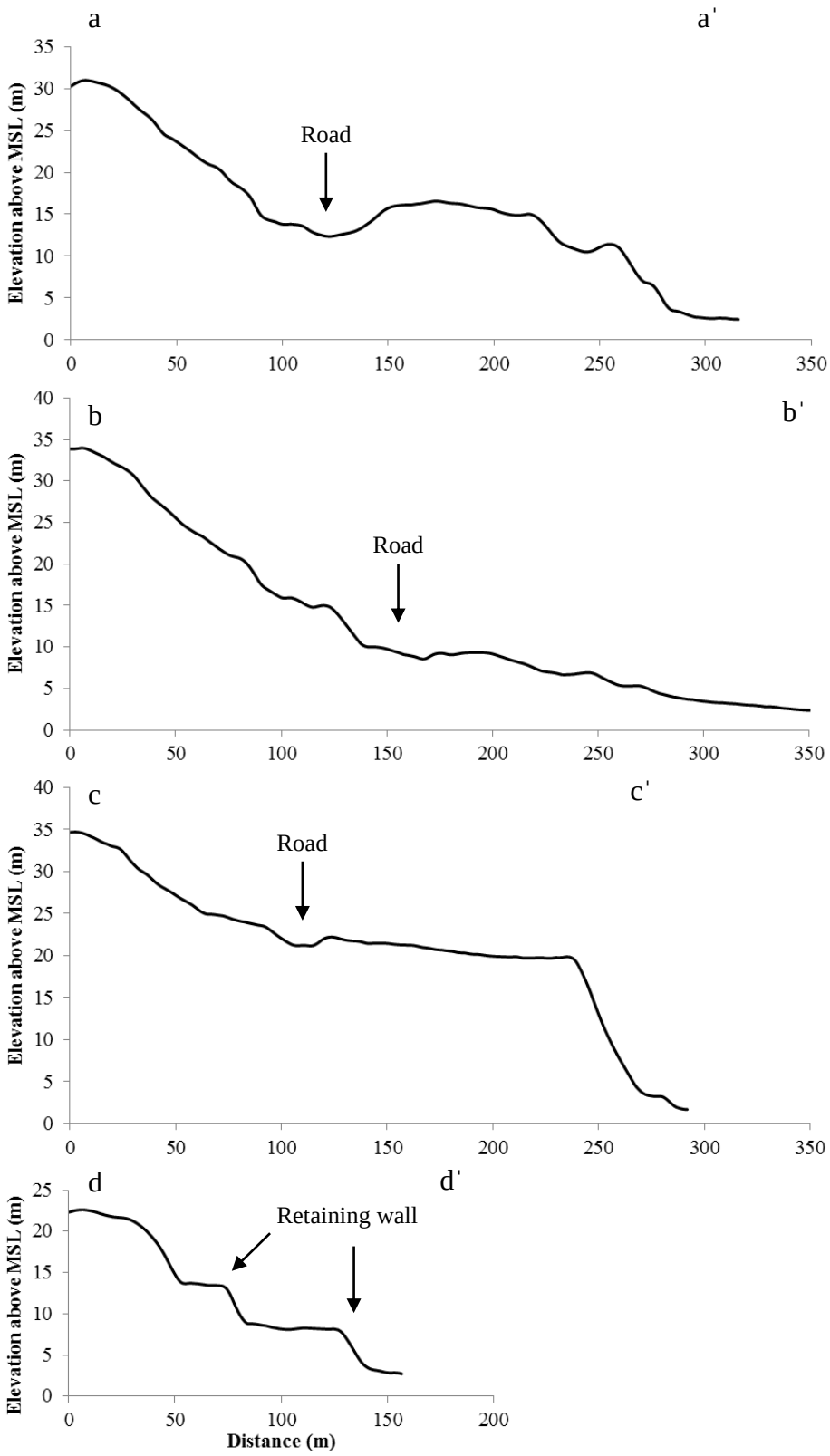

Figure 4.11: Slope profiles of inferred landslides. Profiles correlate to cross sections indicated in Figure 4.10. VE=1.5.

A number of seawalls, identified in Chapter 2, were constructed along the coastal margin to reduce erosion (Figure 4.12). The scour and maintenance required for the seawalls south of the boat ramp indicates an eroding environment, or one with sediment deflect. The resulting effect is that the material is retained north of the boat ramp and unable to supply material downdrift, leading to scouring and collapsing seawalls.

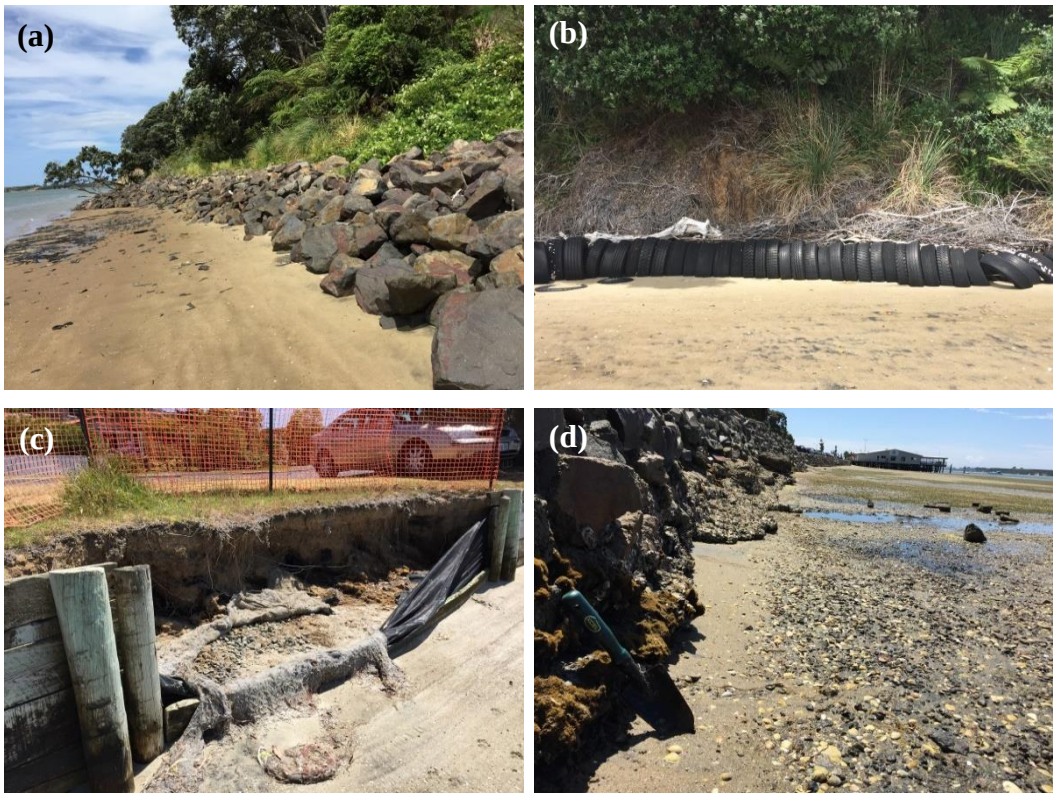

Figure 4.12: Seawalls bordering the Omokoroa Peninsula (a) rock revetment along north western boundary constructed by the Western Bay of Plenty District Council between 2003 and 2010, (b) private home owner places tyres at base of cliffs along the western margin, (c) failure of the timber seawall in 2014, south of the boat ramp and (d) rock grouted seawall south of the boat ramp where minor scouring at the base is evident.

The extent of intertidal flats differs on either side of the Omokoroa Peninsula. On the western and northern margins, the widths of the tidal flats were narrow and the channel passes close to the cliffs. On the eastern margin there are extensive intertidal flats.

4.2.2 Sediment behaviour at the boat ramp

Significant sediment accumulation was evident on the boat ramp and easily entrained into the water column once disturbed. Fine to medium sand with some clay was apparent on the boat ramp. A significant proportion of the sediment was organic material (black fine to medium sand) at the base of the boat ramp. On the upper section of the boat ramp a thin film of light brown, very fine sediment (clay) accumulated. The concrete lip bordering the sides and base of the boat ramp appeared to create a sheltered zone subjected to sediment infill.

After assessing the impact of boats launched from the boat ramp, it was evident that black and/or light brown material was entrained when trailer tyres or people came into contact with the accumulated sediment. Sediment disturbance was affected by water level and sediment thickness, becoming more problematic at low tide over the winter months when accumulated sediment was thicker. It appeared that most of the time sediment entrainment was not problematic and the public who utilised the facility did not recognise sedimentation as a concern provided their boats could still be launched. Some comments were made regarding the danger associated with the sediment on the boat ramp, creating a slip hazard, causing a number of accidents.

The ferry terminal is located adjacent to the boat ramp directly towards the south. The level of the ferry terminal, although slightly higher than the boat ramp, extends further offshore into the channel. The ferry terminal itself is flat with no margins on either side or at the base, which drops steeply into the channel. The flat surface of the ferry terminal means that water is free-flowing, with no evidence of sediment accumulation at the base. At the time this investigation was operated, a thin film of very fine sediment (clay) had accumulated on the ferry terminal, which is, however, frequently cleaned. Clay settlement on the ferry terminal is equivalent to the sediment accumulation on the upper section of the boat ramp, creating a slip hazard to the public.

Ferry arrivals and departures were observed at both high and low tides to identify potential sediment disturbance caused by the propeller wash. Negligible sediment

disturbance was apparent on arrival of the ferry at high and low tide, nor was any obvious sediment disturbance identified during departure at high tide. At low tide, when the ferry departed the terminal, some material was entrained and driven shoreward by the reverse propeller. A large proportion of the entrained material was organic debris such as seagrass leaves. A portion of the suspended material drifted and settled on the boat ramp. While the ferry is docked at the terminal it acts as a barrier to currents and waves from the southern sector.

Eddies are evident at the boat ramp, resulting from adjacent structures. North of the boat ramp, piles for the jetty form small eddies around the boat ramp during the ebb tide whereas south of the boat ramp, eddies form over the flood tide from the piles for the ferry terminal. Minor scouring was observed at the base of the structures adjacent to the boat ramp, therefore negligible sedimentation on the boat ramp was associated with erosion caused by the surrounding structures.

Figure 4.13 shows examples of an episodic suspended sediment plume observed in shallow water along the shoreline adjacent to the boat ramp. Processes contributing to suspended materials are recognised as the turbid fringe, a consequence of wave induced resuspension of muddy sediments during the rise and fall of the tide. Suspended sediment was evident on the boat ramp and a proportion of muddy sediment was naturally deposited on the boat ramp due to the sheltered conditions.

Figure 4.13: Turbid fringe (a) north of jetty, (b) at boat ramp and (c) north of boat ramp.

Figure 4.14: Sediment plume during ebb tide/slack tide. Photo taken from boat ramp facing north towards the jetty.

During fair-weather conditions, a sediment plume was observed in the tidal channel on the ebb tide flowing south past the boat ramp. Over slack tide, light onshore winds forced the sediment plume shoreward onto the boat ramp and eastern shore of the Omokoroa Peninsula (Figure 4.14). Sheltered conditions on the boat ramp allowed the fine sediment to settle and contributed to sediment accumulation on the boat ramp. Over the flood tide no sediment plume was observed. Deposition of suspended sediment was thus dependent on the wind direction at slack tide.

The source of the sediment plume is unknown however there are three potential scenarios that could account for the observations: (1) derived from local, active cliffs exposed to intermitted tidal currents eroding and transporting sediment south past the boat ramp on the ebb tide, (2) migration of the turbid fringe into the channel or (3) derived from the boundary between the intertidal flats and the channel.

4.2.3 Indicators of sediment transport

The Bramley Drive and Ruamoana landslide events were subjected to intermittent wave action at high tide. Entrained material was transported in two divisions: (1)

coarser sediment being redistributed in a band at high tide, accumulating sediment on the adjacent shores and (2) fine sediment created a plume, indicating sediment sourced from the landslide debris was transported north, out of the harbour entrance (Figure 4.15). Runout from the Bramley Drive landslide altered the hydrodynamics and therefore sedimentation patterns. Evidence of sediment transport adjacent to the landslide varied, indicated particularly by structures preventing sediment transport. A small eddy formed around the landslide debris on the flood and ebb tides and redistributed sediment to form small beaches on the southern and northern side, respectively.

Figure 4.15: Sediment transport northeast sourced from the Bramley Drive landslide, image from 2012, after the failure in 2011 (Google Earth).

Figure 4.16 illustrates a distinct zone between the beach sediments and intertidal flats, representing a narrow ribbon of medium to coarse sand along the Peninsula at the high tide mark. Evidence of sorting was identified as indicated by the laminations of sediment. A large proportion of the coarse sediment transport along the Peninsula was concentrated in the swash zone through wave action.

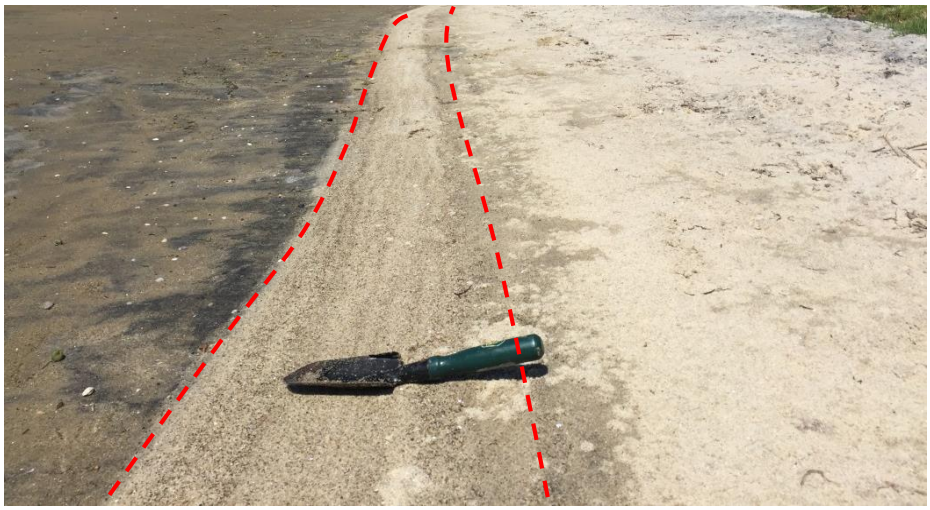

Figure 4.16: Band of sediment transport along high tide mark along the Esplanade.

The shore platform is exposed on the intertidal flats at the northern point and western margin of the Omokoroa Peninsula (Figure 4.17). Matua Subgroup lignites are exposed at the eastern point of the peninsula, whereas on the western side ignimbrites and reworked volcanics are exposed. The exposed shore platform limits sediment availability, of which any available unconsolidated sediment accumulated in depressions.

Figure 4.17: Exposed shore platform on intertidal flats showing (a) lignite on northeast point and (b) ignimbrite west of the Omokoroa Peninsula.

Ripples provided indications into current/wave interactions and dominant directions. Figure 4.18 illustrates slightly asymmetric ripples, steeper on the eastern side, indicating dominant ebb tidal current. Orientations of the ripples are approximately 45˚ to the shoreline, suggesting that a combination of both tide and wave processes influence sediment transport on the intertidal flats.

Figure 4.18: Ripples on intertidal flats north of boat ramp (pen faces north).

Small scale dunes developed along the northern shoreline of Omokoroa Domain between January and May of 2015. Sediment accumulation was approximately 40 cm thick and 1 m wide, extending from the boat ramp north to the slipway (Figure 4.19). Sediment deposition here suggests an increased supply of coarse sediment, a higher frequency of waves large enough to transport sediment onshore and higher water levels due to large spring tides and storm surges.

Figure 4.19: Sand dune development at the high tide mark at the Omokoroa Domain.

4.2.4 Potential sediment sources

Sediment accumulation at Omokoroa Domain appears to be derived from local sources and entered the sediment systems via marine erosion and mass wasting events. A large proportion of the coastline is bound by active cliffs directly exposed to intermittent marine erosion. Here, cliffs comprise a range of clasts sizes that are poorly lithified and thus easily eroded. Localised mass wasting was evident along the Omokoroa Peninsula, providing a large sediment source (Figure 4.20). The suspended sediment load of streams surrounding the Omokoroa Peninsula appeared to be minor and were sourced from runoff and streambank erosion. Fine sediment sourced from streams was either deposited in the upper reaches of the estuary or transported out the harbour entrance. Evidence suggested a large portion of the fine sediment was transported out of the harbour. There was no significant evidence that streams provided a major sediment source contributing to the evolution of Omokoroa Domain.

Figure 4.20: Sources of sediment (a) exposed cliffs subject to marine erosion at Omokoroa Point and mass wasting features (b) Bramley Drive landslide.

4.3 Summary

Initial investigations were based on historic imagery and field observations to provide evidence of sediment sources and processes relating to the evolution of Omokoroa Domain.

- Significant changes in the shape of the shoreline occurred between 1943 and 1982 as a result of human modification including land reclamation and construction of the ferry terminal and seawall hard structures. Construction of the ferry terminal inhibited sediment transport, indicating net sediment transport occurred south along the eastern margin of Omokoroa Peninsula causing sediment deflection. The seawall was subsequently constructed in an eroding environment and exacerbated long-term erosion south of the ferry terminal.
- Evidence suggested Omokoroa Domain was subjected to tidal flooding and thus evolved from a spit enclosed lagoon, not a 'cuspate foreland' as previously considered. The area has been extensively modified and, consequently, a connection to the sea cannot be clearly identified. The present landform suggests the lagoon was breached on the northern side and further modified to aid drainage.
- Sediment accumulation at Omokoroa Domain derived from local sources, primarily through marine erosion and mass wasting of active cliffs along the western side and the northern point of Omokoroa Peninsula.
- Sediment behaviour around Omokoroa Peninsula suggested that sediments were entrained by wave action and further transported by currents. Additionally, sediment patterns indicated two sediment transport processes occurred relative to the grain size. Fine sediment was transported by tidal currents out of the harbour whereas coarser sediment was transported in a narrow band along the shoreline.
- Indicators of sediment transport surrounding Omokoroa Peninsula appeared to be inconsistent. Opposing geomorphic indicators suggested sediment transport was driven by a complex interaction of processes at different scales and time frames. Net sediment transport was south past the boat ramp and ferry terminal, although sort-term variations were also evident.

Chapter Five

HYDRODYNAMICS

The following chapter discusses the hydrodynamics surrounding Omokoroa Peninsula based on wave and current data obtained from field measurement. Meteorological data, initially obtained during the deployment period were here presented and the degree of site exposure was described using the effective fetch. A harmonic analysis was used to analyse tidal and non-tidal components of water level, whereby correlations with meteorological data indicate climatic influences on sea level. Wave characteristics are presented and compared with local wind data to identify relationships with wind patterns. Tidal currents were analysed to determine patterns over the tidal cycle and residual current directions. Sediment threshold and settling velocity were calculated to investigate sediment entrainment and deposition potential. Results from the hydrodynamic analysis are important in determining the influence on sediment transport patterns around the Omokoroa Peninsula.

5.1 Meteorological data

Meteorological data was examined for the deployment period (from 19 February to 19 March 2014) in order to identify relationships between weather patterns and wave conditions recorded around Omokoroa Peninsula. Data included wind records from Omokoroa Weather Station (referred to as Omokoroa WS) (Figure 5.2c) and archived weather observations supplied by Meteorological Service of New Zealand Ltd (2014), from the Tauranga Aerodrome Automatic Weather Station (referred to as Tauranga Aero AWS) (Figure 5.1 & Figure 5.2a,b). The analysis presented in this chapter refers to Tauranga Aero AWS, located 14 km SE of Omokoroa, as the Omokoroa WS was affected by obstructions that limited reliability of wind records (see Chapter 2).

The wind recorded at the Omokoroa WS does not show a dominant wind pattern in comparison to the Tauranga Aero AWS, although does indicate most common prevailing winds from the southwest, however weaker than Tauranga. The

Omokoroa WS indicates strongest winds prevail from the northwest followed by east. The most frequent wind at Omokoroa is from the west, southeast and northwest (Figure 5.2). There are limited readings from the north and northeast at Omokoroa suggesting that the entire wind direction is not represented. Inspection of the instrument confirms it is working correctly and there is no explanation for the gap in the wind direction (Figure 5.4). The Tauranga Aero AWS is situated 5 m above M.S.L whereas the Omokoroa WS is approximately 2 m above ground level, on a 40 m high cliff. It is important to note that the observed winds at the Tauranga Aero AWS are stronger than the actual wind at water level due to the logarithmic wind profile. The Omokoroa WS is subject to obstructions, limiting reliability of wind records. For this reason, and to consider the wind conditions over the entire Tauranga Harbour, the Tauranga Aero AWS is referenced throughout the analysis, located approximately 14 km southeast of Omokoroa.

Wind records during the deployment period indicated fair-weather conditions of low energy, with wind speeds generally less than 5 m/s. Wind direction during fair-weather conditions varied, although a daily northeast (onshore) afternoon sea breeze was evident. Occasionally, in calm conditions, a land breeze was apparent approximately 12 hours after the sea breeze (Figure 5.2). The strongest and most frequent winds were southwesterlies, evident in Figure 5.4. Easterly and westerly winds were strong and infrequent, while regular light northerlies were recorded. During the deployment period there were three high-energy episodes with the potential to cause storm surge and increase wave heights at Omokoroa, including Julian Day 54 – 56 (*Event 1*), Julian Day 59 – 65 (*Event 2*) and Julian Day 73 – 76 (*Event 3*), described in the following period.

Event 1: Julian Day 54 – 56 (23 – 25 February)

Event 1, short-duration disturbed west-to-southwest airflows associated with a cold front, recording wind speeds from 12 m/s gusting to 15 m/s. Sea level pressure dropped to 1004 hPa and light showers accumulated 9.6 mm of rainfall over 48 hours.

Event 2: Julian Day 59 – 65 (28 February – 6 March)

Event 2 was characterised by disturbed west to southwest airflows that prevailed in both strength and duration. Strong winds were driven by a number of fronts that moved across the country attached to a low pressure system in the Southern Ocean, moving up the east coast of the South Island. Over a six day period the sea level pressure reduced to 1005 hPa and wind speeds varied between 5 and 10 m/s, gusting to 17 m/s.

Event 3: Julian Day 73 – 76 (14 – 17 March)

Event 3 is associated with Extra-Tropical Storm Lusi (ETS Lusi) arriving in the Bay of Plenty on 14 March 2014, bringing gale force winds and heavy rain. During *Event 3*, strong easterly winds of 13 m/s preceded ETS Lusi with maximum gusts reaching 22 m/s. As the extra-tropical storm progressed, wind speed decreased and shifted to the north. A total of 24.2 mm of rainfall was recorded ahead of the extra-tropical storm. Decreased sea level pressure (1008 hPa) followed the heavy rain and strong winds as ETS Lusi migrated down the west coast of the country.

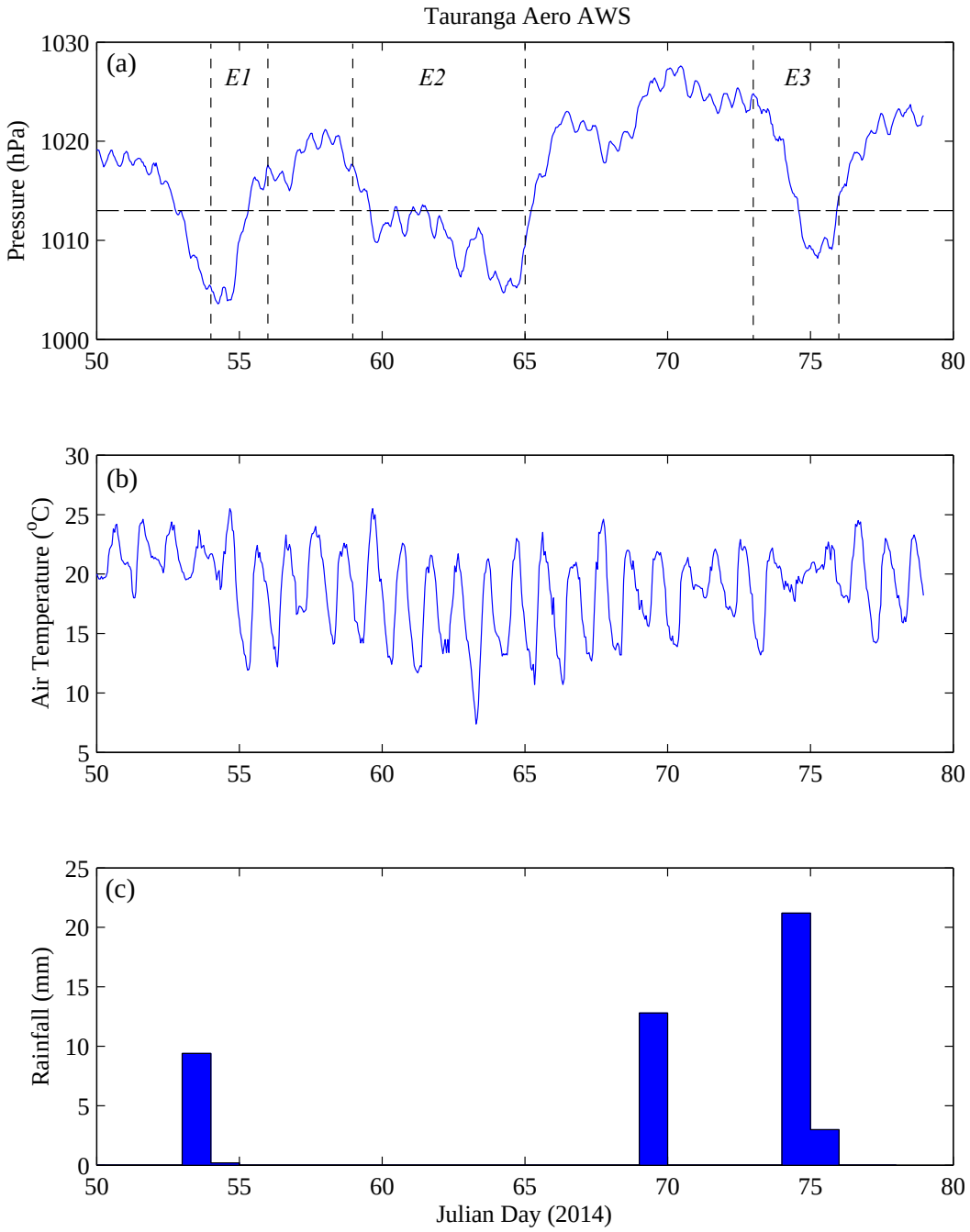

Figure 5.1: Weather data from Tauranga Aero AWS over the deployment period showing (a) atmospheric pressure, (b) air temperature and (c) rainfall.

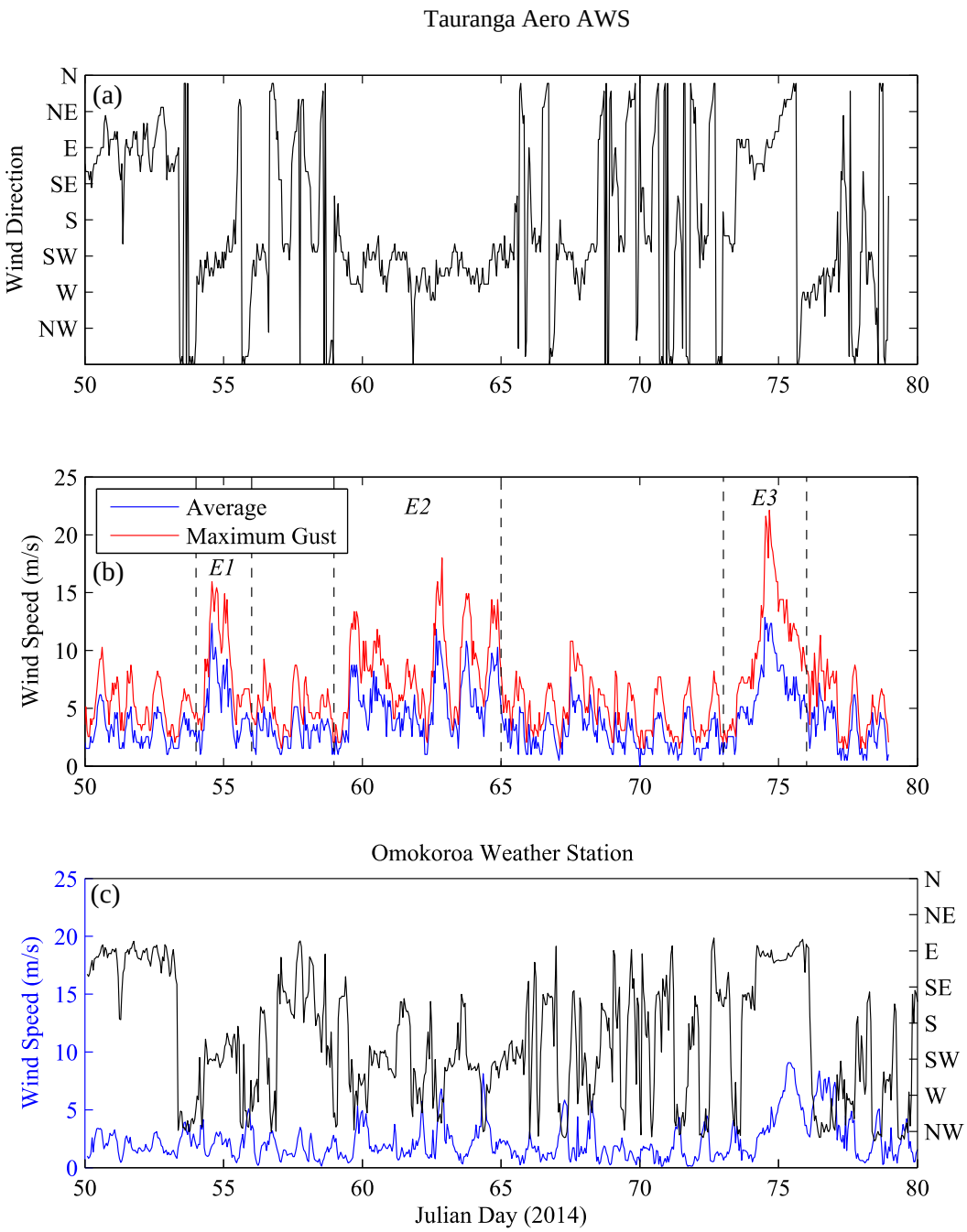

Figure 5.2: Weather data over the deployment period of the (a) wind direction, (b) wind speed including average and gusts from the Tauranga Aero AWS and (c) wind speed and direction obtained from the Omokoroa weather station.

5.2 Effective Fetch/Site Exposure

Omokoroa is sheltered from the open coast by Matakana Island, hence swell energy penetrating to Omokoroa is negligible and waves surrounding the Omokoroa Peninsula were considered entirely locally generated wind waves. Wave heights

generated from of local winds are a function of wind conditions, basin dimensions and water depth. The available fetch at Omokoroa is limited by the surrounding topography and the tidal range causing intermittent subaerial exposure of intertidal flats. Additionally, Motuhoa Island, east of Omokoroa, shelters the boat ramp from easterlies and south-easterly winds. The available fetch at Omokoroa is largely influenced by the tidal range as the exposure of intertidal flats reduces the available fetch.

Tidal influence is significant on the western shore of Omokoroa where extensive intertidal flats are exposed in the middle reaches of the Tauranga Harbour, forming a boundary that divides the harbour into two tidal compartments during most of the tidal cycle, limiting the available fetch. The eastern shore is affected by the locations of islands which shelter the eastern margin and channels and were split by intertidal flats causing intermittent exposure, limiting the fetch over the tidal cycle.

Each site was exposed to different wind directions due to the location relative to the surrounding coastline, further restricted by the tidal cycle. At each of the three sites that measured wave height, the effective fetch has been calculated along four profiles including: longest fetch, onshore wind direction, dominant prevailing wind direction and prevailing wind direction during ETS Lusi. Figure 5.5, Figure 5.6, Figure 5.7 and Figure 5.8 illustrate the available fetch at each site and document the effected fetch calculated along each profile. Fetch profiles are presented in Figure 5.9, Figure 5.10, Figure 5.11 and Figure 5.12 illustrating bathymetry and effect of the tidal cycle. The first two profiles are site specific, whereas the dominant prevailing wind direction was determined from historic records that indicated prevalence of south-westerly winds in both strength and frequency (Figure 5.4); and winds associated with ETS Lusi were strong easterlies. In order to consider the influence of the tidal cycle, effective fetch along each profile has been determined at high, mid and low tide. The respective water depths are -1.9 m, -1.05 m and 0 m relative to chart datum (LAT). The effective fetch was calculated based on the Shore Protection Manual (1984).

The longest fetch reaching Omokoroa was from the northwest at Bramley Drive (Figure 5.4 & Figure 5.10). However, the longest effective fetch was the onshore direction at Bramley Drive due to the restricted gap between Kauri Point and Matakana Island. The effective fetch to the west of Omokoroa was significantly reduced during mid and low tide due to the extensive intertidal flats in the middle reaches of the Tauranga Harbour. Bramley Drive was sheltered by the Omokoroa Peninsula from southeast winds.

Opureora Point had the largest effective fetch relative to the dominant wind direction (southwest). However, effective fetch was affected by the exposure of tidal flats at low tide, in effect eliminating the fetch (Figure 5.6 & Figure 5.11). Opureora Point is sheltered from the north by Matakana Island, to the south by Motuhoa Island, and in the east by Rangiwaea Island. Exposure at Opureora Point was reduced by the surrounding topography, and the fetch was also significantly reduced by intermittent subaerial exposure of the intertidal flats.

Te Puna is sheltered by Motuhoa Island to the northeast and in the south by local geography (Figure 5.7 & Figure 5.12). However, Te Puna is exposed to the east and, therefore, has the largest effective fetch relative to the winds associated with ETS Lusi. Further east of Te Puna, the deep channels east do not significantly restrict fetch during low tide.

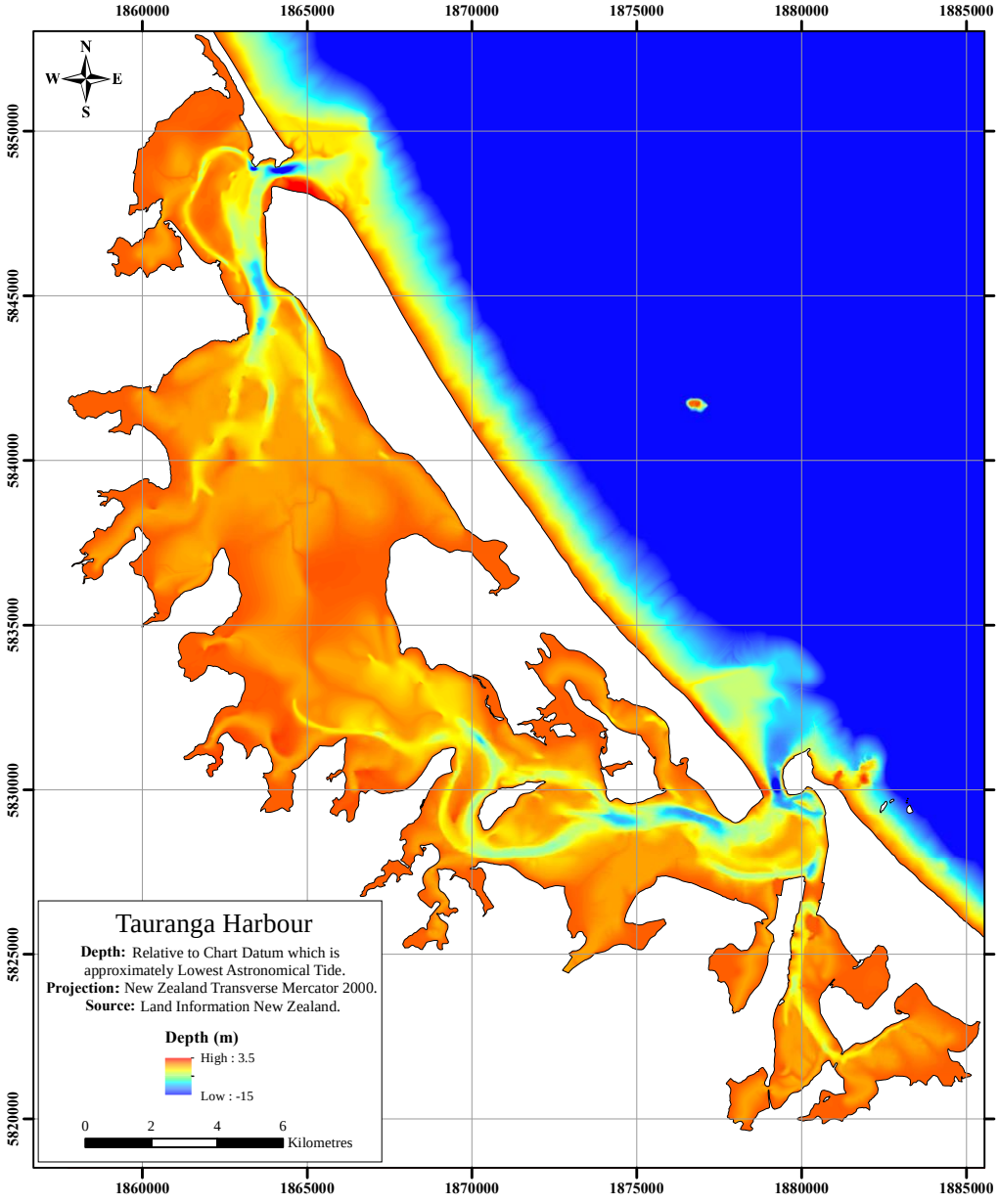

Figure 5.3: Bathymetric map of the Tauranga Harbour.

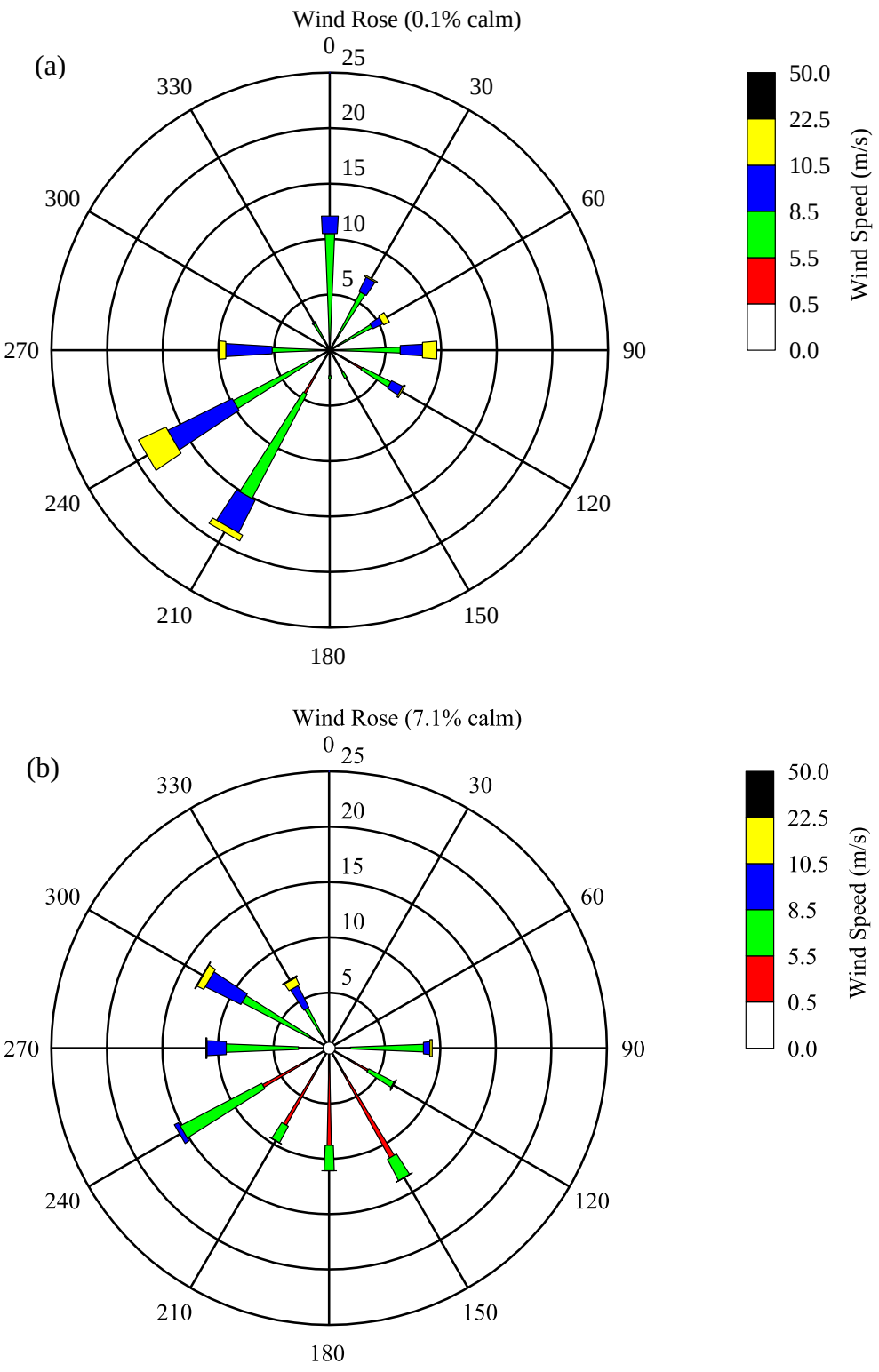

Figure 5.4: Wind Rose over the deployment period, between 19 February and 19 March at (a) Tauranga Aero AWS and (b) Omokoroa WS.

(a)

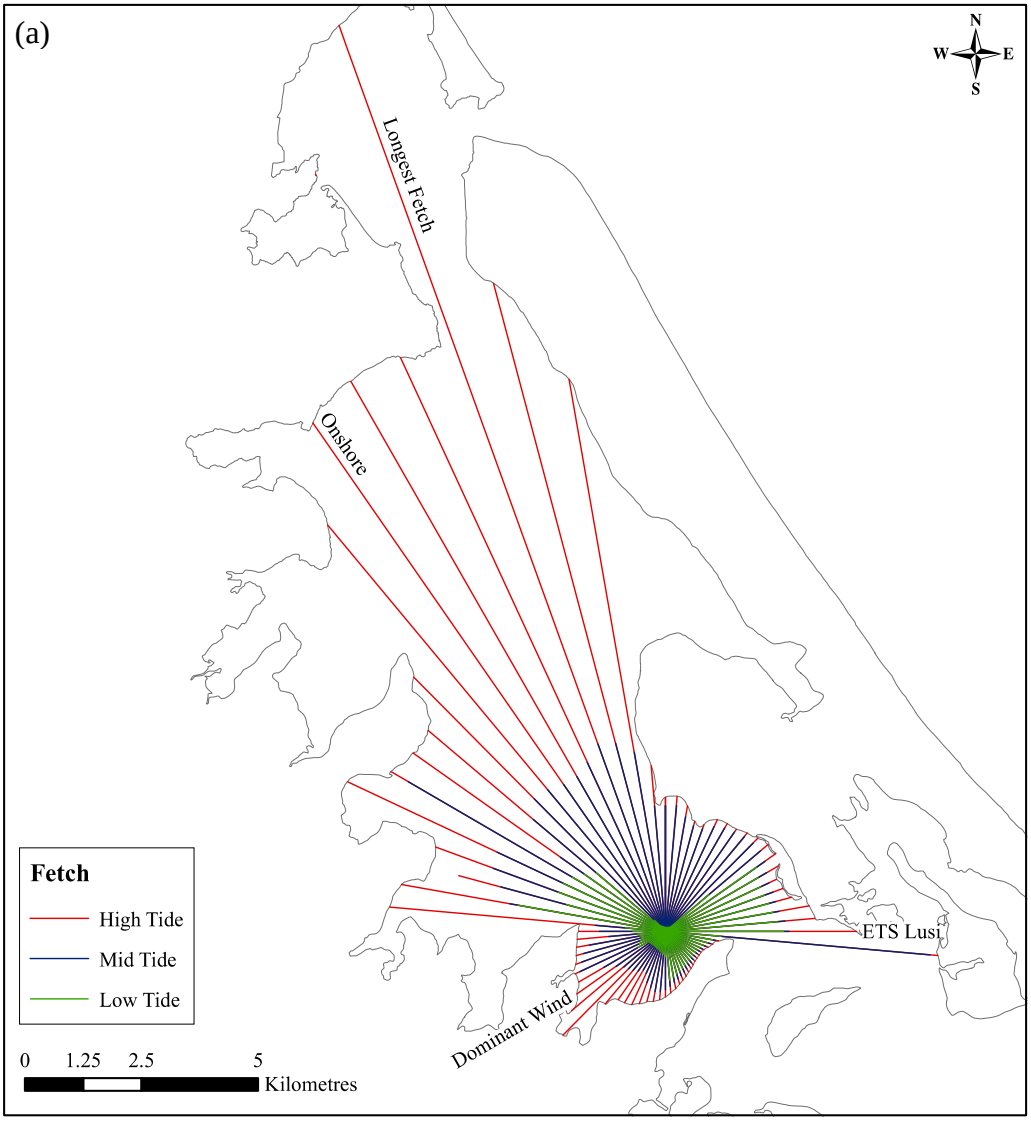

(b)

Fetch Profile	Effective Fetch (m)		
	High Tide	Mid Tide	Low Tide
Longest Fetch (340˚)	10591.6	3729.9	478.7
Onshore Direction (325˚)	11474.2	4041.2	680.1
Dominant Wind (240˚)	2186.4	1449.3	515.4
ETS Lusi (90˚)	2540.4	2258.2	1735.2

Figure 5.5: Fetch at Bramley Drive (a) available fetch showing limits at high, mid and low tide and (b) effective fetch calculated based on longest fetch, onshore, dominant and ETS Lusi at high, mid and low tide.

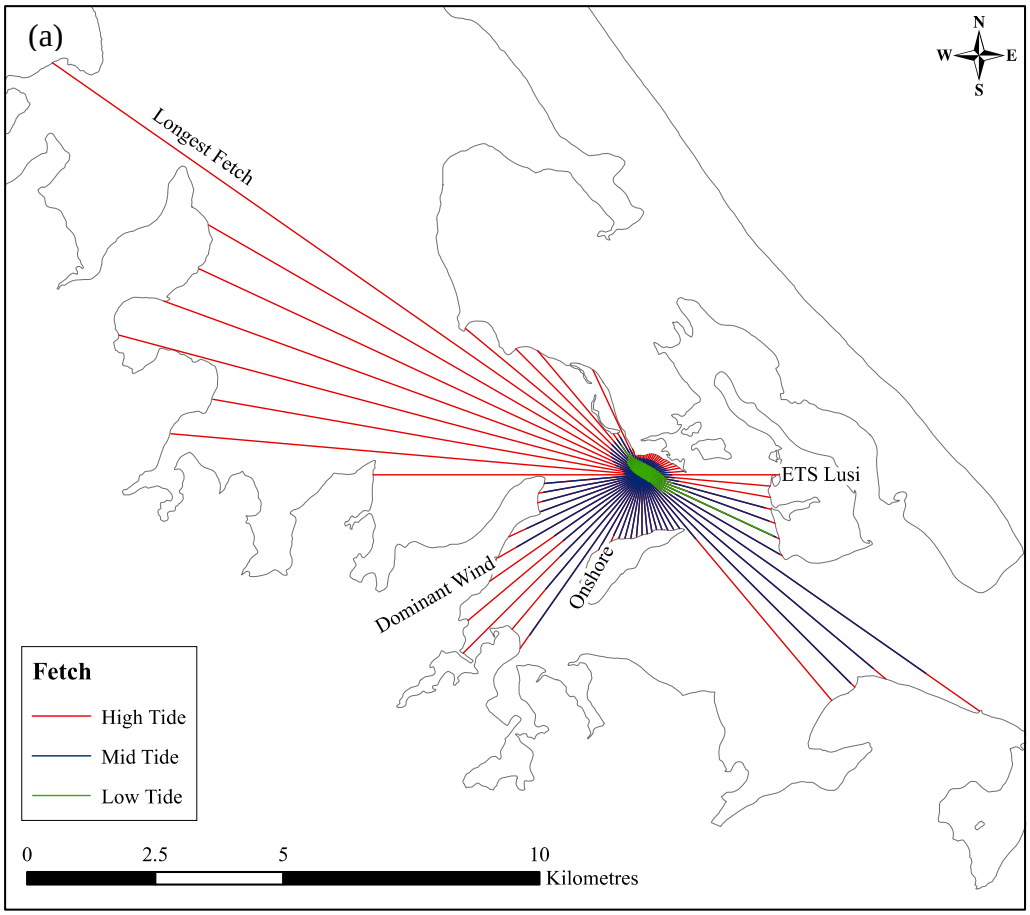

(b)

Fetch Profile	Effective Fetch (m)		
	High Tide	Mid Tide	Low Tide
Longest Fetch (305˚)	6900.0	690.0	332.1
Onshore Direction (205˚)	2421.9	1834.2	42.5
Dominant Wind (240˚)	3217.5	2385.8	49.4
ETS Lusi (90˚)	1778.5	1105.6	654.6

Figure 5.6: Fetch at Opureora Point (a) available fetch showing limits at high, mid and low tide and (b) effective fetch calculated based on longest fetch, onshore, dominant and ETS Lusi at high, mid and low tide.

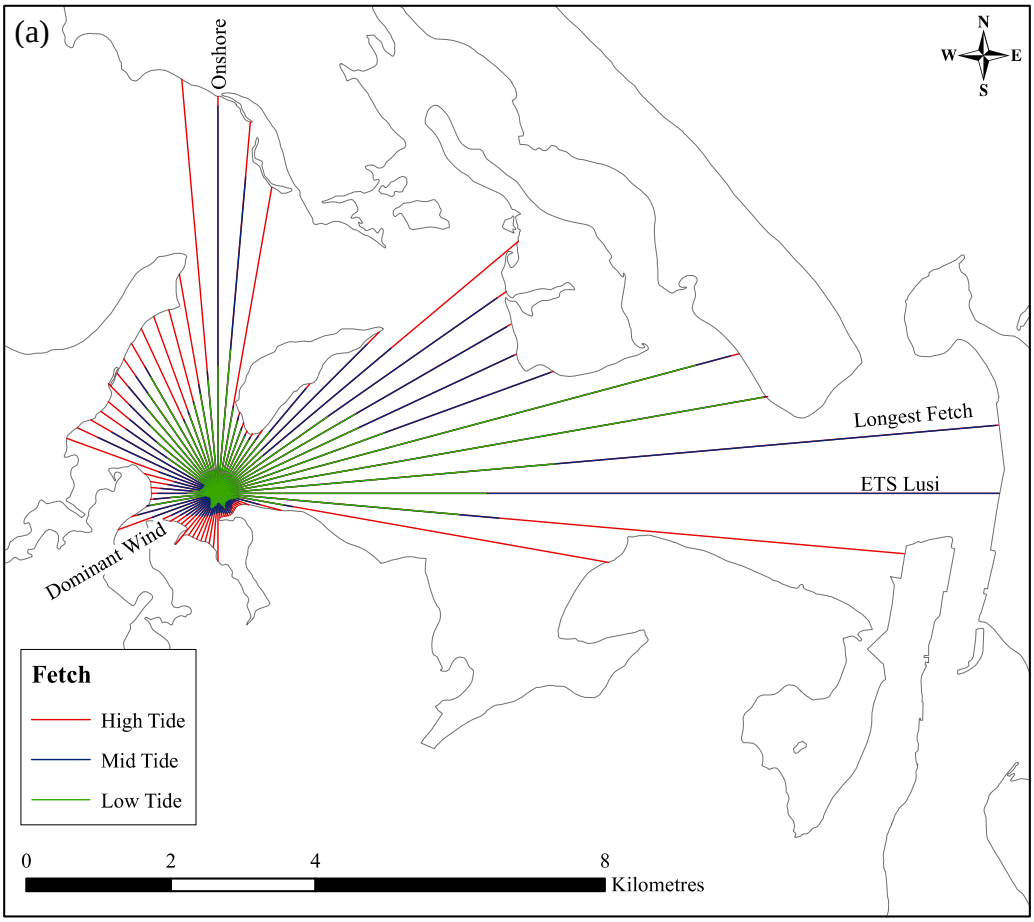

(b)

Fetch Profile	Effective Fetch (m)		
	High Tide	Mid Tide	Low Tide
Longest Fetch (85˚)	6217.7	5214.3	3191.4
Onshore Direction (0˚)	3193.5	1920.2	1306.0
Dominant Wind (240˚)	895.8	684.0	257.1
ETS Lusi (90˚)	5824.6	4209.3	2844.2

Figure 5.7: Fetch at Te Puna (a) available fetch showing limits at high, mid and low tide and (b) effective fetch calculated based on longest fetch, onshore, dominant and ETS Lusi at high, mid and low tide.

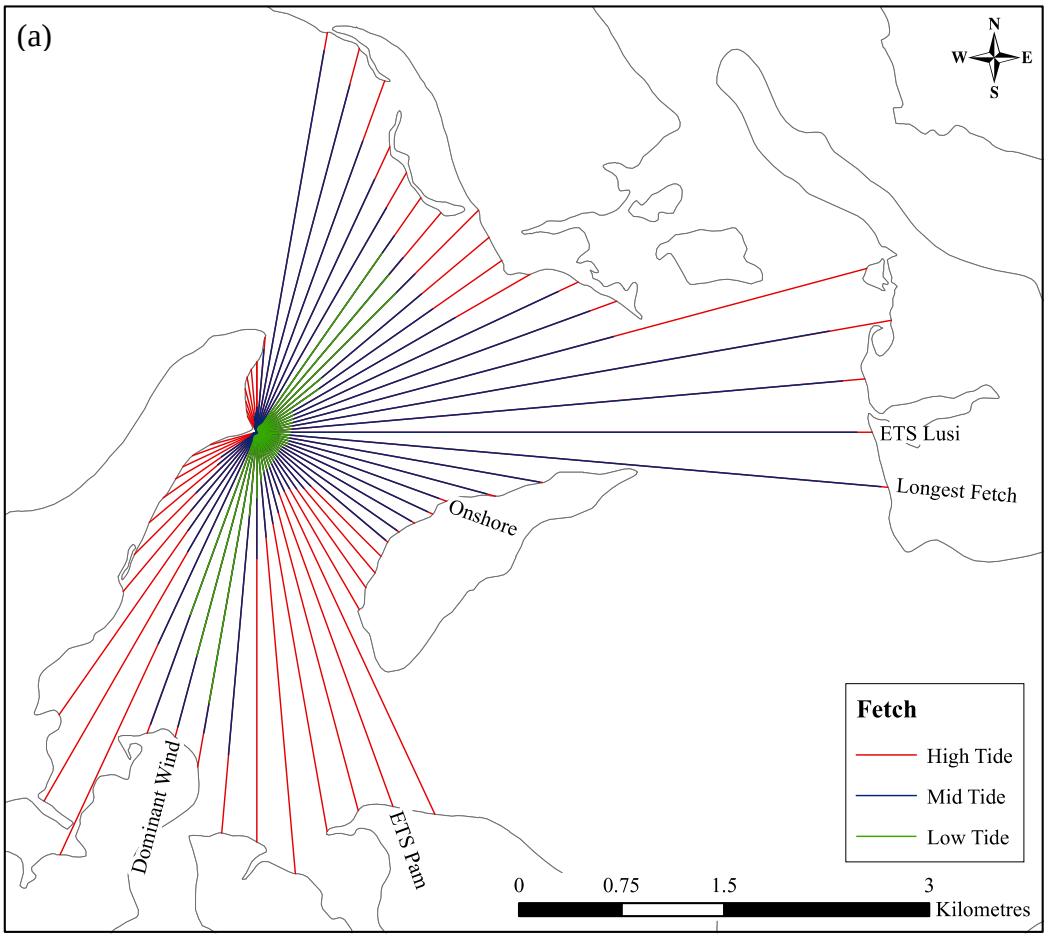

(b)

Fetch Profile	Effective Fetch (m)		
	High Tide	Mid Tide	Low Tide
Longest Fetch (95˚)	3097.0	2816.0	238.2
Onshore Direction (110˚)	3204.9	2189.1	220.8
Dominant Wind (190˚)	2830.6	1443.0	658.7
ETS Lusi (90˚)	3224.9	2926.2	245.8
TC Pam (160˚)	2418.0	753.7	246.7

Figure 5.8: Fetch at the boat ramp (a) available fetch showing limits at high, mid and low tide and (b) effective fetch calculated based on longest fetch, onshore, dominant, ETS Lusi and TC Pam at high, mid and low tide.

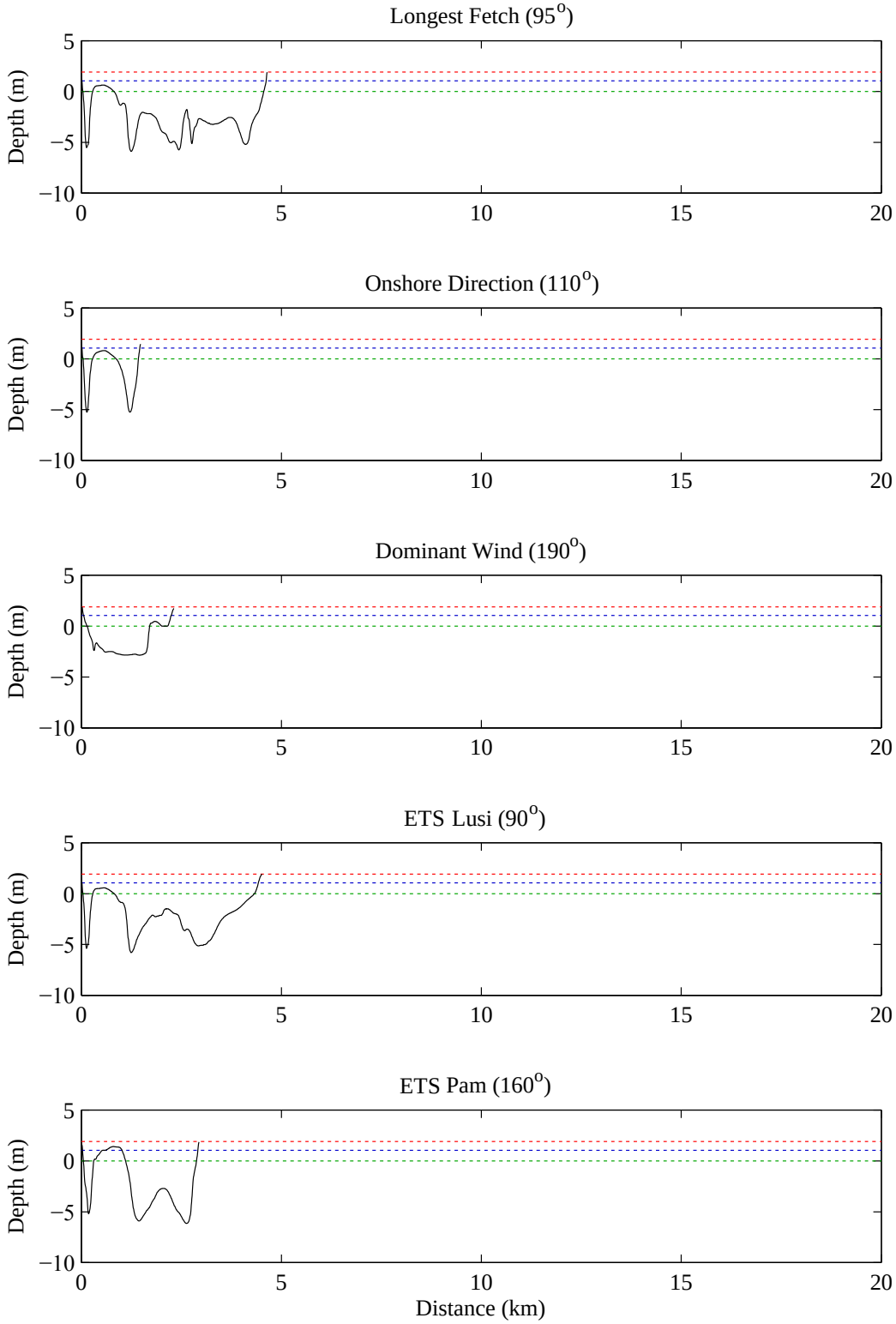

Figure 5.9: Bathymetric profiles along effective fetch transects at the boat ramp. Dotted lines indicate water depth at high (red), mid (blue) and low (green) tides. VE=250.

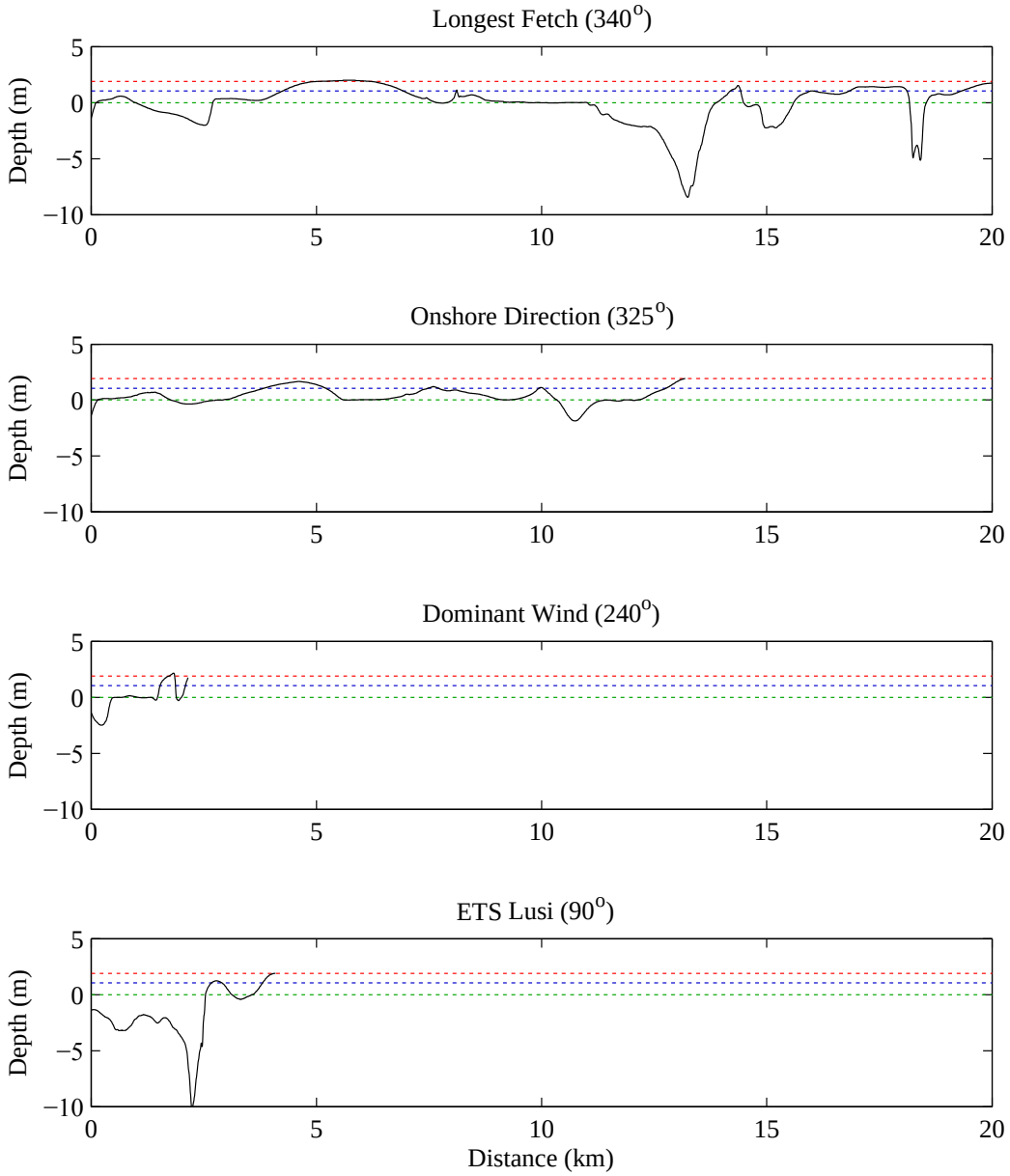

Figure 5.10: Bathymetric profiles along effective fetch transects at Bramley Drive. Dotted lines indicate water depth at high (red), mid (blue) and low (green) tides. VE=250. All profiles are drawn to the same scale.

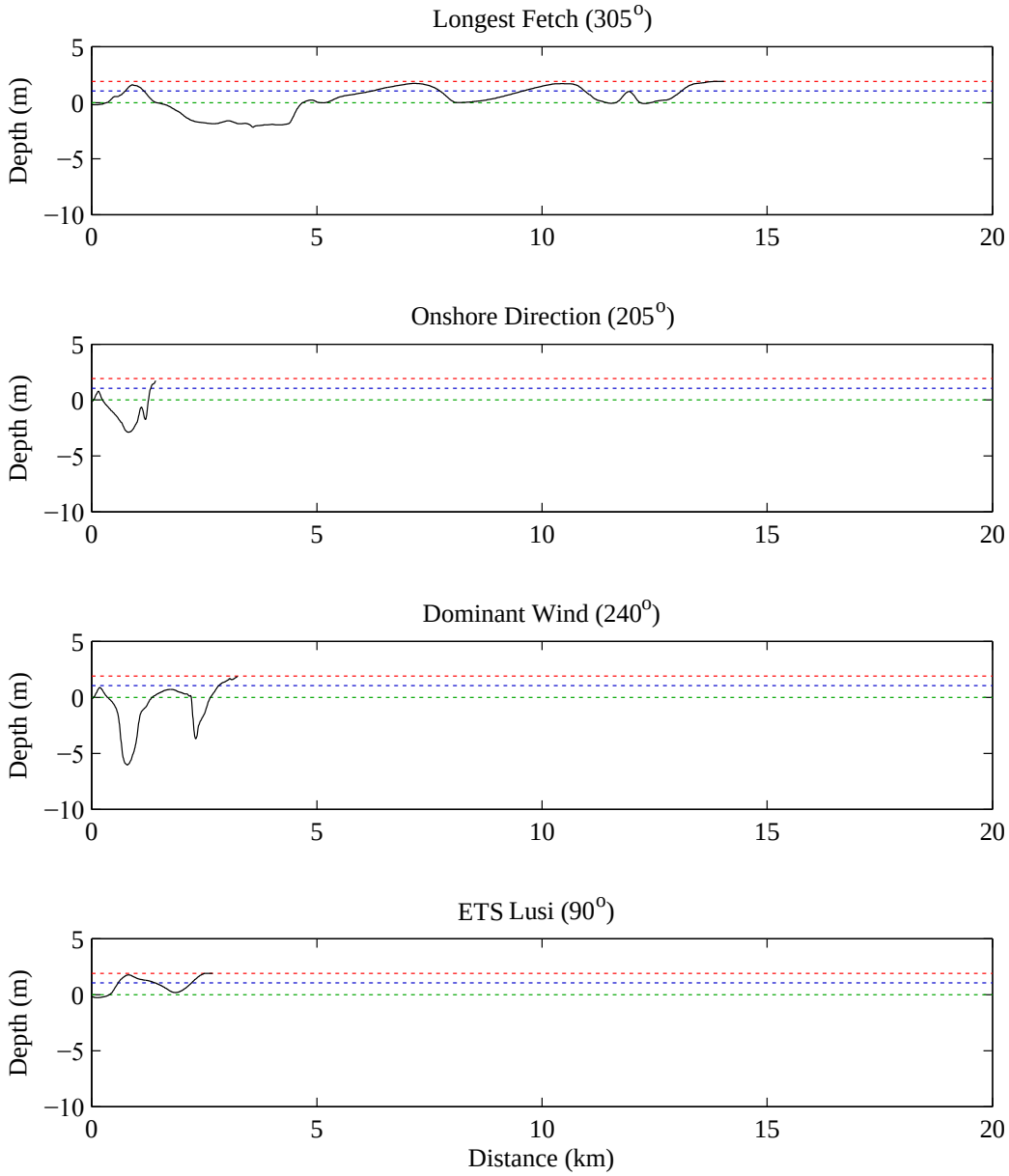

Figure 5.11: Bathymetric profiles along effective fetch transects at Opureora Point. Dotted lines indicate water depth at high (red), mid (blue) and low (green) tides. VE=250.

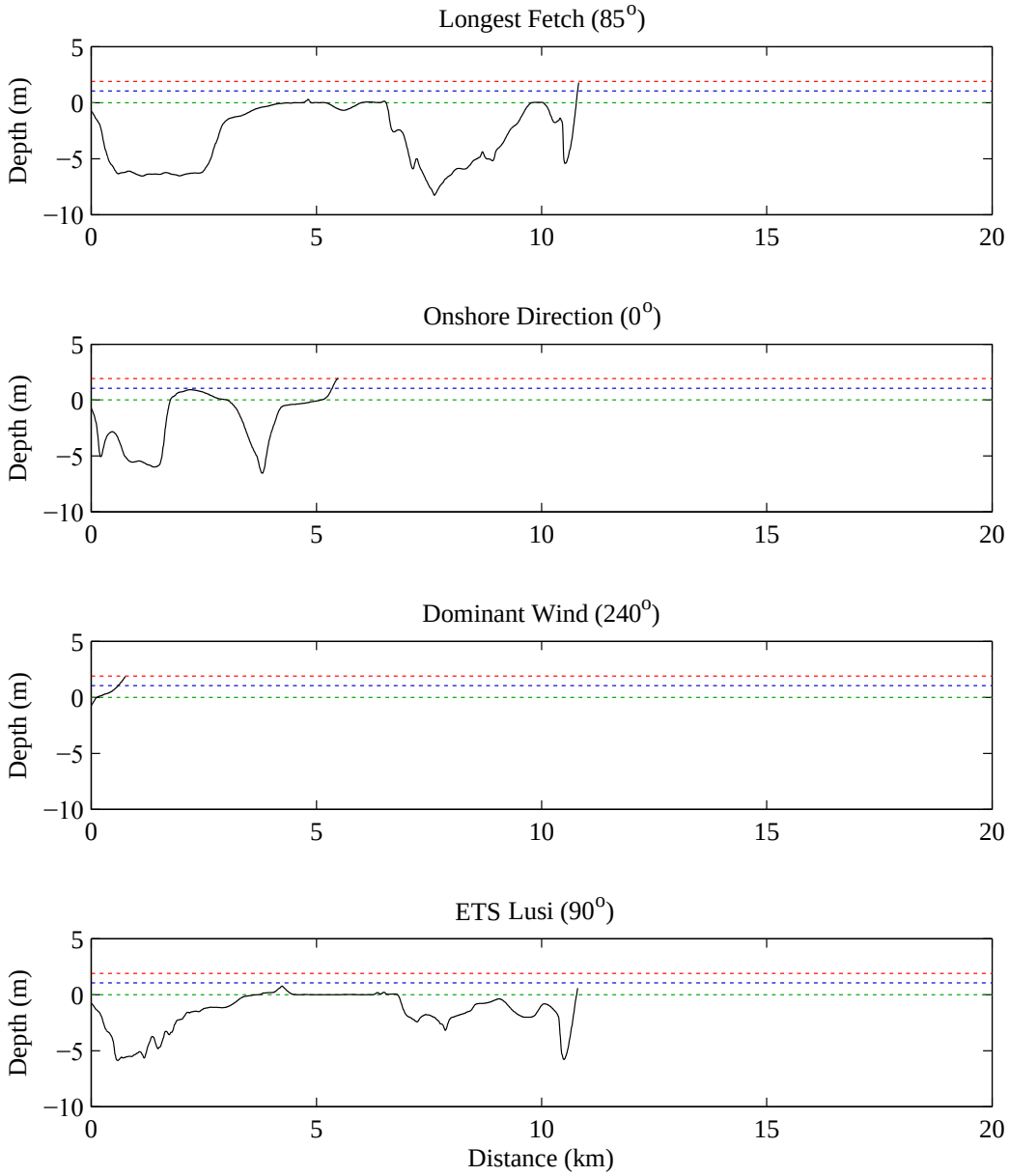

Figure 5.12: Bathymetric profiles along effective fetch transects at Te Puna. Dotted lines indicate water depth at high (red), mid (blue) and low (green) tides. VE=250.

5.3 Tidal Analysis

5.3.1 Tides

Tidal records over the deployment period covered a spring-neap cycle. Results indicate the Omokoroa tidal regime is semi-diurnal, recording two high and low tides daily. Successive high tides varied in height, illustrating a diurnal inequality (Figure 5.18). Measured tidal levels, presented in Table 5-1 indicate that the minimum neap tidal range was at Te Puna (1.116 m) while the maximum spring tidal range was recorded at Bramley Drive (2.170 m). Based on the spring tidal range, Tauranga Harbour is categorised as meso-tidal, although micro-tidal ranges were recorded during neap tides. The minimum neap tide occurred during the storm surge of *Event 3*, which is after the predicted neap tide.

A change in water level is observed at all of the sites during *Event 3*, increasing water elevation by approximately 0.3 m. The increase in water level was driven by the storm surge and superimposed with the tidal signal. Additionally, the predicted maximum spring tide was depressed, caused by high atmospheric pressure (Figure 5.18). At Bramley Drive, maximum spring elevation occurred after the predicted maximum because of the storm surge associated with *Event 2*. At Opureora Point and Te Puna the maximum spring tide arrived before the predicted tide due to a decrease in barometric pressure which increased the water level. It was evident from the deviation between the predicted and observed tide that storm surges significantly alter the water elevation. Storm surges are further outlined below.

Table 5-1: Tidal elevations for spring and neap tides around Omokoroa.

Tidal Level	Bramley Drive	Opureora Point	Te Puna
Mean Depth (m)	3.978	3.286	4.664
Maximum Spring Elevation (m)	1.022	0.962	0.963
Minimum Spring Elevation (m)	-1.202	-1.117	-1.140
Maximum Neap Elevation (m)	0.964	0.905	0.914
Minimum Neap Elevation (m)	-0.362	-0.356	-0.343
Maximum Spring Range (m)	2.170	2.021	2.061
Minimum Neap Range (m)	1.167	1.178	1.116

Note does not take into account for atmospheric pressure

5.3.2 Tidal asymmetry

Tidal asymmetry around Omokoroa was irregular as variations were evident over the deployment period. Figure 5.13 illustrates differing tide behaviours over the tidal cycle. Based on current velocities, flood tides were dominant during spring tides and the duration over the flood tide was shorter, hence faster currents occurred to maintain continuity of mass. During neap tides, the ebb tide dominated, although due to the short record available, there was no evidence to suggest why this occurs.

Tidal asymmetry associated with the storm tide recorded during *Event 3* behaved differently for the duration of the event. The storm tide occurred during a neap tide with a ~30 cm storm surge, approximately the same water elevation as a spring tide. Over the first two tidal cycles, when the storm surge was at its highest, ebb tides dominated. In contrast, over the following two tidal cycles when the storm surge decreased, flood tides dominated. It would be expected that the storm tide, based on water elevation, followed the tidal asymmetry of spring tides.

In general, the flow velocity is related to the cross-sectional area of the channel (Pugh & Woodworth, 2014). This means there is a variation in behaviour during the tidal cycle in response to depth, hence the change should be systematic (ie regular). However, there are three channels associated with tides reaching Omokoroa. The relative distribution of flows in these channels may be affected by

wind stress altering the distribution of flow between the three channels. Since the channels have different dimensions, the effect on tidal flows at Omokoroa is difficult to predict.

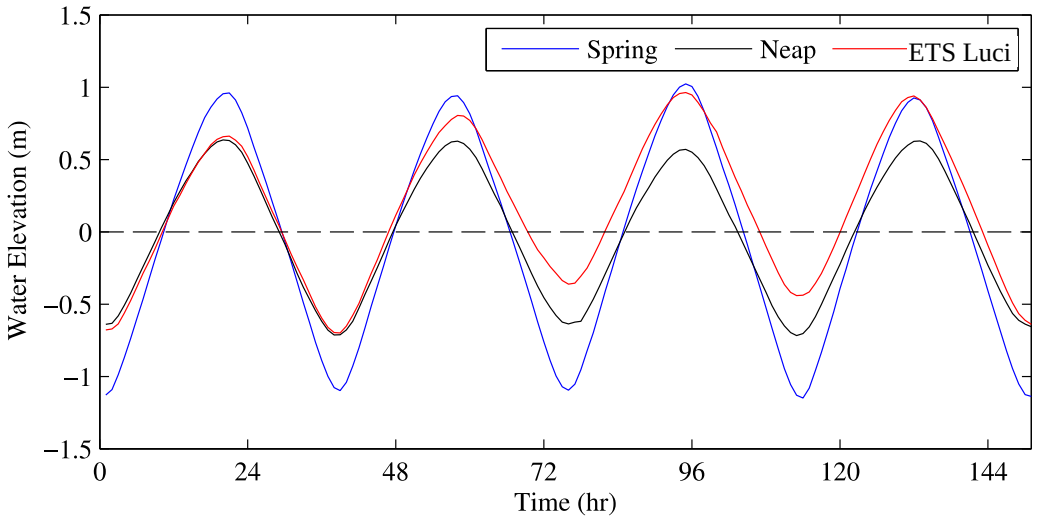

Figure 5.13: Time series of water elevation at Bramley Drive over three different tidal variations beginning at low tide: spring tide (3:20, 2 March – 5:20, 4 March), neap tide (10:40, 11 March – 12:40, 13 March) and ETS Lusi (13:20, 14 March – 15:20, 16 March).

5.3.3 Harmonic analysis

Tidal harmonic analysis was applied to differentiate tidal and non-tidal components. Analysis was implemented using a t-tide MATLAB routine (Pawlowicz *et al.*, 2010).

5.3.3.1 Tidal constituents

The observed tide at any given location is the result of constructive and destructive interference between numerous tidal constituents (Brown *et al.*, 1999).

Main tidal constituents identified in the upper Tauranga Harbour are displayed in Table 5-2. The principle lunar semidiurnal constituent, M2, was the largest at all locations, followed by the larger lunar elliptic semidiurnal (N2) and principal solar semidiurnal (S2) constituents. Constituents of less significance include the lunar declinational diurnal (O1) and luni-solar declinational diurnal (K1). A full list of tidal constituents are presented in Appendix 3. Of the main tidal constituents, the amplitude and phase generally increased in the upper reaches of the harbour.

Table 5-2: Main tidal constituents.

Constituent	Location	Frequency	Period (hours)	Amplitude (m)	Phase (˚GMT)
M2	Bramley Drive	0.0805	12.42	0.7377	238.32
	Opureora Point	0.0805	12.42	0.7031	245.00
	Te Puna	0.0805	12.42	0.7053	242.79
S2	Bramley Drive	0.0833	12.00	0.1093	326.37
	Opureora Point	0.0833	12.00	0.1046	318.00
	Te Puna	0.0833	12.00	0.1052	315.64
N2	Bramley Drive	0.0790	12.66	0.1432	202.36
	Opureora Point	0.0790	12.66	0.1387	213.96
	Te Puna	0.0790	12.66	0.1423	212.10
K1	Bramley Drive	0.0418	23.93	0.0404	36.18
	Opureora Point	0.0418	23.93	0.0384	210.79
	Te Puna	0.0418	23.93	0.0384	212.15
O1	Bramley Drive	0.0387	25.82	0.0117	358.08
	Opureora Point	0.0387	25.82	0.0133	190.38
	Te Puna	0.0387	25.82	0.0123	190.85

Table 5-3 presents the time differences between phases at each site for the major tidal constituents. Phase differences of the dominant M2 tidal constituent suggest that the flood tide arrived at Te Puna first, correlating to the dominant current direction via the channel south of Motuhoa Island. The time difference between Te Puna and Opureora Point is small (5 minutes) as they are fed from the different channels diverging around Motohua Island. The location of the RBR at Opureora Point (within a minor channel) is likely to differ from the tide travelling in the main channel past Omokoroa. From Te Puna, the tide takes 23 minutes to travel to Bramley Drive and 19 minutes from Opureora Point to Bramley Drive, located in the upper reaches of the harbour.

Table 5-3: Phase difference between location of main tidal constituents.

Constituent	Te Puna to Opureora Point (minutes)	Te Puna to Bramley Drive (minutes)	Opureora Point to Bramley Drive (minutes)
M2	4.57	23.16	18.59
S2	4.72	81.6	76.88
N2	3.92	-2.32	-6.25
K1	-5.42	57.07	62.50
O1	-2.02	-18.89	-16.87

In a recent study, McKenzie (2014) recorded sea levels at six locations within the Tauranga Harbour including Omokoroa (instrument located at Te Puna) and Tug Berth, located at the Port of Tauranga (Section 2.2.8.2). The phase and amplitude documented at Omokoroa by McKenzie (2014) closely correlated to those recorded at Te Puna in this study, verifying the results obtained. Comparison of results from this study to the measurements at Tug Berth indicates a greater difference between amplitude and phase at each location, the difference increasing away from the tidal inlet.

Propagation of the tide into the Tauranga Harbour was modified by convergence and frictional dissipation due to changes in the cross-sectional area of the channels operating in the Tauranga Harbour. An increase in amplitude landward from the tidal inlet was caused by a reduced cross-sectional area of the channels as the channel split and narrowed around Motuhoa Island. As a result, tidal amplification (due to hypersynchronous behaviour) was observed landward of the tidal inlet as tidal convergence outweighed the frictional effects.

In this study, the tidal constituents are fitted over a short period of data as the deployment was restricted to a period of 19 days. At minimum, a period of 29 days should be used to resolve diurnal tidal constituents (de Lange *et al.*, 1993). Consequently, the record in this study is not long enough to resolve some of the longer duration tidal constituents. The implications for the results obtained generally overestimated the amplitude, as the energy associated with the

unmeasured tidal constituents was aliased and hence added to the measured tidal constituents. Period is fixed aliased whereas phase is estimated by fitting fixed period sine waves to time series. Phase was calculated by finding the time of peak energy and is consequently affected by aliasing. Longer duration record is required to gain more accurate results and to differentiate between tidal constituents.

5.3.3.2 Storm surge

Storm surge is a non-tidal component that significantly altered the tidal elevation within the Tauranga Harbour. Two significant storm surges were recorded over the deployment period following *Event 2* and during *Event 3*. During *Event 2*, the impact from the storm surge was largest at Bramley Drive (0.16 m) (Figure 5.14), whereas during *Event 3* the storm surge was greatest at Te Puna (0.32 m) (Figure 5.16). Opureora Point (Figure 5.15) recorded the lowest storm surge throughout both events (Table 5-4).

Comparing the relative sea level response, driven by the change in atmospheric pressure (inverse barometric effect), to storm surge indicates that storm surge, although delayed, responds to atmospheric pressure. The difference in magnitude suggests that increases in water level driven by atmospheric depressions were enhanced and decreases associated with high pressure were suppressed. During *Event 1*, however, increase of the inverse barometric pressure was supressed. The difference between the inverse barometric effect and storm surge was thus a function of wind (Table 5-4).

A minor storm surge was recorded as a lagged response following *Event 1*. However, in relation to the inverse barometric effect, the storm surge was suppressed, potentially because the wind and pressure was not sustained for a long enough duration. Alternatively, the offshore wind direction may have pushed water away from the area, counteracting the pressure effect.

The prevailing wind direction during *Event 2* was southwest and coincided with a drop in atmospheric pressure. The storm surge associated with *Event 2* was delayed, indicating the strong winds associated with *Event 2* had a limited effect on the storm

surge as the wind conditions changed when the storm surge occurred. The dominant force causing the storm surge subsequent to *Event 2* was a sustained decrease in the atmospheric pressure. It is likely that the storm surge subsequent to *Event 2* was driven by the series of cold fronts attached to a low pressure system that developed southeast of New Zealand during *Event 2*, resulting in a storm surge that propagated around the east coast of the North Island.

During *Event 3* the prevailing wind direction was from the east, with wind speeds up to 12.9 m/s and gusts reaching 22.1 m/s, swinging to north-east as the wind-speed dropped. The inverse barometric pressure response suggested that the extra-tropical storm and associated low pressure system did not impact the storm surge as the decrease in pressure occurred subsequent to the storm surge. The main factor causing the storm surge during *Event 3* was gale force winds associated with the edge of ETS Lusi. The largest storm surge was recorded at Te Puna, as water was forced shoreward by strong winds into the Te Puna Estuary, exposed to the easterly winds (Figure 5.7). Opureora Point recorded the lowest storm surge as it was sheltered and had the smallest fetch (Figure 5.6).

Table 5-4: Maximum heights of storm surge and components during *Event 1*, *2* and *3*.

Location	Max Surge Effect (m)	Inverse Barometric Height (m)	Resulting Wind Setup (m)
Event 1			
Bramley Drive	0.008	0.104	-0.096
Opureora Point	0.038	0.104	-0.066
Te Puna	0.028	0.104	-0.076
Event 2			
Bramley Drive	0.164	0.093	0.071
Opureora Point	0.137	0.093	0.044
Te Puna	0.149	0.093	0.056
Event 3			
Bramley Drive	0.299	0.058	0.241
Opureora Point	0.294	0.058	0.236
Te Puna	0.316	0.058	0.258

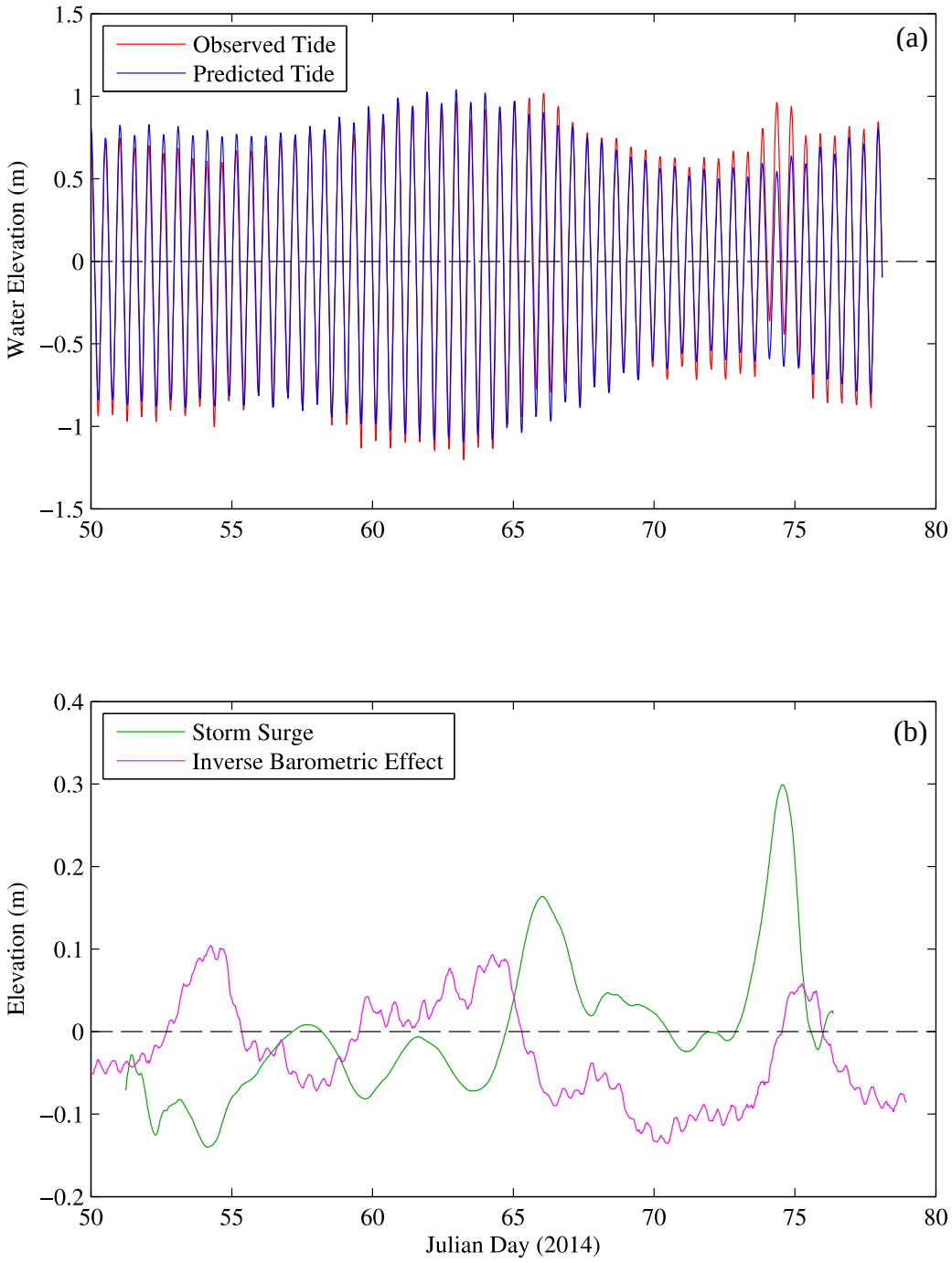

Figure 5.14: Bramley Drive (a) observed and predicted water elevation and (b) storm surge and inverse barometric effect.

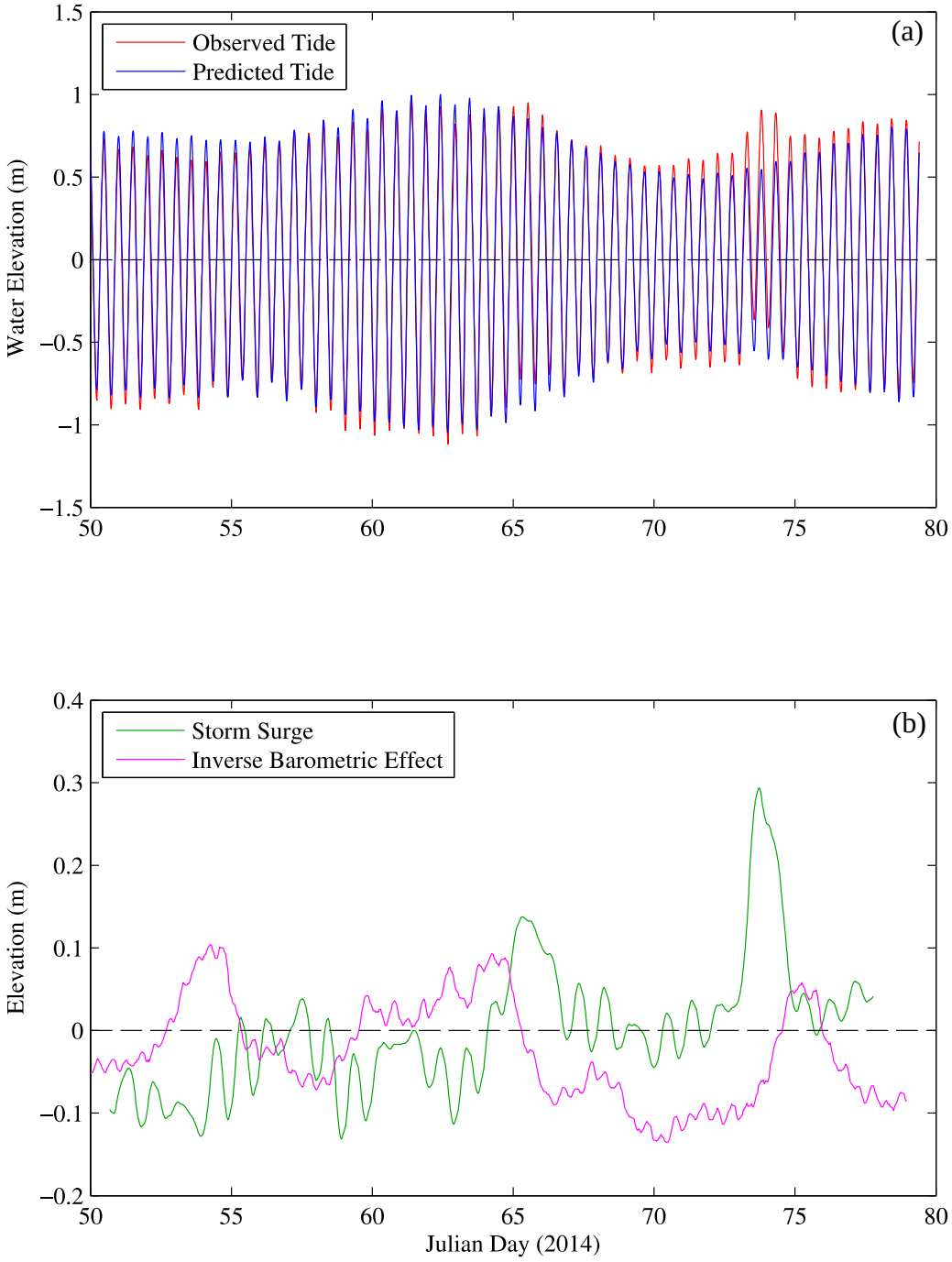

Figure 5.15: Opureora Point (a) observed and predicted water elevation and (b) storm surge and inverse barometric effect.

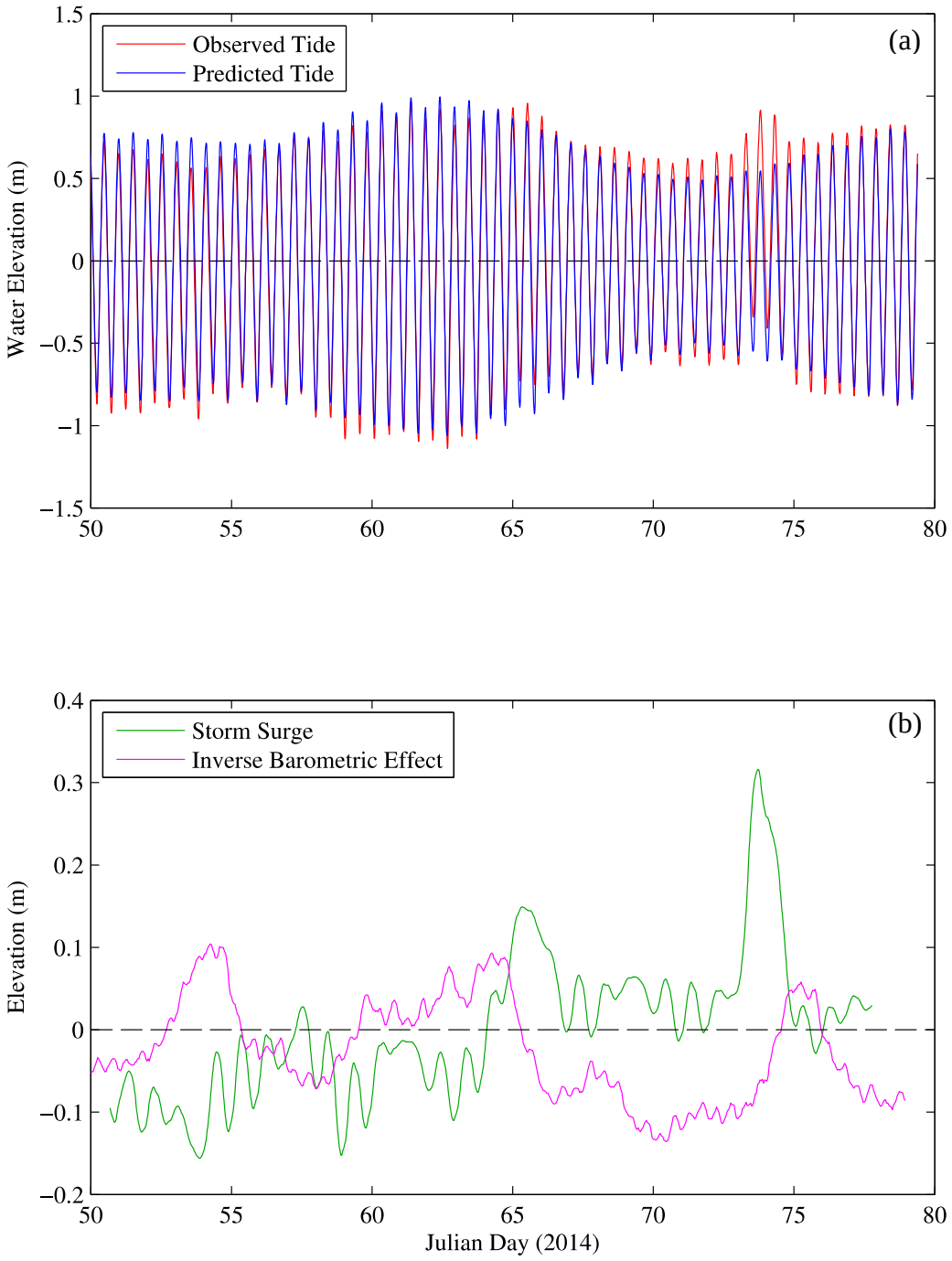

Figure 5.16: Te Puna (a) observed and predicted water elevation and (b) storm surge and inverse barometric effect.

5.4 Wave Characteristics

The measured (RBR) hydrodynamic results (water level, period and significant wave height) at Bramley Drive, Opureora Point and Te Puna, as well as wind speed data recorded at the Tauranga Aero AWS, are presented in Figure 5.18, Figure 5.19 and Figure 5.20, respectively. Significant wave height (H_s) recorded during the deployment period was small, with maximum H_s ranging between 0.059 and 0.211 m (Table 5-5). Bramley Drive had the highest waves of the three sites and exceeded 0.05 m 5% of the time during the deployment period. A large proportion of waves measured at Opureora Point (98%) and Te Puna (97%) were less than 0.02 m high (Figure 5.17). The small wave heights recorded surrounding Omokoroa were difficult to distinguish from noise. If the wave heights are too small to detect, the instrument records noise, returning long periods showing chaotic results.

Table 5-5: Wave statistics

Location	Max H_s (m)	Mean H_s (m)	Mean T (s)
Bramley Drive	0.211	0.012	3.7
Opureora Point	0.059	0.008	5.1
Te Puna	0.152	0.008	4.0

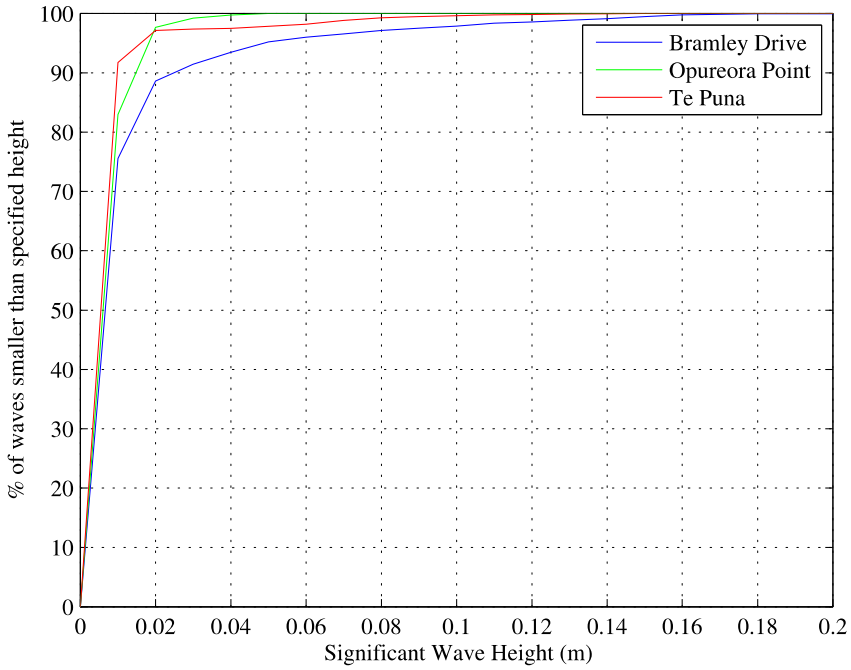

Figure 5.17: Exceedance probability of wave heights.

Wave height was largest at Bramley Drive, recording between 0.10 and 0.21 m with periods between 2.3 and 3.2 s during storm periods (Figure 5.18). Bramley Drive responded to all three high energy events as it is the most exposed site (Figure 5.5). The available fetch at Bramley Drive increased the wind driven stresses, and therefore the wave height. H_s during *Event 1* and *2* were driven by southwesterlies, the larger H_s were recorded during *Event 2* as the water level was higher due to a spring tide. H_s responded to the strong easterly winds associated with ETS Lusi, increasing the wave height. The Bramley Drive RBR is located offshore and was subjected to easterly winds while the western side of the Omokoroa Peninsula was sheltered from easterlies.

Opureora Point results displayed very small significant wave heights. Three minor increases in wave height was recognised at Opureora Point, coinciding with *Event 1, 2* and *3,* reaching a maximum significant wave height of 0.05 m. The effective fetch at Opureora Point was significantly influenced by the periodic subaerial exposure of the intertidal flats, limiting the duration of available fetch for wave generation (Figure 5.6).

No significant increase in wave height was recorded during *Event 1* or *2* at Te Puna, being sheltered by the surrounding topography from southwesterlies (Figure 5.7). A minor increase in H_s is evident over the spring tide as water depths were higher. H_s reached 0.15 m coinciding with *Event 3* driven by the long effective fetch and strong easterly winds.

H_s is a collective function of wind speed, direction and water depth, therefore, stronger winds at exposed sites correlate to larger wave heights. Increased water depth over the spring tidal cycle increased the wave height and lengthened the period. Hence the largest waves occur during spring tides with strong winds.

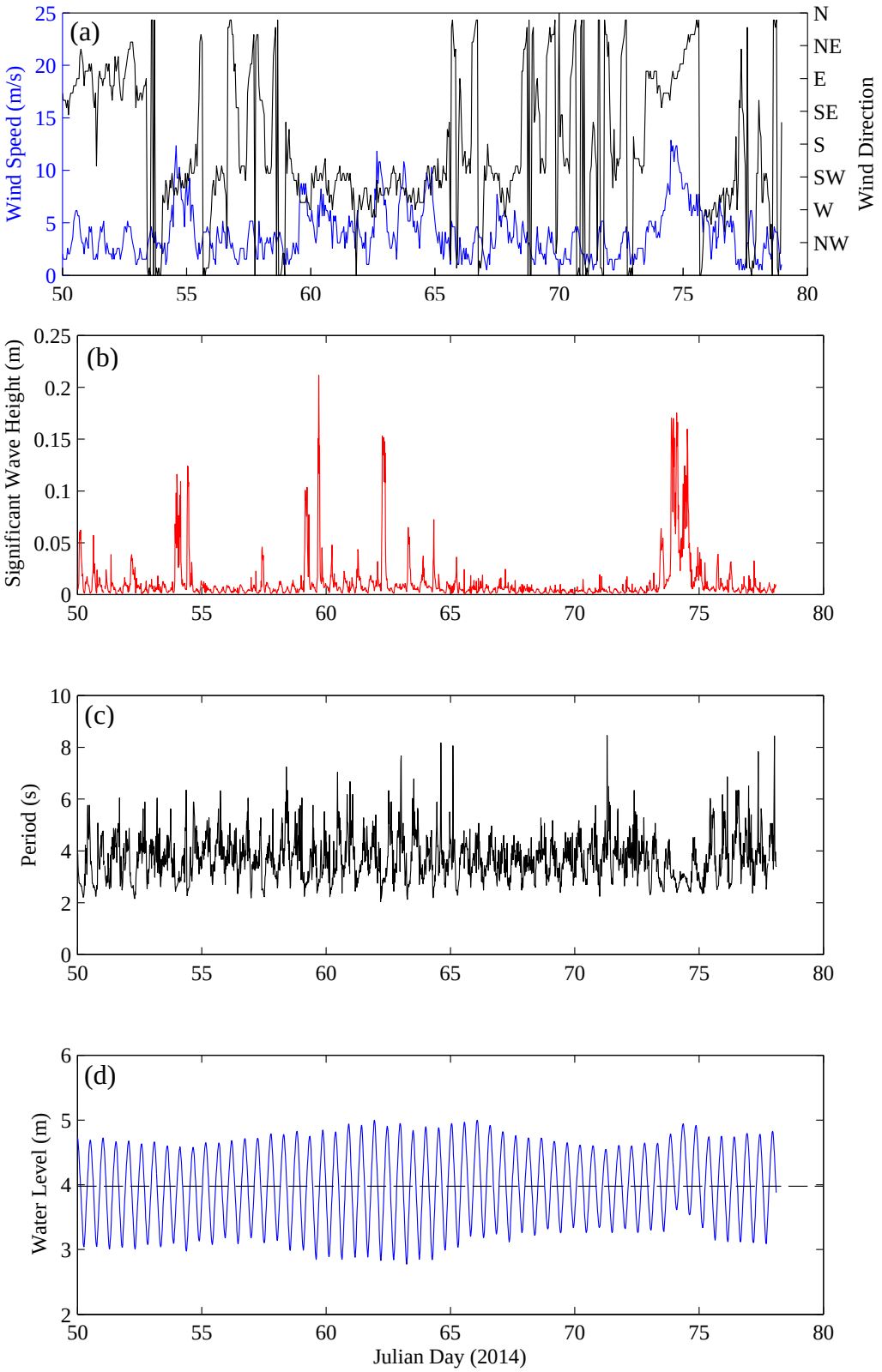

Figure 5.18: (a) wind speed and direction at the Tauranga Aero AWS correlating to (b) significant wave height, (c) wave period and (d) water level at Bramley Drive.

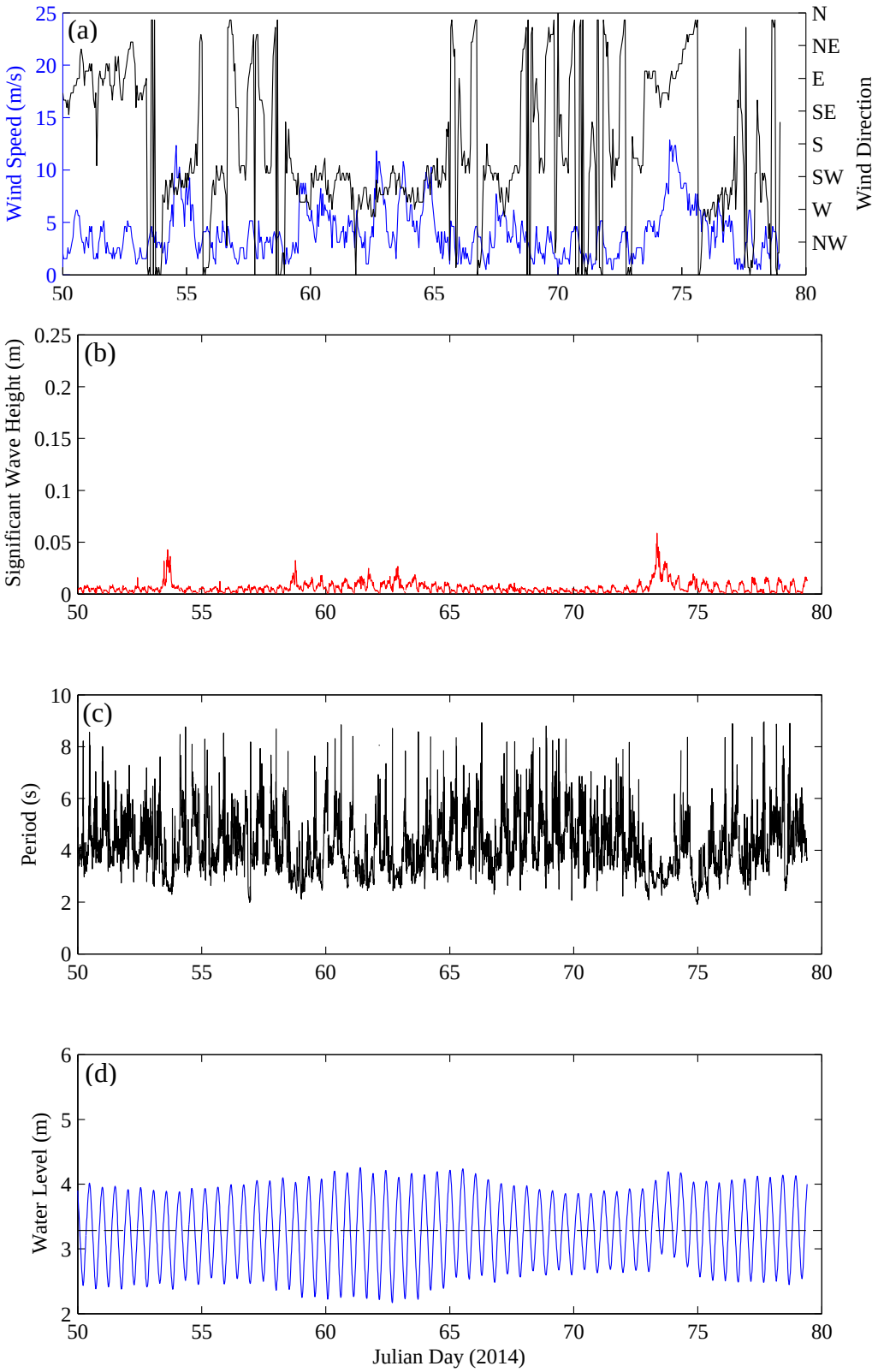

Figure 5.19: (a) wind speed and direction at the Tauranga Aero AWS correlating to (b) significant wave height, (c) wave period and (d) water level at Opureora Point.

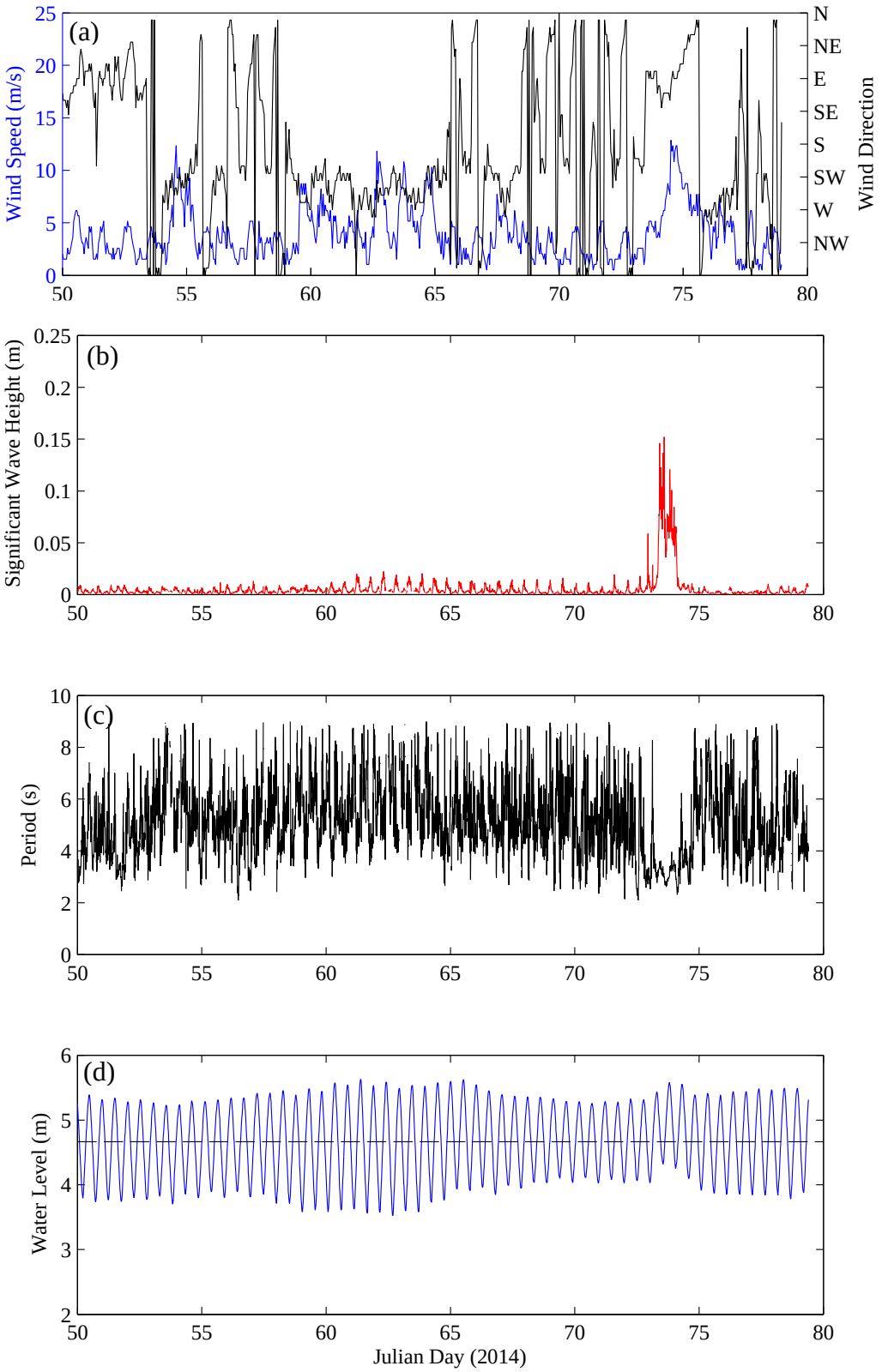

Figure 5.20: (a) wind speed and direction at the Tauranga Aero AWS correlating to (b) significant wave height, (c) wave period and (d) water level at Te Puna.

The largest H_s recorded over the tidal cycle occurred during mid tide, when currents were strongest and opposed the prevailing wind. The largest waves generally occurred during the flood tide over a spring cycle as the tidal prism was larger, thus increasing current speed and water depth. Furthermore, wave heights were elevated at mid tide when the tidal flow opposed the prevailing wind (Figure 5.21a). Opposing wind direction reduced the wavelength in comparison to the wave height, forming steeper waves, recognised as wind-against-tide. Wind-against-tide is subject to wind speed and direction in relation to the current speed and direction.

Wind-against-tide influences H_s during high energy events. The largest H_s corresponding with *Event 3* occurred during the ebb tide as the strong easterly winds opposed the east flowing ebb current (Figure 5.21b). Opureora Point differed from the other sites due to the tidal cycle limiting the duration of fetch. Under normal conditions, the largest wave heights at Opureora Point occur at mid tide, driven by wind-against-tide. However, the larger wave heights recorded during high energy events generally occurred at, or near, high tide as the available fetch increased wind generated waves (Figure 5.21c).

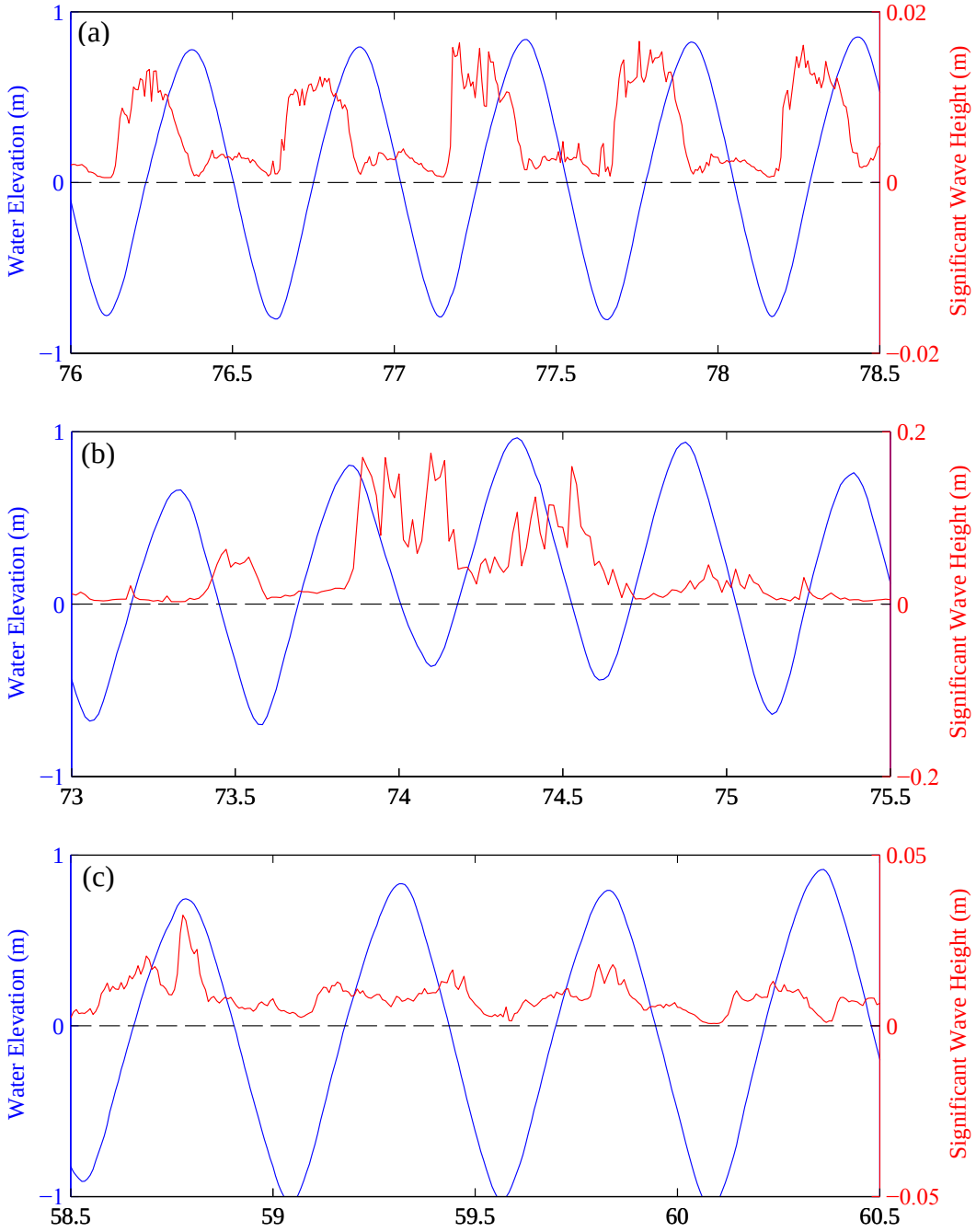

Figure 5.21: Wave height and water elevation at (a) Te Puna, (b) Bramley Drive and (c) Opureora Point. Note (c) has a different x-axis to (a) and (b).

5.4.1 Sediment threshold

Figure 5.22 and Figure 5.23 provides an indication of wave steepness based on wave height and wave period. Results suggest locally generated waves, of which no waves have been recorded as breaking, although those close to the critical wave steepness may break depending on the wind conditions. Results correlate to those

by de Lange and Healy (1990) who demonstrated that the harbour entrance filters out most of the wave energy, therefore waves in the upper harbour must be locally generated.

The breaking wave height is controlled by water depth which determines the ability of waves to transport sediment. Within the tidal channels (approximately 3 m water depth) the waves are not considered an important factor controlling sediment transport as the water is too deep (Figure 5.22a). Applying the wave characteristics measured to progressively shallower water depths illustrates an increase in the ability of waves to transport sediment (Figure 5.22). In shallower water, on the intertidal flats, sediment transport by waves becomes important. At Bramley Drive, in 0.5 m water depth few waves were large enough to transport sediment (Figure 5.22b). Water depth reduction to 0.2 m indicated that a larger proportion of waves breaks and were therefore capable of shifting sediment (Figure 5.22e).

The threshold depth for sediment transport differed at each location. Bramley Drive recorded the largest wave heights and hence had a higher proportion of waves capable of transporting sediment. The sediment transport threshold at Bramley Drive was ~0.2 m water depth, while at Te Puna, few waves exceeded the sediment threshold in 0.1 m water depth. Sediment transport by waves will hence occur in water depths shallower than ~0.1 m (Figure 5.23b). Results from Opureora Point suggest that in 0.1 m water depth, the small wave heights recorded do not have the ability to transport sediment (Figure 5.23a).

Sediment transport driven by waves tends to move coarse sediment onshore whereas fine material was transported out of the harbour as the settling time is much longer. Fine sediment transport away from the site correlated with observations of the removal of debris at the Bramley Drive landslide.

Sediment transport by waves in shallow water, identified in the results, highlights the effect of the turbid fringe. The results suggest that sediment transport by waves occurs in shallow water on the intertidal flats on the rising and falling tide. These findings are consistent with Dolphin (2003) who found that in the Manakau Harbour, the suspended sediment transport was confined to a near bed layer of approximately 10 cm thick.

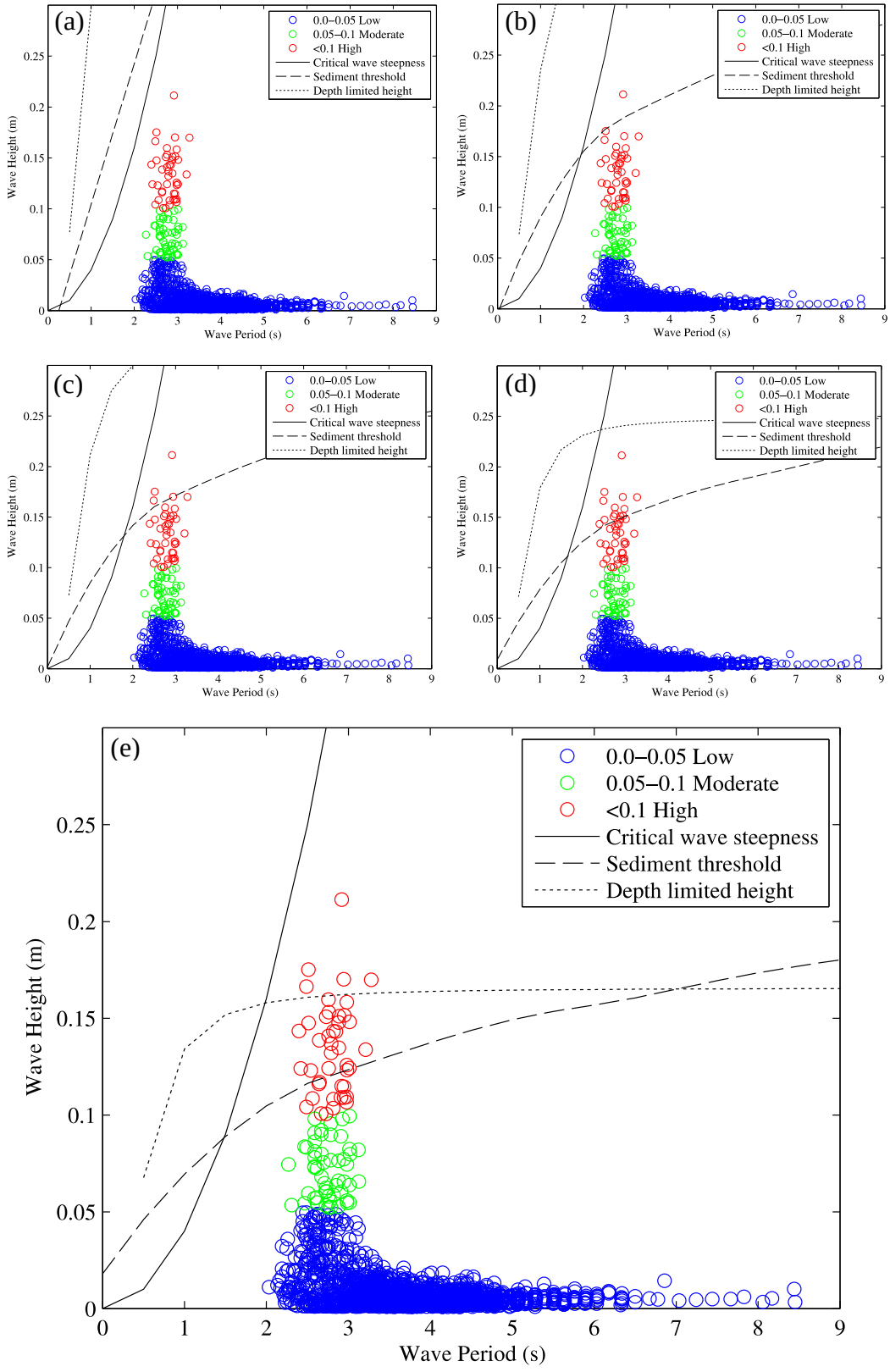

Figure 5.22: Joint probability of wave height and wave period indicating wave steepness at Bramley Drive. Series of shallowing water depths to depict relationship between wave steepness and sediment threshold. Water depths; (a) 3 m, (b) 0.5 m, (c) 0.4 m, (d) 0.3 m and (e) 0.2 m.

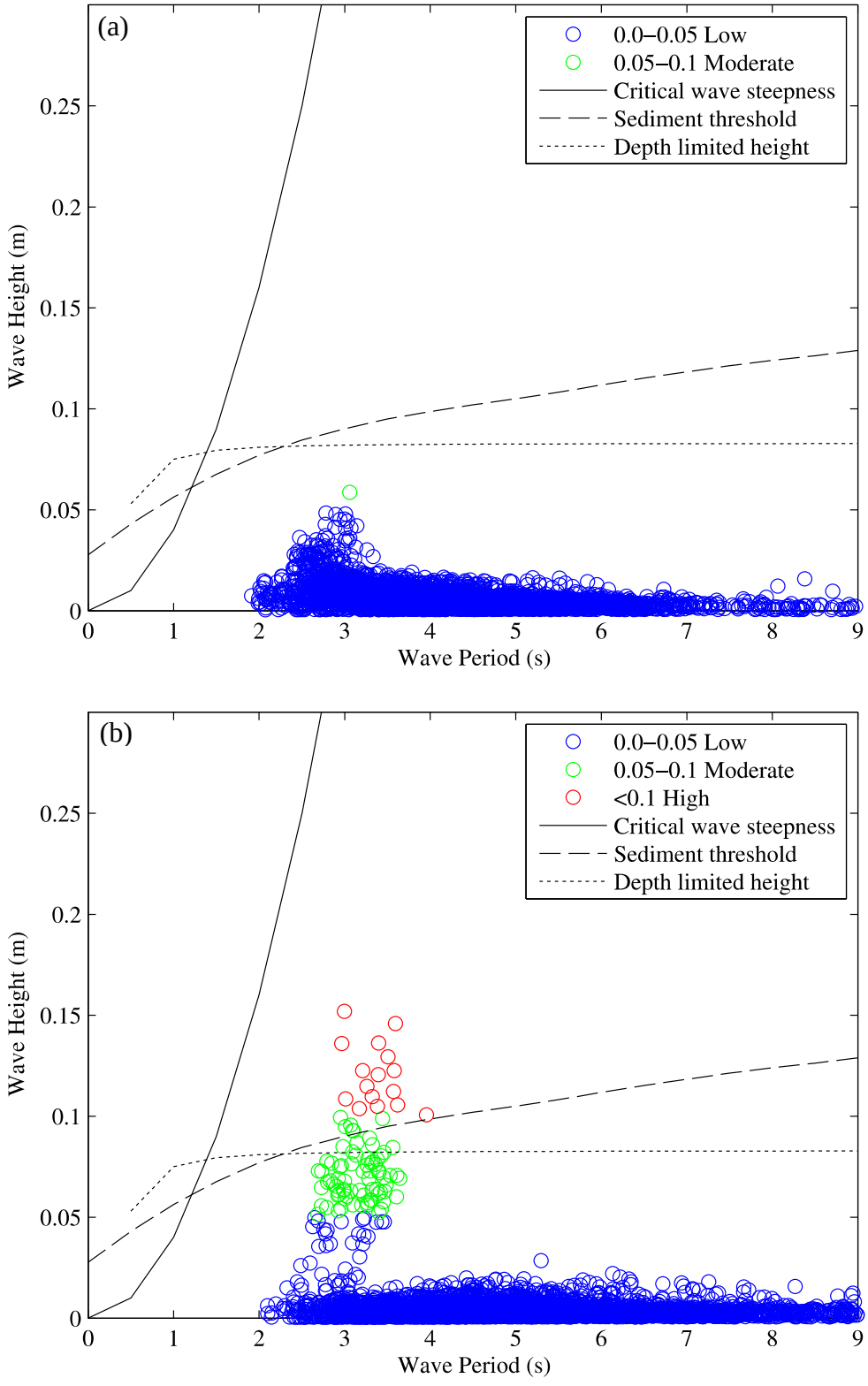

Figure 5.23: Joint probability of wave height and wave period indicating wave steepness at (a) Opureora Point in 0.1 m water depth and (b) Te Puna in 0.1 m water depth.

5.5 Currents

Current measurements (S4), including north and east mean velocity and water elevation at OMO North, OMO Wharf and Western Channel, are presented in Figure 5.25, Figure 5.26 and Figure 5.27, respectively. Strongest mean velocities were observed at OMO North (12.09 cm/s) and Western Channel (12.05 cm/s). OMO Wharf recorded a lower mean velocity (10.13 cm/s). Strongest currents occurred essentially at mid tide, correlating to the largest wave heights as H_s is a function of wind-against-tide. The dominant tidal flow varied at each site, with Western Channel and OMO Wharf being flood dominant and OMO North ebb dominant (Table 5-6). Previous studies indicate that inside the harbour, currents are predominately flood dominated (Davies-Colley & Healy, 1978). Kwoll (2010) found that the Western Channel was ebb dominant, however, the instrument was located east of that in this study, and was likely to be influenced by the behaviour of the flood tidal delta.

de Lange (1988) predicted entrainment velocities of marine sand between 30-35 m/s. The maximum current velocities recorded (10-12 m/s) are well below the velocity required to erode and transport sediment.

Table 5-6: Average current velocity and direction.

Location	Mean Depth (m)	Mean Velocity (cm/s)	Mean Direction (degN)	Mean Flood Velocity (cm/s)	Mean Flood Direction (degN)	Mean Ebb Velocity (cm/s)	Mean Ebb Direction (degN)
OMO North	2.9269	12.1	124.7	21.9	275.8	43.2	112.1
OMO Wharf	4.1304	10.1	345.0	36.8	0.0	17.7	196.9
Western Channel	2.8781	12.1	235.9	43.7	255.3	23.4	95.5

The recorded currents reflect the tidal behaviour within the Tauranga Harbour as the predominant flood tidal flow travels through the Western Channel which splits either north or south of Motuhoa Island. The mean flood direction at Western Channel (255.3 degN) suggests the dominant flood flow is south past Motuhoa Island. Currents south of Motuhoa Island, during flood, pass Omokoroa Wharf

heading north. The ebb tide flows east-southeast past the Omokoroa Peninsula, splitting either side of the exposed intertidal flats, between Motuhoa Island and Omokoroa, or north of Motuhoa Island, before flowing south past Omokoroa Wharf. The behaviour of the tidal currents were governed by the three operating channels around the Omokoroa Peninsula.

Current velocities at all of the sites are asymmetric about zero, indicating a residual tidal flow. Current velocities respond to spring-neap tidal cycles. Stronger currents were recorded during spring tides associated with an increased tidal prism. Furthermore, all sites show a decrease in current velocity over the deployment period. The decrease in current velocity is more pronounced on the ebb tide, particularly in the Western Channel (Figure 5.27). The decrease in tidal range, and hence the reduced currents, correlates to the perigee to apogee lunar cycle. Tidal ranges during 2014 at Moturiki Island are presented in Figure 5.24. The spring and neap range decreased during the deployment period which were responsible for reduced current velocities.

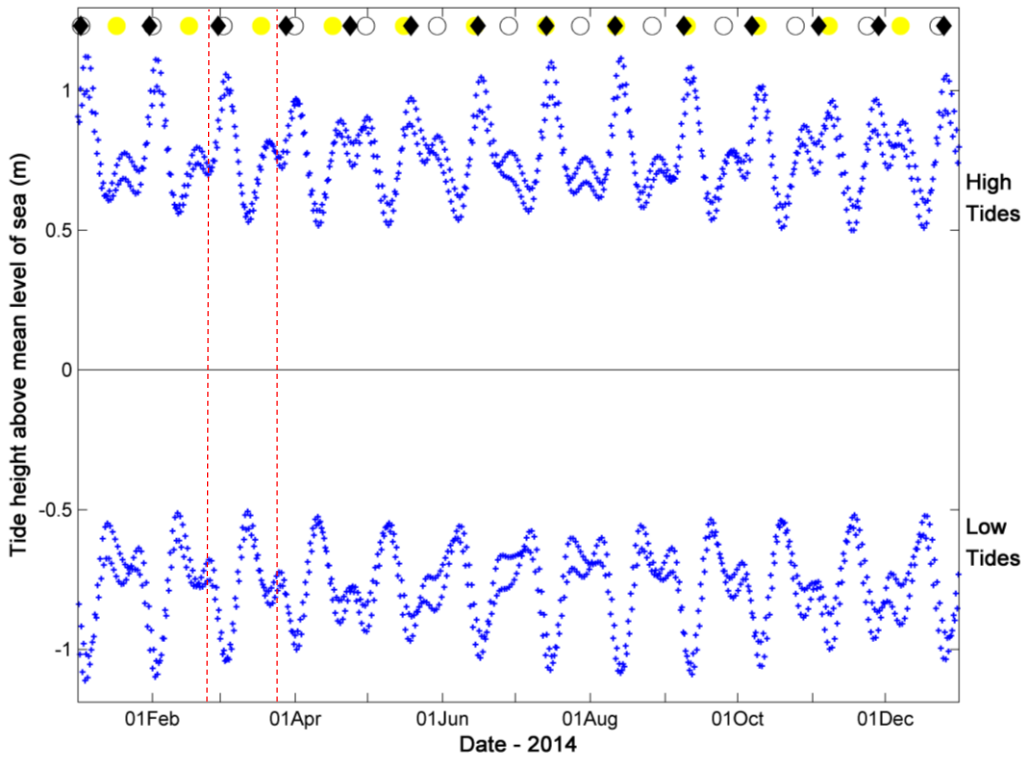

Figure 5.24: Tidal envelope at Moturiki Island, Mount Maunganui, dotted lines indicate deployment period (NIWA, 2014).

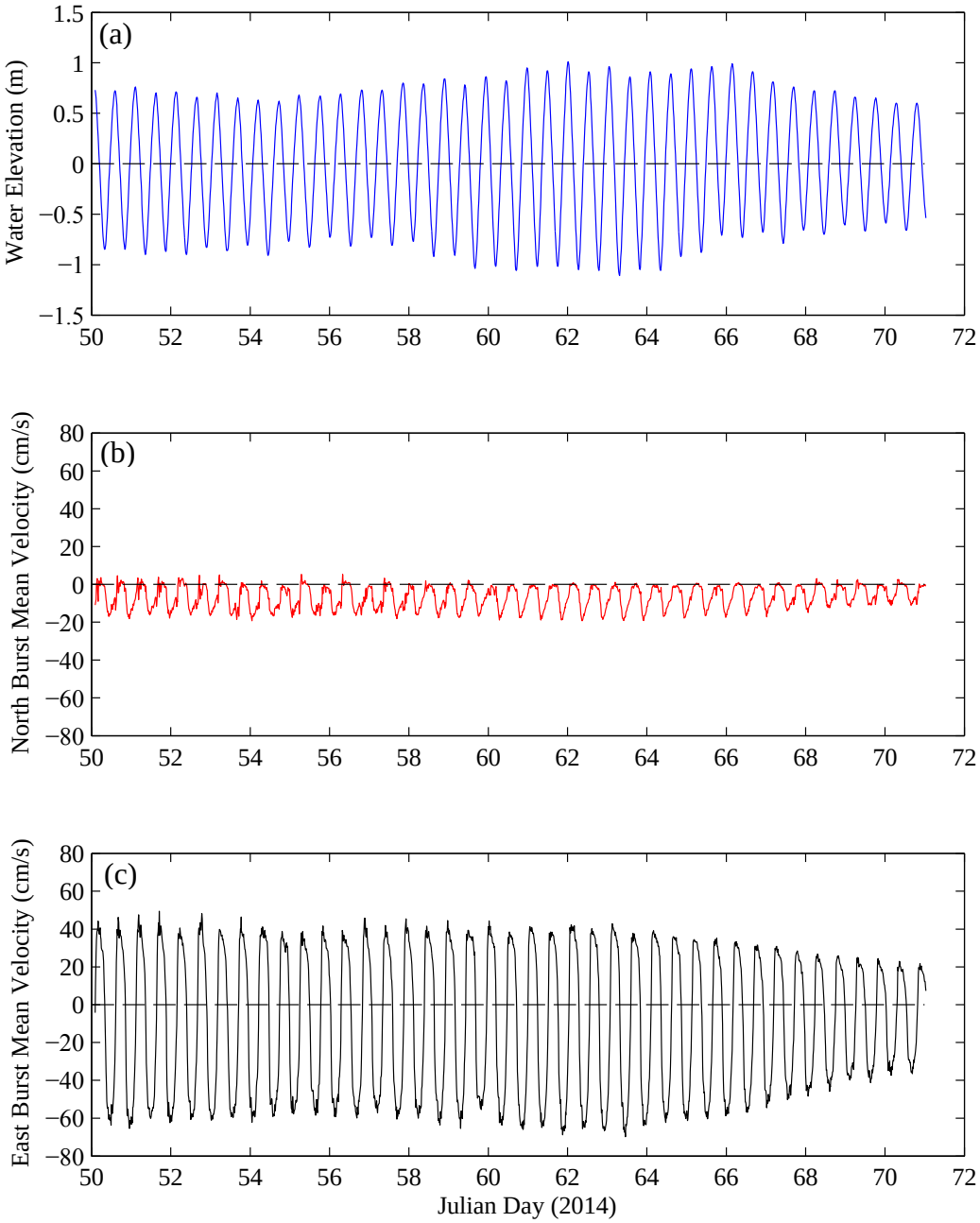

Figure 5.25: (a) water elevation, (b) north mean velocity and (c) east mean velocity at OMO North.

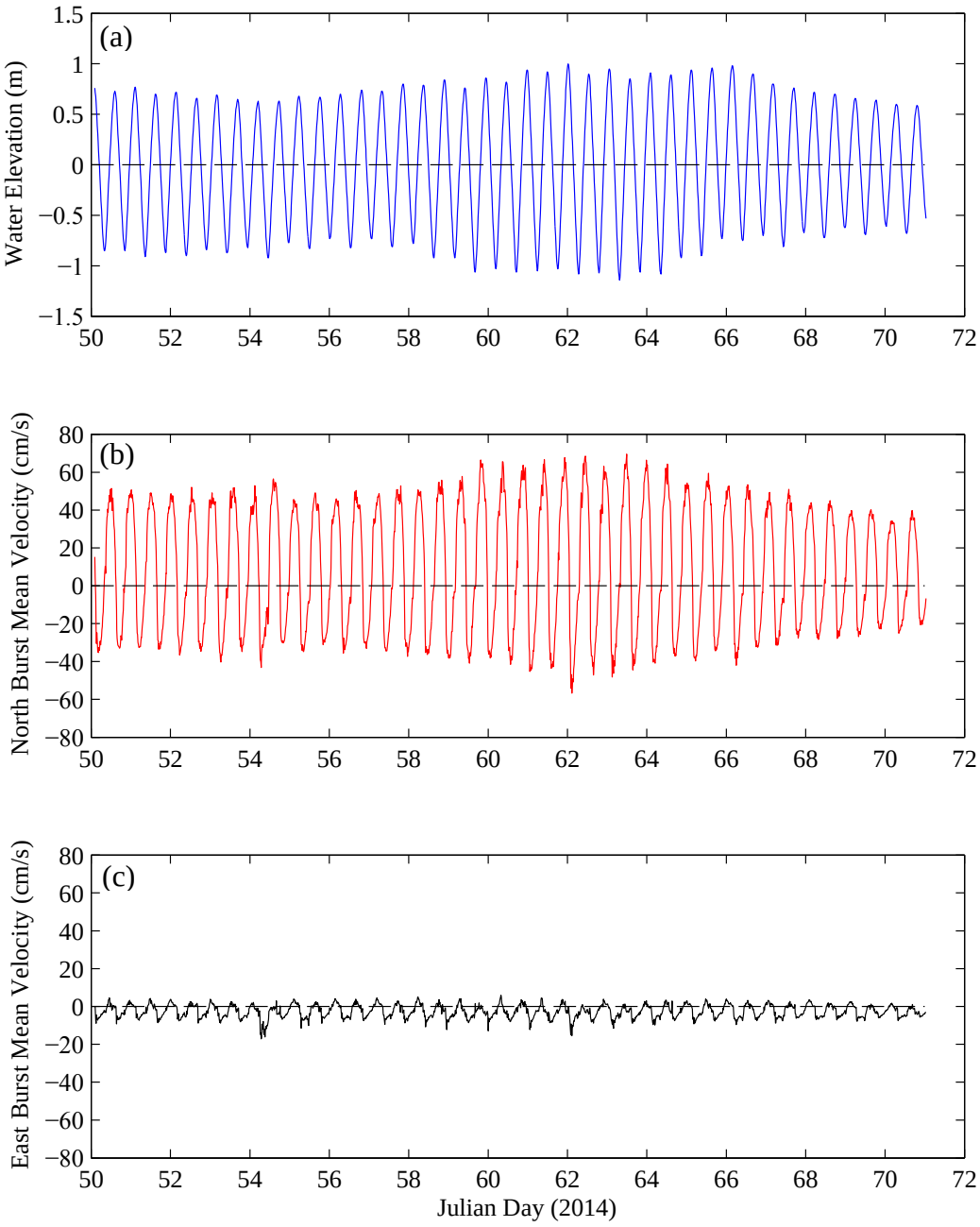

Figure 5.26: (a) water elevation, (b) north mean velocity and (c) east mean velocity at OMO Wharf.

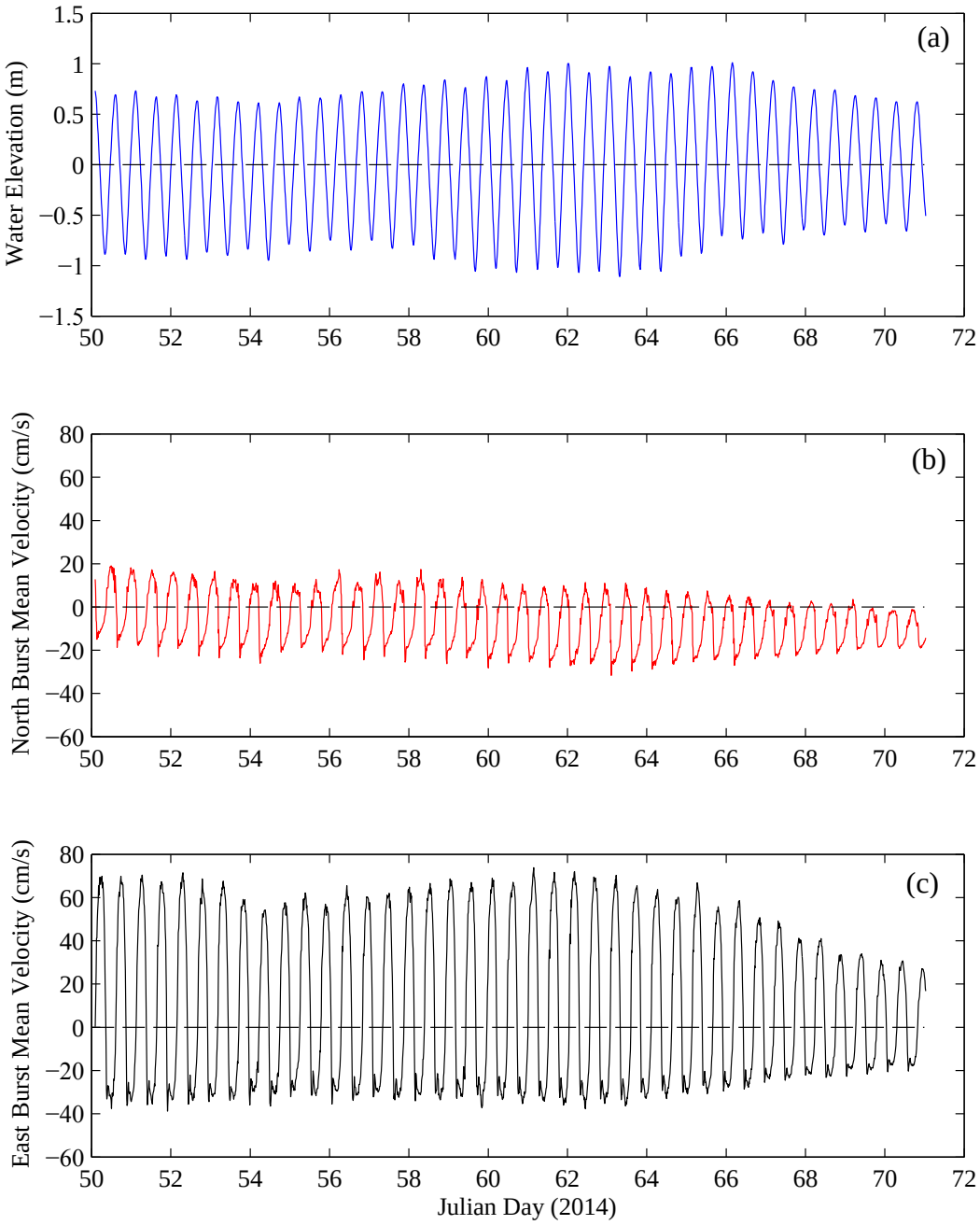

Figure 5.27: (a) water elevation, (b) north mean velocity and (c) east mean velocity at Western Channel.

5.5.1 Influence of the ferry

Figure 5.28 illustrates the direction of currents at OMO wharf, suggesting that the ferry influences the currents at the boat ramp. Deviations from the mean tidal currents were evident on the ebb tide, with greater impact when the ferry was manoeuvring close to slack water. Overall, effects of the ferry propeller wash were minor.

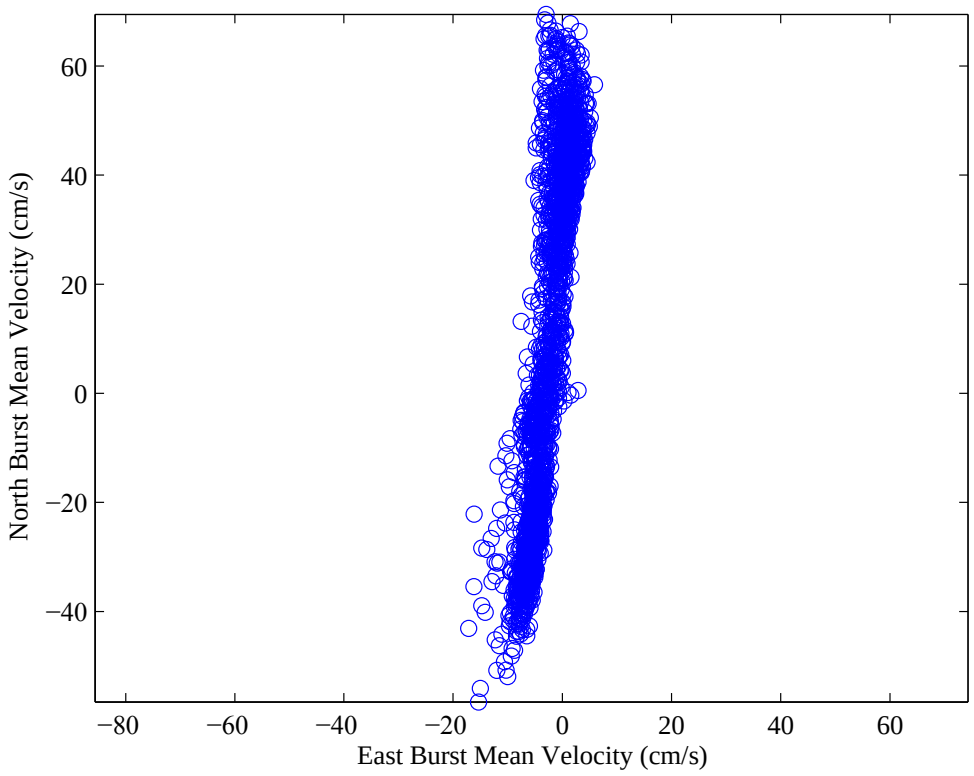

Figure 5.28: Current directions at OMO wharf showing influence of the ferry.

5.6 Predicted wind wave generation

Monochromatic wave parameters were calculated for given wind generation conditions using Carter (1982). Calculated wave characteristics were determined at the three sites where wave parameters were measured (Bramley Drive, Opureora Point and Te Puna), as well as at the boat ramp. Input parameters included wind speed, available fetch and wind duration. Two scenarios were calculated for normal and storm conditions. Wind speed was determined based on meteorological data attained from Tauranga Aero AWS. Average wind speeds during normal conditions was 3 m/s and 10 m/s in storm conditions. The duration of wind speed was limited

to 3 hours, taking into consideration the available fetch restrictions over the tidal cycle. The longest effective fetch calculated previously at each site was applied (Figure 5.5, Figure 5.6, Figure 5.7 & Figure 5.8).

Results of the calculated monochromatic wave parameters are presented Table 5-7. Wave generating conditions show wave growth was fetch-limited, apart from at Bramley Drive during normal conditions which is duration-limited. Fetch-limited wave generation indicates that the distance over which the wind is in contact with the surface is not sufficient to enable full development of the wave. Calculating H_s during normal conditions overestimated the mean measured H_s by an order of 16 at Opureora Point, 15 at Te Puna and 13 at Bramley Drive. During storm conditions the calculated H_s was an order of 2.6 at Bramley Drive, 7.3 at Opureora Point and 2.7 at Te Puna, greater than the measured H_s.

The relative measured H_s at the boat ramp was determined by using an average of that the calculated H_s overestimated the measured H_s. The mean H_s at the boat ramp would be 0.006 m and max H_s 0.109 m. The max H_s determined for the boat ramp did not consider the magnitude difference at Opureora Point.

Applying the longest effective fetch, of which waves are fetch-limited, significantly overestimated the wave height and suggest that further obstructions inhibited the generation of waves surrounding the Omokoroa Peninsula. Field observations suggest that waves were depth-limited, which explains to some degree the overestimate of wave height.

Table 5-7: Wind wave generation based on Carter (1982) of the longest fetch at each site.

	Bramley Drive	Opureora Point	Te Puna	Boat ramp
Normal Conditions				
Wind speed (m/s)	3	3	3	3
Effective fetch (km)	11.5 (325˚)	6.9 (305˚)	6.2 (85˚)	3.2 (90˚)
Critical duration (h)	4.2	2.9	2.7	1.7
Generating conditions	Duration-limited	Fetch-limited	Fetch-limited	Fetch-limited
H_s (m)	0.13	0.13	0.12	0.09
Peak period (s)	1.62	1.57	1.52	1.25
Crest period (s)	1.26	1.22	1.18	0.97
Storm Conditions				
Wind speed (m/s)	10	10	10	10
Effective fetch (km)	11.5 (325˚)	6.9 (305˚)	6.2 (85˚)	3.2 (90˚)
Critical duration (h)	2.6	1.8	1.7	1.1
Generating conditions	Fetch-limited	Fetch-limited	Fetch-limited	Fetch-limited
H_s (m)	0.55	0.43	0.41	0.29
Peak period (s)	2.96	2.53	2.46	2.02
Crest period (s)	2.29	1.97	1.91	1.57

5.7 Settling velocity

For suspended sediment, the flow velocity must be greater than the settling velocity in order for sediments to remain in suspension. Ahrens' (2000) method was applied to calculate settling velocity based on the mean grain size of sediments on the eastern side of the Omokoroa Peninsula, adjacent to the boat ramp at high and low tides and on the boat ramp. Additionally, settling velocity was calculated at high and low tides surrounding Plummers Point. Further input parameters included fluid temperature (15˚C), fluid salinity (30) and sediment density (2650 kg/m^3), which remained constant for all calculations.

Results illustrate that the settling velocity at both Omokoroa and Plummers Point at high tide was significantly greater than that calculated for low tide, reflecting the difference in grain size (Table 5-8). Correlating the settling velocity to the maximum currents recorded in the surrounding channels (10-12 m/s) suggests that entrained sediments from the high tide zone will rapidly drop out of suspension and will not be transported far from the source. The finer sediments on the intertidal flats and boat ramp are likely to be transported further by currents, dropping out of suspensions as currents decrease towards slack tide.

Table 5-8: Settling velocity calculated based on Ahrens (2000).

Location	Mean grain size (phi)	Settling velocity (cm/s)
Omokoroa		
High tide	0.89	6.2
Low tide	1.97	2.6
Boat ramp	2.27	2.0
Plummers Point		
High tide	0.90	6.2
Low tide	2.21	2.1

5.8 Summary

Results from the hydrodynamic analysis illustrate the dynamic wave and tidal processes occurring at Omokoroa Peninsula, influencing the sediment transport patterns.

- The fetch is influenced by the surrounding topography and tidal range. The surrounding topography shelters the Omokoroa Peninsula from ocean swells and is further limited by the location of islands. The tidal range restricts the available fetch due to intermittent subaerial exposure of the intertidal flats.
- Tidal asymmetry around Omokoroa is irregular as the behaviour of the tide differs over the tidal cycle. The tidal flows surrounding the Omokoroa Peninsula are hard to predict as the three operating channels have different dimensions and are likely to be influenced by wind stress.

- The harmonic analysis illustrates that the principle lunar semidiurnal constituent, M2, was the largest at all locations. The propagation of the tide into the Tauranga Harbour is subjected to tidal amplification due to hypersynchronous behaviour as tidal convergence outweighs the frictional effects.
- Two significant storm surges were recorded over the deployment period following *Event 2* and during *Event 3* being driven by atmospheric pressure differences of which strong winds significantly increased the height of the storm surge.
- H_s were largest at Bramley Drive, although overall recorded H_s were small and each site only exceeded 0.05 m in stormy conditions. H_s is a function of wind speed and direction, water depth and current speed and direction.
- The currents reflect the behaviour of the operating channels surrounding the Omokoroa Peninsula. Over the deployment period a reduction in tidal currents occurred due to the perigee to apogee lunar cycle. The residual tidal currents differed at each location. At the boat ramp, residual tidal currents were north whereas north of Omokoroa residual tidal currents were east.
- Continuous tidal action and episodic wind generated waves are the primary factors influencing sediment transport at Omokoroa. Sediment entrainment is driven by waves and is confined to shallow depths (10-20 cm) on the rising and falling tides, defined as the turbid fringe. Current velocities do not have the ability to entrain sediment into suspension, however, once entrained, are capable of transporting sediment.

Chapter Six

SEDIMENTS

This chapter investigates the underlying geology and surficial sediments surrounding the Omokoroa Peninsula. Initially, the stratigraphy of the area is presented, based on descriptions of cliffs sections and cores retrieved from the intertidal flats to reveal historic sedimentation patterns. Present sedimentation patterns are determined through the application of a Sediment Trend Analysis (STA), based on sediment textural parameters of surficial sediments. Finally, sedimentation on the boat ramp is correlated to weather episodes to establish any sedimentation patterns associated with storm events. Establishing sedimentation patterns is essential in determining the morphodynamic evolution of the Omokoroa Peninsula.

6.1 Stratigraphy

6.1.1 Cliffs

Figure 6.1 illustrates the geology forming the Omokoroa Peninsula based on exposures at coastal cliff sections (Figure 3.2), including the stratigraphy obtained from a borehole at Bramley Drive described by B. Steinborn (pers. comm. 2015). The geological units identified include Matua Subgroup, Te Puna Ignimbrite, Pahoia Tephras, Hamilton Ash and Rotoehu Ash.

At Site 1, the shore platform is lined by a discontinuous unit identified as a fluvial, overbank deposit (grey estuarine mud), capped with a thin lignite deposit. The unit is 1.3 m thick and subject to undercutting. Orange brown fluvial sands overlie the estuarine mud at Site 1 (2.8 m). The units identified at Site 1 do not appear to correlate with other sites described along the peninsula. The Matua Subgroup comprises a wide variety of lithologies which have been classified into four facies. Lignite beds are the lowermost unit identified at Site 2, exposed on the shore platform at the north eastern point. The lignite beds do not further outcrop along the peninsula but were identified below sea level at Bramley Drive as a much thicker

unit. At Bramley Drive, an olive brown paleosol is identified above the lignite beds. A dark brown fluvial sand unit overlies lignite beds at Site 2 and is further overlain by pumiceous fluvial sands and silts (~1 m), correlating with descriptions of the lower section at Bramley Drive. Te Puna Ignimbrite is evident from Site 2 though to Site 5. The thickness of the unit varies, illustrating a significant degree of relief over both the upper and lower surfaces. A thick sequence of Pahoia Tephras covers Te Puna Ignimbrite. At Sites 3 and 4, formation of a well-developed paleosol is evident at the top of the Pahoia Tephras. At Bramley Drive, thickness of the Pahoia Tephras exceeds 10 m and is interrupted by a paleosol in the middle section and at the top of the unit. Hamilton Ash is evident above the paleosol of the Pahoia Tephras at Sites 3 and 4, as well as at Bramley Drive. At Sites 3 and 4, the upper paleosol of the Hamilton Ash is not observed. Thickness of the Hamilton Ash sequence increases at Bramley Drive and includes the upper paleosol. At Bramley Drive, Rotoehu Tephra overlies the Hamilton Ash. A thin layer of modern topsoil is evident at locations where the surface is exposed.

Due to site restrictions limiting access to the upper units, a textural analysis could not be conducted and is therefore estimated by visual inspection.

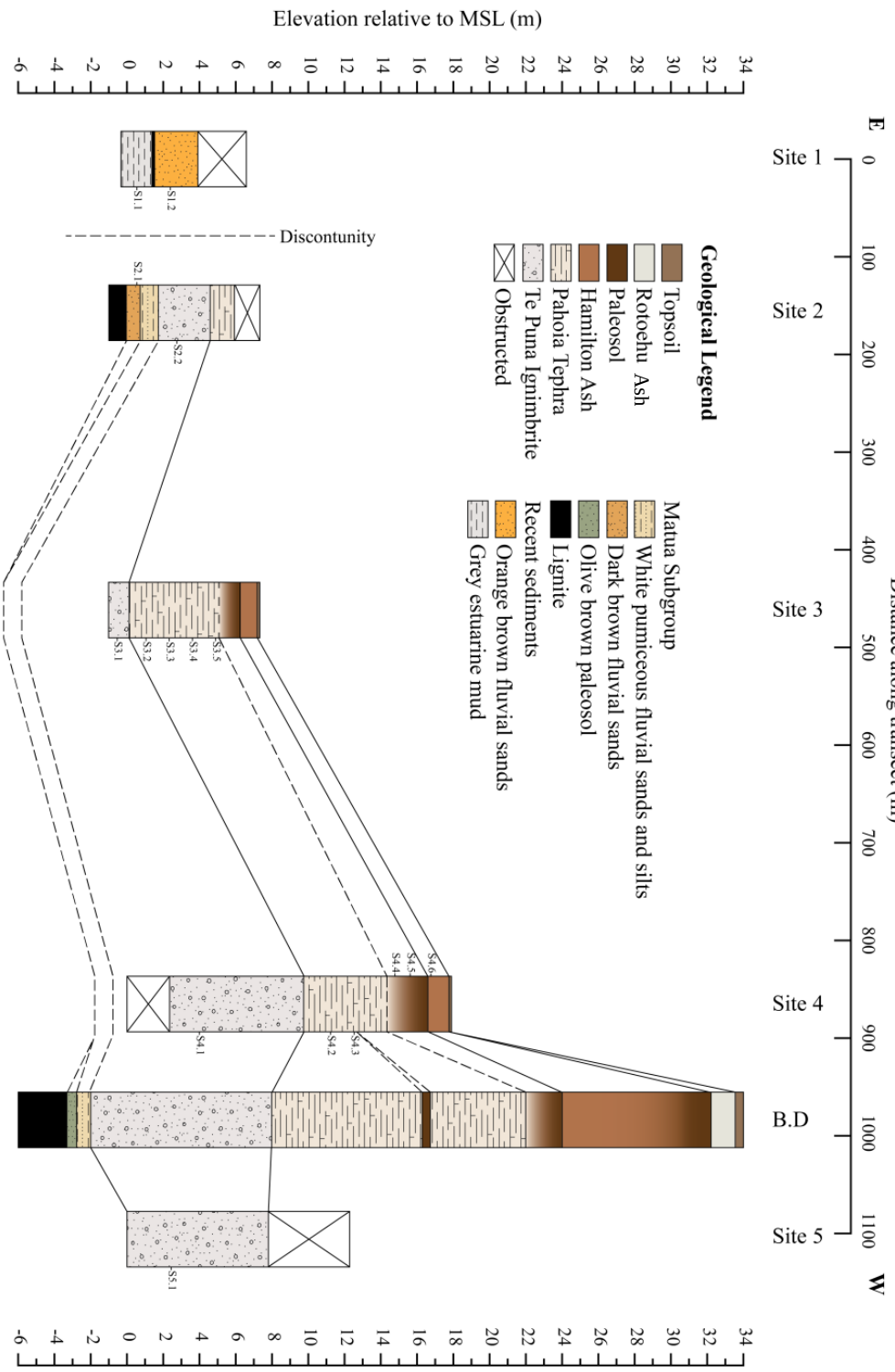

Figure 6.1: Fence diagram of the stratigraphy along the Omokoroa Peninsula.

6.1.2 Estuarine sediments

Subsurface stratigraphy, retrieved from cores surrounding the Omokoroa Peninsula, displays significant changes in lithology both vertically and laterally, representing a complex sedimentary sequence with a number of depositional environments (Figure 6.2, Figure 6.3 & Figure 6.4). Core logs are presented in Appendix 1.

General stratigraphy comprises a lowermost unit of fluvial volcaniclastic sediments which can be correlated to Pleistocene sediments onshore. The lowermost Pleistocene fluvial sediments are only encountered along the western margin, illustrating significant relief over the surface. Pleistocene fluvial sediments are overlain by marine sands and shells that infill depressions. An erosional unconformity separates these units. The uppermost unit consists of organic rich fine estuarine sand on the intertidal flats or, at some sites, fluvial deposits are situated above the marine sediments.

Underlying Pleistocene sediments reflect the regional underlying geology and can be correlated to cliff sections. A laminated sequence of the Pahoia Tephras is identified underlying transect 5, whereas Te Puna Ignimbrite is evident underlying transect 6.

On the eastern margin, the overlying marine sediments that infill depressions include various thicknesses of silts and sands with layers of shell fragments and disarticulated bivalves.

The uppermost unit, identified from intertidal cores (cores 2 and 3 along any transect), is comprised of organic rich fine sand deposited in the present day environment. The contact between the underlying marine sand and organic rich fine sand varies. In some locations there is a gradational contact, whereas at other sites there is a sharp boundary, the differences between which indicate the presence of an unconformity. On the western margin, only a thin layer of organic rich fine sand overlies the Pleistocene fluvial sediments, indicating very low accumulation rates. Core 1 of transects retrieved from the eastern margin contains terrestrial sediments.

Material includes medium to coarse sand and laminated silts and sands, collectively indicative of beach reworking and pulses of sediment from a fluvial input.

6.1.2.1 Radio carbon ages

Radiocarbon ages of sediments are from cores at localities 1.1, 2.1 and 4.1. Results are presented in Figure 6.2, Figure 6.3 and Figure 6.4, respectively, illustrating the stratigraphic relations. Age reports and calibrations are presented in Appendix 2.1.

The lowermost unit in core 1.1 is an estuarine silt, further overlain by silt with disarticulated bivalves which dated at 1,652 ± 20 BP, before grading into a coarsening-upwards estuarine silt sand intermix. The overlying unit is comprised of medium sand capped with a thin layer of organics. Medium to coarse sand overlies the organic material with laminations of increased fine sand/silt followed by beach sand, rich in heavy minerals, indicative of the current environment.

Core 2.1 comprises a lower sand silt intermix with few disarticulated bivalves at the top. This was followed by medium to coarse sand overlain by a gravelly sand unit with shell and rock fragments. Coarse beach sand continued before a thin layer of organic material which has an age of 20,131 ± 66 BP. Above the organic material a thin layer of sand is subject to oxidisation. This is followed by beach sand containing heavy minerals, followed by a chaotic clay intermix overlain by beach sand with layers of increased heavy minerals and rubble likely from construction of roads or the seawall. The chaotic nature of sediments surrounding the sample dated, and the history of human modification in this area, suggest the radiocarbon age may not be from sediments deposited *in situ*.

The lower section of core 4.1 contains fluvial pumiceous sediments. The lowermost part contains a silt sand intermix with gravel size pumice pieces, grading into a silt with sand stringers and rootlets overlain by a tephra with bioturbation at the base. Overlying the tephra is ~5 cm thick organic layer with an age of 7,676 ± 30 BP, followed by a coarse sand with stringers of heavy minerals. The uppermost unit consists of beach sand with disarticulated bivalves with an age of 1970 AD.

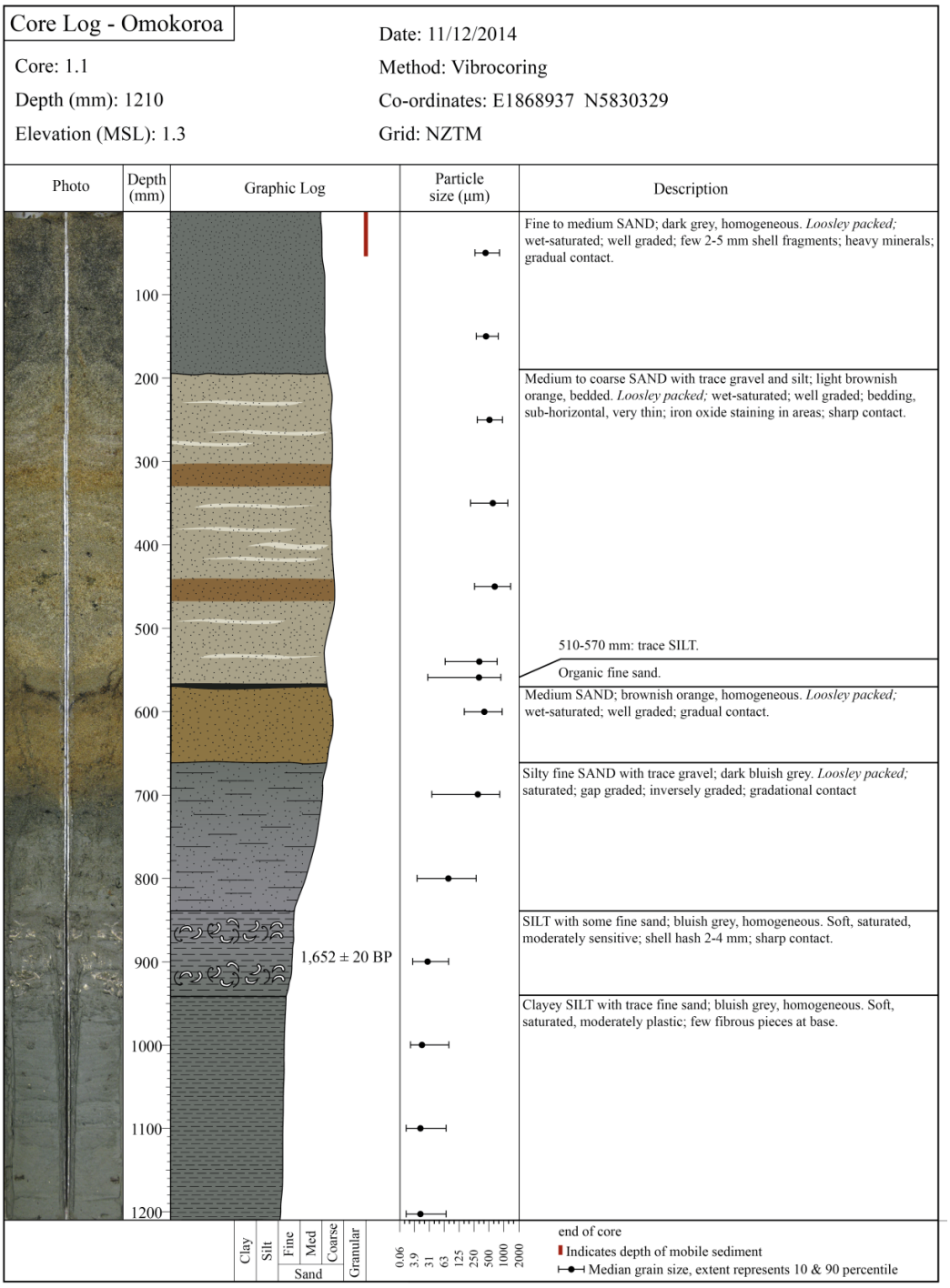

Figure 6.2: Stratigraphic log of core 1.1.

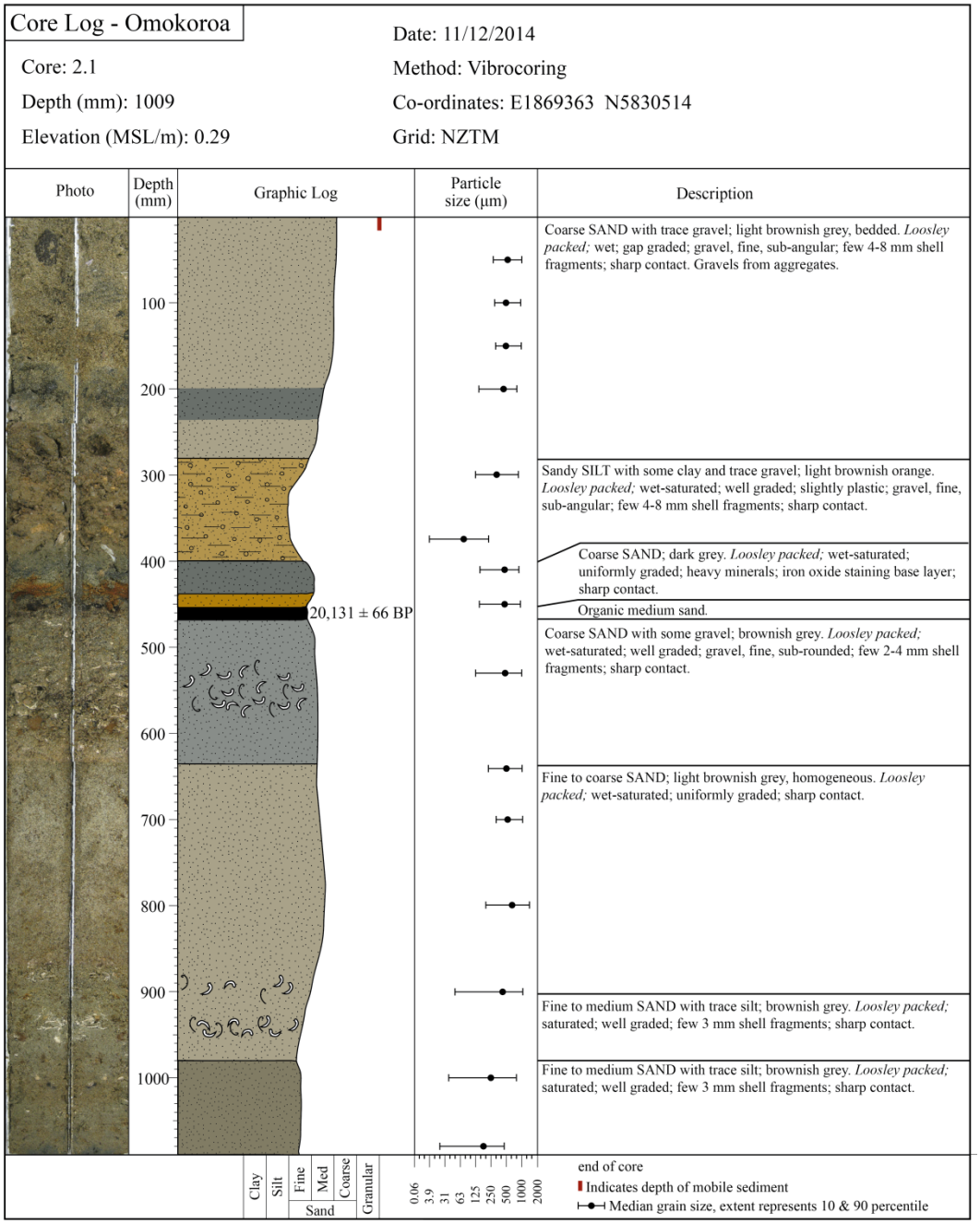

Figure 6.3: Stratigraphic log of core 2.1.

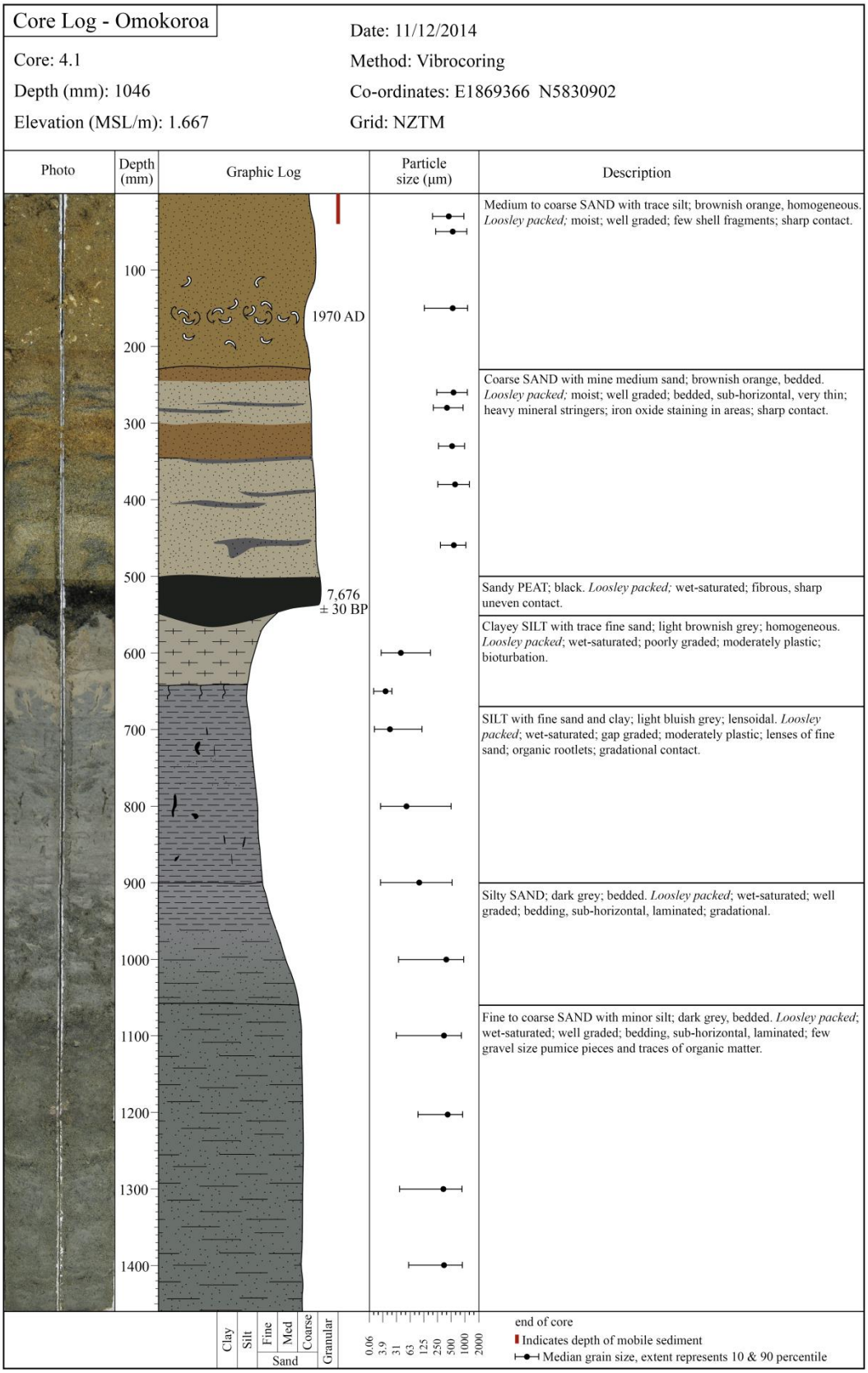

Figure 6.4: Stratigraphic log of core 4.1.

6.1.2.2 Sedimentation rates

Sedimentation rates at each site have been calculated based on radiocarbon dates and the inferred Holocene – Pleistocene boundary identified from cores (Figure 6.5). It is apparent that the sedimentation rates on the eastern side of the Omokoroa Peninsula are greater than the western side. Furthermore, sedimentation rates have varied during the Holocene. Between 7,676 ± 30 BP and 1970 AD, sedimentation rates on the northern side of the Omokoroa domain were low (0.00445 mm/yr). South of the Omokoroa Domain, increased sedimentation rates since 1,652 ± 20 BP were calculated (0.0524 mm/yr). Since 1970 AD, sedimentation rates have significantly increased north of the Omokoroa Domain (0.455 mm/yr). Sedimentation rates within the southern Tauranga Harbour (0.75 and 1.57 mm/yr) calculated by Hancock *et al.*, (2009) are significantly higher than at Omokoroa.

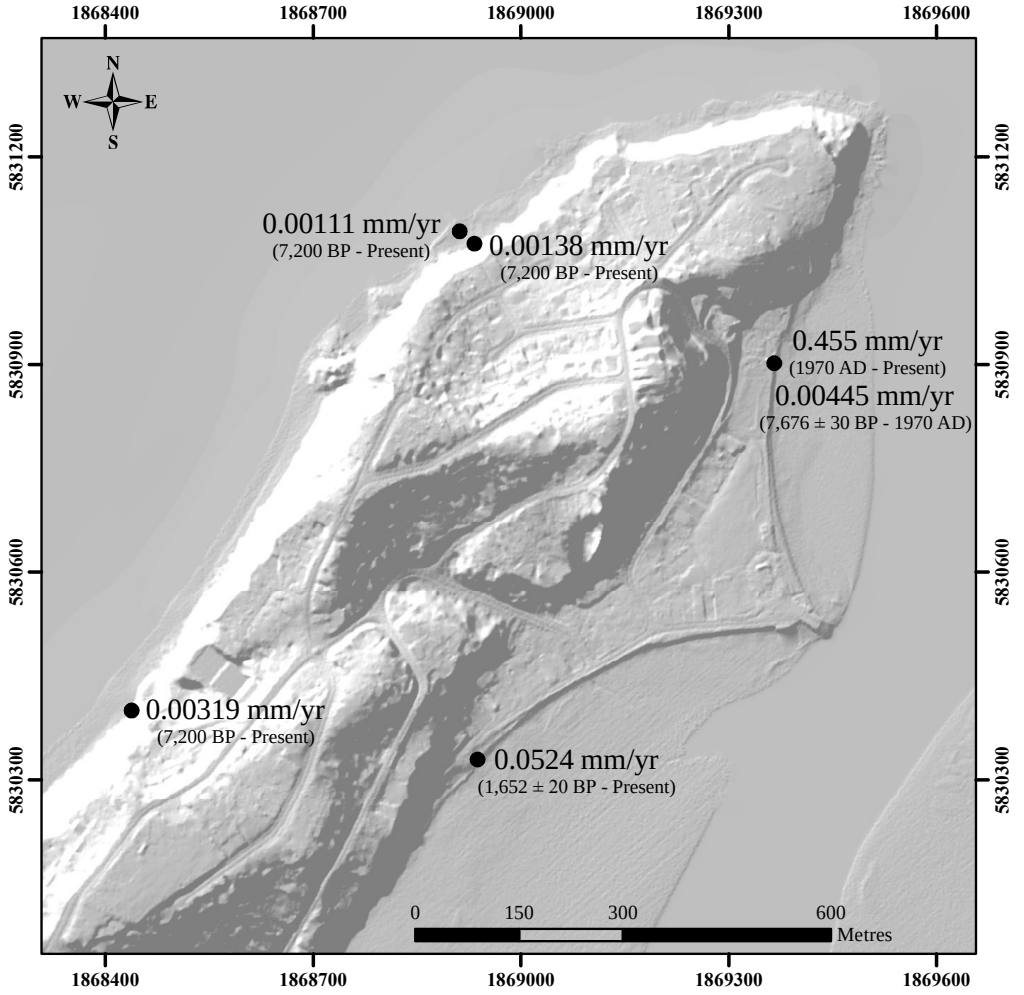

Figure 6.5: Sedimentation rates calculated based on radiometric dates and inferred Holocene – Pleistocene boundary.

6.1.2.3 Correlation of estuarine and cliff sediments

The sequence of sediments identified in Core 4.1 correlates to descriptions of the cliff outcrop at Site 1 (Figure 6.6). The lignite bed in Core 4.1 was dated at 7,676 ± 30 BP. The correlating sequence of sediments identified is not continuous along the cliff and stratigraphically appears near the elevation of the Te Puna Ignimbrite (known age of 0.93 Ma) and are significantly older than the dated material. It is therefore evident that a discontinuity separates Sites 1 and 2 (Figure 6.1). Assuming the identified sequences relate, the tilt on the lignite bed is approximately 0.15˚ south-southwest.

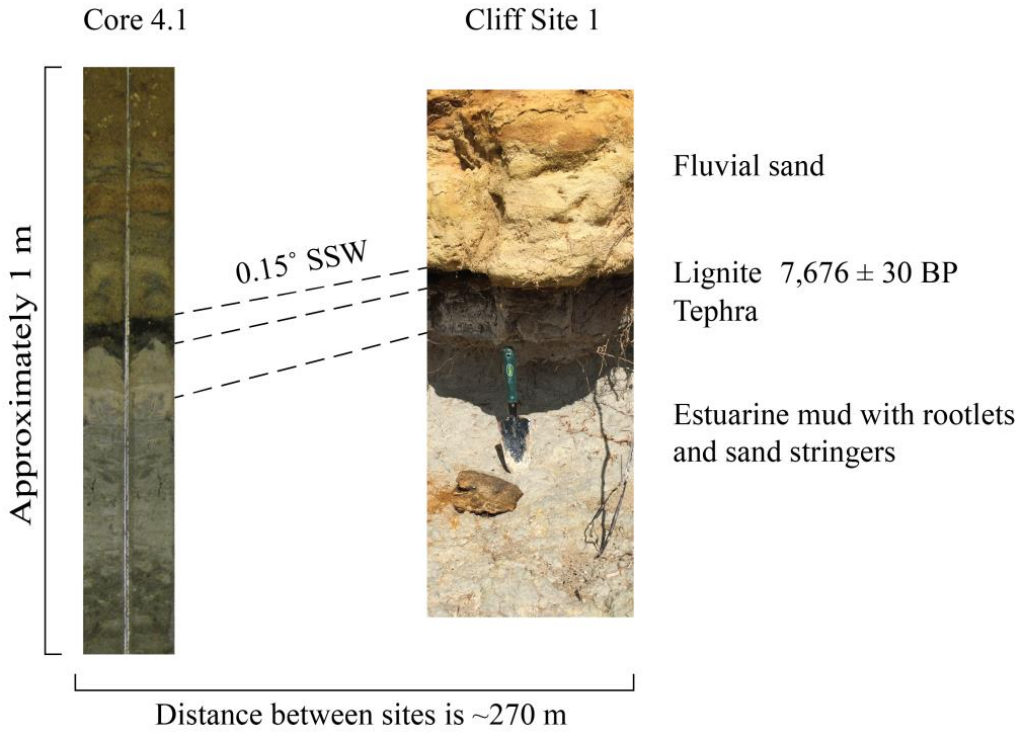

Figure 6.6: Stratigraphic correlation between Core 4.1 and cliff section Site 1.

6.1.3 Mineralogy

Minerals identified from surficial sediments and cliff samples are presented in Table 6-1. A full record of the results is presented in Appendix 2.3. A significant proportion of both surficial sediment and cliff samples contained quartz, plagioclase and kaolin group clays. Additional uncommon minerals include aragonite, heavy minerals, clinopyroxene and olivine. Halite, a coastal environment salt contaminant, is present in a number of samples located at the base of cliffs or intertidal sediments. The aragonite present in X2 and X4 of the surficial sediments is shell material.

Based on the mineral composition, it cannot be concluded that the beach sediment is derived from local cliffs exclusively. The dominance of quartz and plagioclase identified in the beach and intertidal sediments corresponds to the abundance of quartz and plagioclase present in each of the geological units, suggesting that cliffs provide a source of sediment to the surrounding beaches. However, the streams draining the surrounding catchment contains the equivalent geology, therefore the mineral composition would not differ as there are no distinguishing minerals.

Table 6-1: Mineral assemblages of surfical sediments and cliff samples identified by XRD.

Sample	Quartz	Plagioclase	Kaolin group clays	Other	Environment/ Geological Unit
Surficial sediments					
X1	●	●			Boat ramp
X2	●	●		Aragonite	Boat ramp
X3	●	●	●		Intertidal
X4	●	●	●	Aragonite Heavy minerals Halite	Beach
X5	●	●	●		Beach
X6	●	●	●		Intertidal
X7	●	●		Heavy minerals Clinopyroxene	Intertidal
X8	●	●			Beach
X9	●	●			Beach
X10	●	●			Beach
Cliff samples					
S1.1	●	●			Estuarine mud (MS)
S1.2	●	●	●		Fluvial sand (MS)
S2.1		●		Halite	Fluvial sand (MS)
S2.2	●	●			Te Puna Ignimbrite
S3.1	●	●	●		Te Puna Ignimbrite
S3.2	●	●	●	Halite	Pahoia Tephra
S3.3	●	●	●		Pahoia Tephra
S3.4	●		●		Pahoia Tephra
S3.5	●		●		Pahoia Tephra
S4.1	●	●	●		Te Puna Ignimbrite
S4.2	●	●	●		Pahoia Tephra
S4.3	●	●	●	Olivine	Pahoia Tephra
S4.4	●		●		Pahoia paleosol
S4.5	●		●		Pahoia paleosol
S4.6	●	●			Hamilton Ash
S5.1	●	●	●		Te Puna Ignimbrite

6.2 Sediment Trend Analysis

6.2.1 Pilot study

Results obtained from the initial Sediment Trend Analysis (STA) undertaken surrounding the Omokoroa Peninsula are inconclusive. No sediment transport pathways were identified. The data collection was based on potential sources of sediment and observations of changes in grain size. The method of sample collection created a bias which affected the outcome. Further sampling and analyses was completed to remove the assumption of sediment sources and processes influencing sediment transport surrounding the Omokoroa Peninsula.

After further field investigations, it became evident that the triangle feature forming the Omokoroa Domain and the location of the boat ramp was not a 'cuspate foreland'. Long-term net sediment transport and historic photographs suggest that the area developed as a recurved spit, similar to the feature observed at Plummers Point. Therefore, a sediment trend analysis was undertaken surrounding the Omokoroa Peninsula and also at Plummers Point to identify current patterns associated with a recurved spit that potentially formed at Omokoroa in the past.

6.2.2 Omokoroa STA

Grainsize analysis reveals that sand dominates the study area (Figure 6.9). The predominant grain size at high tide is coarse sand, with increasing fine material on the intertidal flats, particularly on the south eastern margin. Increased mud content was measured on the boat ramp and is associated with the landslide debris from Bramley Drive.

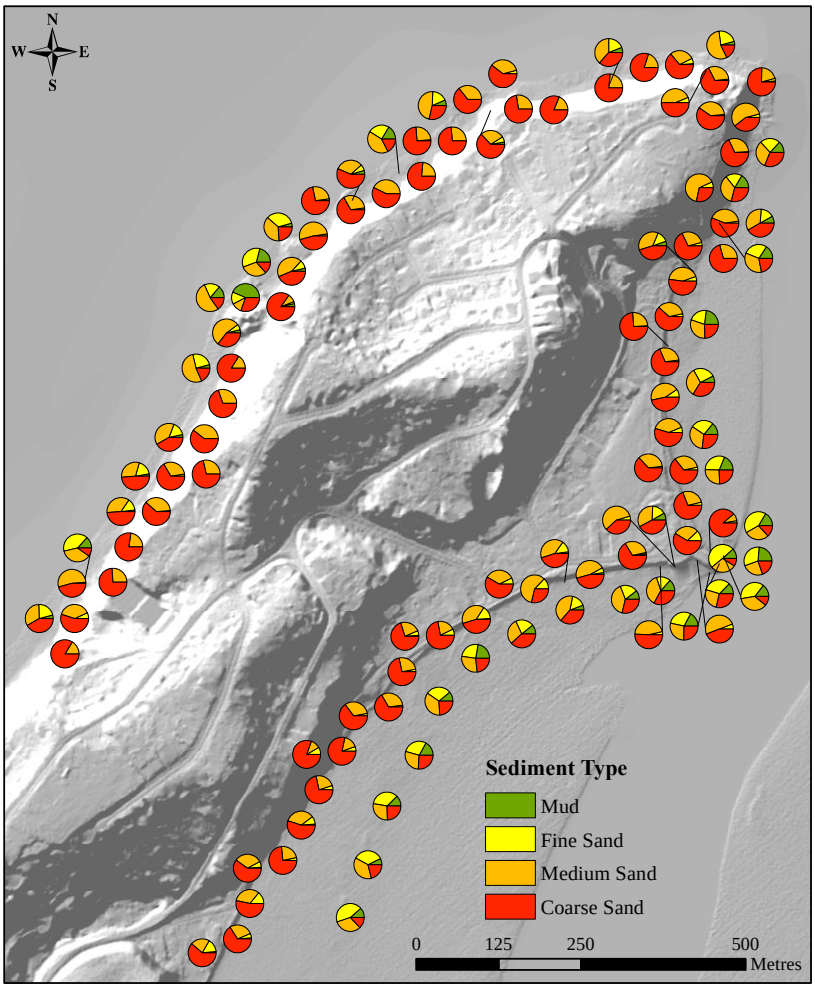

Figure 6.7: Grainsize distribution of surficial sediments surrounding Omokoroa.

Figure 6.8 illustrates the sediment transport pathways based on the analysis using GiSedTrend. A weighted function was used of the four sediment trend combinations (CB+, FB−, CB−, FB+). The characteristic distance was set to 250 m, defined by the maximum sampling interval (Poizot *et al.*, 2006). The shoreline was used as a boundary condition and no smoothing was applied as this significantly modifies the results, only showing a general trend. Sediment transport directions identified following the parameters defined above, not considering environmental factors, illustrates chaotic results with no clear transport pathways identified.

Based on knowledge of the environmental factors at Omokoroa, a number of different scenarios were applied. Firstly, samples from high tide were considered independent from low tide sediments, as it was clear from field observations that sediment transport occurred in a narrow band at high tide. At Omokoroa, high tide

sediments were also separated into identified transport environments divided by the boat ramp which acts as an impoundment structure, inhibiting sediment bypassing. North of the boat ramp, a boundary was defined based on the shoreline environment, transitioning from a beach setting to one dominated by active coastal cliffs. The weighted function was applied between the two sediment trend combinations identified as statistically significant to the study area (CB+ and FB-). Observations indicate sediments are derived from local sources, of which wave action tends to remove fine sediments. Depending on the distance from source and the time sediments were subjected to wave action, either CB+ or FB- may be identified. The following sections present the most sensible results obtained from the sediment trend analysis.

No clear sediment transport pathways can be identified along the western margin of the Omokoroa Peninsula, illustrating the complex nature of the sediments. It is likely that the material is derived from local cliffs, which are not transported far from the source, hence the textural parameters indicate a chaotic nature as the constant local sediment inputs do not allow sufficient time for sorting and transport to occur via wave action and tidal currents. On the eastern side of Omokoroa Peninsula, north of the boat ramp, it is evident that sediment transport is south. South of the boat ramp, the relationship between textural parameters indicates bidirectional sediment transport. The sediment trends identified from textural parameters correlate to field observations discussed in Chapter 4. Sediment impoundment at the boat ramp and ferry terminal suggests long-term sediment transport south along the eastern margin of the peninsula.

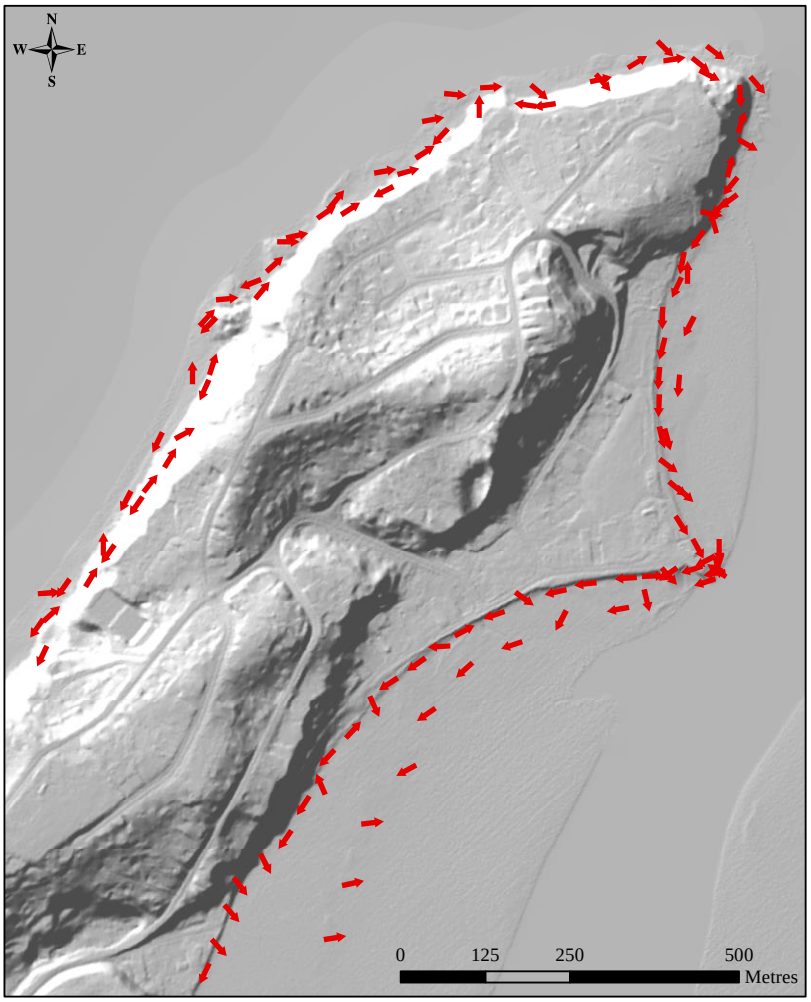

Figure 6.8: Sediment pathways based on sediment textural parameters at Omokoroa.

6.2.3 Plummers Point STA

Analysis of grainsize at Plummers Point shows medium to coarse sand comprises a large proportion of the material at high tide. Sediments on the intertidal flats include a range of grain sizes, of which the proportion of fine sediment increases away from the stream outlet (Figure 6.9).

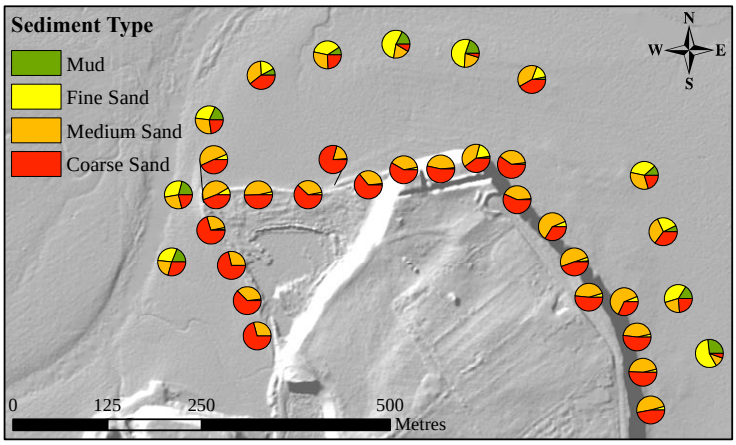

Figure 6.9: Grainsize distribution of surficial sediments surrounding Plummers Point.

Figure 6.10 displays the sediment transport pathways derived from the STA. The same input conditions and parameters that were used at Plummers Point were applied to Omokoroa. A boundary defining the transport environments was applied between active coastal cliffs (east) and the beach environment (west).

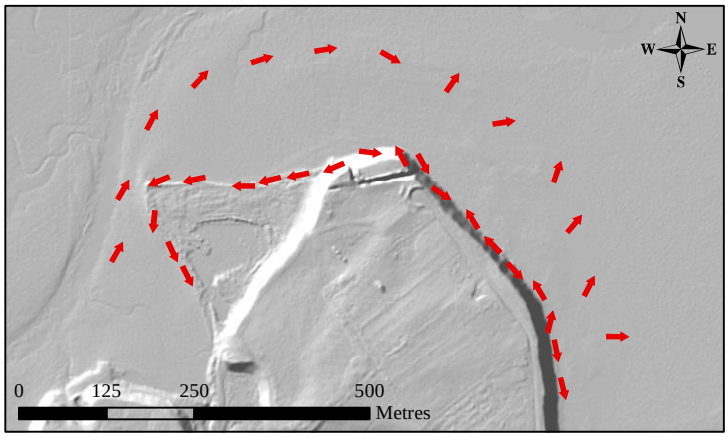

Figure 6.10: Sediment pathways based on sediment textural parameters at Plummers Point.

Chaotic sediment transport is observed on the northeastern boundary of Plummers Point. In a result similar to the western margin of Omokoroa, local sediment inputs from cliffs obscure long-term sediment transport patterns. Along the northern and western boundaries at Plummers Point, the sediment transport pattern traces parallel to the shoreline, consistent with the formation of a recurved spit. The intertidal sediments on the western side of Plummers Point indicate northeastern sediment transport, driven by river discharge.

6.3 Sedimentation associated with extra-tropical storm Pam

Sediment accumulation on the boat ramp was measured before and after extra-tropical storm Pam (ETS Pam) to determine the impact storm events have on the sediment transport around Omokoroa and accumulation of sediment on the boat ramp.

6.3.1 Weather

ETS Pam arrived in the Bay of Plenty on 15 March 2015 (Julian Day 74), bringing heavy rain, gale force winds and large swells. Winds were initially strong south easterlies that swung southwest. Average wind speed reached 16 m/s, gusting to 25 m/s. A total of 15.6 mm of rainfall was recorded over the first 24 hours. A significant drop in atmospheric pressure associated with ETS Pam recorded a low of 987 hPa (Figure 6.12 & Figure 6.13). Water level during ETS Pam at Te Puna, recorded by the Bay of Plenty Regional Council (2014), was passed through a low pass wavelet filter to extract the tidal and non-tidal components. A storm surge height of approximately 2.468 m was recorded with a 0.287 m surge component (Figure 6.13c). Figure 6.11 illustrates the inland extent following ETS Pam, flooding the beach and overtopping the small dunes formed over the recent summer months (see Chapter 4).

Figure 6.11: Storm surge at Omokoroa Domain during ETS Pam.

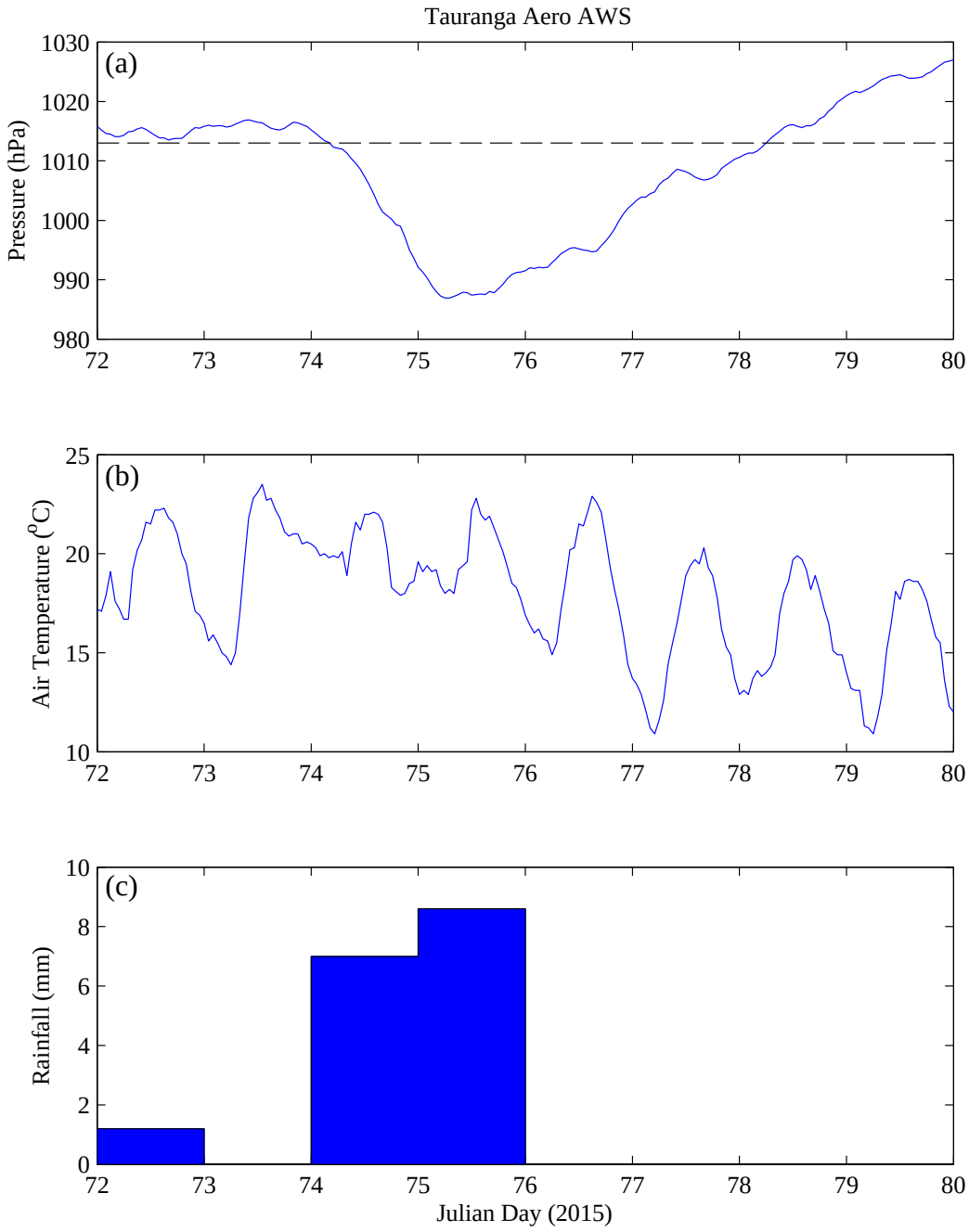

Figure 6.12: Weather data from Tauranga Aero AWS during ETS Pam showing (a) atmospheric pressure, (b) air temperature and (c) rainfall.

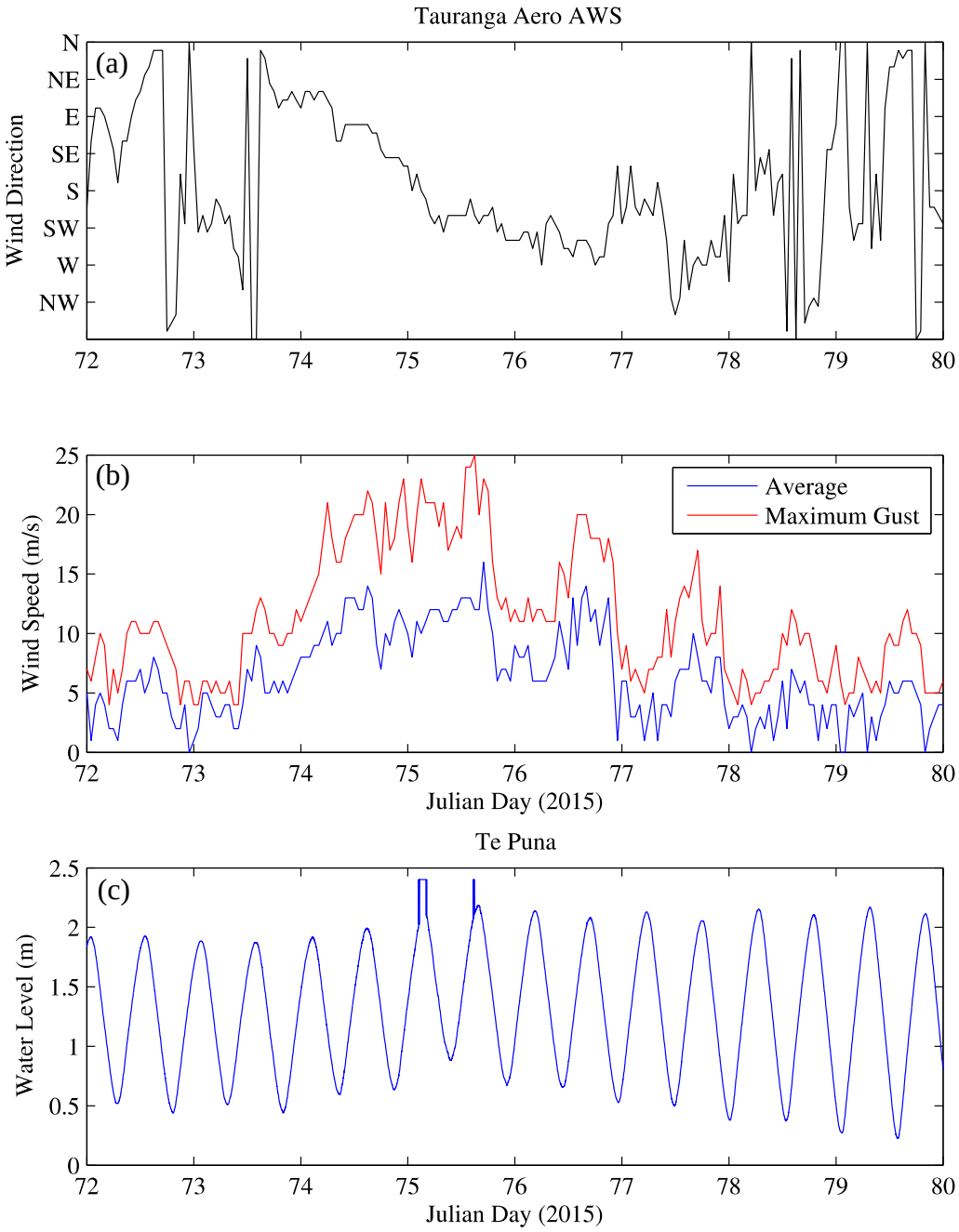

Figure 6.13: Weather data during ETS Pam of the (a) wind direction, (b) wind speed including average and gusts from the Tauranga Aero AWS and (c) water level at Te Puna (EBOP, 2014).

6.3.2 Sediment associated with ETS Pam

Prior to the storm, measurements of sediment thickness illustrate the significant sediment build up on the boat ramp (Table 6-2). On the northern side, sediment accumulation was thickest, overtopping the base of the boat ramp and extending 4 m up the ramp. Furthermore, it was evident that sediment accumulation was enough

so that boat trailers had reversed into the sediment. In the centre of the boat ramp, the thinnest layer of sediment that was measured did not extend far up the boat ramp (1.8 m). The southern side of the boat ramp had a moderate build-up of sediment, extending 2.4 m up the ramp.

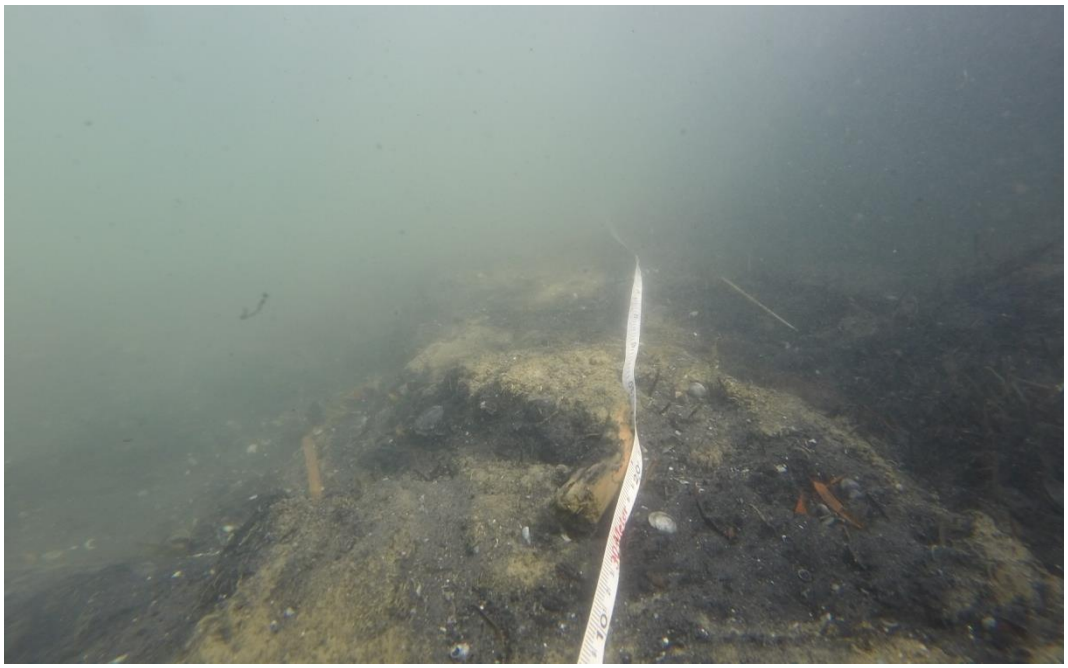

Figure 6.14: Sedimentation on the boat ramp.

Following ETS Pam, sediment accumulation on the boat ramp increased (Table 6-2). The most significant change in sediment thickness on the boat ramp was the accumulation of sediment on the southern side and the increase of sediment further up the boat ramp. The northern side still had the thickest sediment, although evidence suggests that sediment has eroded and/or redistributed on the boat ramp.

The residual tidal currents at the wharf are north, explaining the accumulation of fine sediment against the raised lip on the northern side. It is probable that during storm conditions the wind direction alters the distribution of sediment on the boat ramp. The onshore easterly winds may have transported sediment further up the boat ramp. The accumulation of sediment on the southern side may be attributed to sheltering from the lip on the boat ramp, enabling sediments to accumulate. In comparison, the northern side of the boat ramp is exposed to southerlies, and as the

sediment was overtopping the lip of the boat ramp, sediments could have easily been eroded and transported away from the site.

Table 6-2: Difference in sediment thickness on the boat ramp after ETS Pam.

Distance (m)	Transect 1 (South)			Transect 2 (Middle)			Transect 3 (North)		
	Before	After	Diff.	Before	After	Diff.	Before	After	Diff.
4.4								1	**1**
4.2								1	**1**
4.0								3	**2**
3.8							1	4	**2**
3.6							2	4	**0**
3.4							4	5	**-3**
3.2		1	**1**				8	6	**-3**
3.0		2	**2**				9	8	**-5**
2.8		3	**3**				13	10	**-3**
2.6		6	**6**				13	7	**-6**
2.4	1	5	**4**				13	9	**-1**
2.2	1	7	**6**		1	**1**	10	12	**0**
2.0	1.5	6	**4.5**		1	**1**	12	17	**1**
1.8	3	6	**3**	2	3	**1**	16	19	**4**
1.6	4.5	11	**6.5**	4	6	**1**	15	17	**-2**
1.4	4	11	**7**	7	6	**2**	19	21	**2**
1.2	2.5	15	**12.5**	6	6	**-1**	19	15	**-5**
1.0	7	14	**7**	5	11	**0**	20	15	**-5.5**
0.8	8	16	**8**	7	11	**4**	20.5	20	**-2**
0.6	8	15	**7**	6	12	**6**	22	23	**-2**
0.4	9	12	**3**	10	14	**4**	25	25.5	**0.5**
0.2	10	10	**0**	4	13	**9**	23.5	25.5	**2**
0.0	8	11	**3**	11	17	**6**	25	28	**3**
On lip	0	0	**0**	0	0	**0**	4	13	**9**
Base	28	25	**-3**	18	23	**5**	90	90	**0**

6.3.2.1 Organic material

Organic content of surficial sediments derived from intertidal flats surrounding the Omokoroa Peninsula is compared to sediments retrieved from the boat ramp. Results indicate that the content of organic matter on the boat ramp is significantly higher than on the intertidal flats surrounding the Omokoroa Peninsula (Table 6-3).

Table 6-3: Organic matter content.

Sample	Location	Organic content (%)
O1	Boat ramp – north	12.62
O2	Boat ramp – south	9.65
O3	Adjacent to boat ramp – north at low tide	5.74
O4	Intertidal flats - northeast	4.19
O5	Intertidal flats southeast	2.90
O6	Intertidal flats – west	3.87

6.4 Summary

The underlying geology and sedimentation patterns surrounding the Omokoroa Peninsula displays evidence that a number of factors contribute to the evolution of the Omokoroa Domain.

- The onshore regional Pleistocene stratigraphy, identified from cliff sections along the Omokoroa Peninsula, can be correlated to underlying offshore geology. It is evident that the underlying surface of Pleistocene fluvial sediments has significant relief. Marine sands and silts accumulate in the depressions of the underlying surface. On the western margin, the thickness of sediment accumulation is much smaller than on the eastern margin, reflected by a significantly lower sediment accumulation rate.
- Based on mineralogical assemblages, the source of sediment accumulating at the Omokoroa Domain cannot be correlated with cliff sediments exclusively. However, the abundance of quartz and plagioclase identified in

the surrounding beach sediments is evident in a large proportion of geological units forming the surrounding cliffs.

- Sediment transport pathways inferred from sediment textural parameters reflect the degree of sorting relative to the location of the source material. No trends are apparent adjacent to active coastal cliffs, suggesting that sediments have not been exposed to sufficient sorting, indicating recent sediment inputs. On the eastern margin of the Omokoroa Peninsula, sediments trends indicated southwards sediment transport, of which some bidirectional flow is observed south of the boat ramp. The sediment transport patterns are consistent with field observation of sediment impoundment at the boat ramp. At Plummers Point, sediment transport at high tide is unidirectional, consistent with the formation of a recurved spit. At low tide, sediment transport is influenced by freshwater flows. It is important to note that environmental factors have been considered prior to the computation of the results presented. Analysis of results with no understanding of the environmental setting produced inconclusive results.
- Sedimentation patterns on the boat ramp indicate that the residual tidal currents are the primary control on the distribution of sediments. The impact of storm events increases the volume of sediment on the boat ramp, and depending on the prevailing wind direction, tend to redistribute sediments.

Chapter Seven

DISCUSSION

Considering the multiple line of evidence found in this research, the following chapter discusses the evolution of the Omokoroa Domain. Firstly, the geological architecture identified at Omokoroa is correlated to the wider structure of the Tauranga region, followed by a paleogeomorphic reconstruction of the Omokoroa Domain.

7.1 Tauranga Region

Pleistocene fluvial volcaniclastic sediments, of both primary and secondary origin, form the Omokoroa Peninsula. The underlying Pleistocene surface exhibits considerable relief which has been attributed to the topography of the stream and valley system during the last glacial, infilled by marine sediments during the marine transgression. Since sea level reached its current position (7,200 BP) it has fluctuated up to 2 m (Gibb, 1997) causing periods of erosion and deposition.

From evidence based on stratigraphic relations between geological units identified at coastal sections and in cores from the intertidal flats, I believe there are vertical displacements between the cliffs and the surrounding intertidal flats. Te Puna Ignimbrite cannot be traced along the length of the northern point of the coastal cliff section and no outcrops visibly contain the unit on the eastern margin. This correlates with alignment of the Te Puna Ignimbrite as mapped by Briggs *et al.*, (1996), indicating a significant age difference between sediments on the western and eastern margins of the Peninsula. No faults have been mapped along the Omokoroa Peninsula, however, Briggs *et al.,* (1996) envisage a series of NNE trending faults within the basement that likely control the alignment of the Omokoroa Peninsula.

Since the last glacial, marine sediments were deposited in a depression of the fluvial surface. On the eastern margin of the Omokoroa Peninsula, cores revealed a thick sequence of marine sediments underlying the recent sediments of the present day

environment. The sedimentary sequence on the western margin consists of a thin layer of recent sands overlaying Pleistocene sediments with no evidence of marine deposits, providing further evidence of vertical land movements through Pleistocene sediments at Omokoroa. The stratigraphic relationship between the Pahoia Tephras on the western margin, identified at cliff sections and underlying recent sediments along core transect 5, indicates a sharp discontinuity, here attributed to vertical displacement. The displacement cannot be identified as the lithology is highly variable, however I suspect that there may be a series of stepped blocks west of the peninsula.

Timing of the vertical movements is unknown. It can be inferred that displacement occurred following deposition of the Te Puna Ignimbrite, which Briggs *et al.* (1996) dated at 0.93 Ma, although it cannot be established if the marine sediments were deposited on the western margin and vertical movement has subsequently caused erosion. A belt of Pleistocene sediment is evident between Omokoroa and Matakana Island. It is possible that the Pleistocene sediments forming the ridge through the middle of the Tauranga Harbour represent a boundary between two calderas that once formed the two basins of the Tauranga Harbour that have been subsequently infilled with more recent Holocene deposits.

On the eastern margin of the Omokoroa Peninsula there is evidence of tilting south-southwest. Studies conducted regarding the development of Matakana Island (Shepherd, 1997; Shepherd *et al.*, 2000) identified tilted sediments in the opposite direction to that identified in this study. Schofield (1985) identified regions of subsidence within the Tauranga Harbour. However, based on Shepherd's evidence, I believe that the middle section of the Tauranga Harbour is doming (higher), extending from Omokoroa north to Matakana Island, with some deformation having occurred since 7,626 ± 30 BP. Shepherd (1997) identifies that at least one tidal inlet was located through the centre of Matakana Island during the Holocene.

It is possible that the region surrounding the Omokoroa Peninsula previously drained though the inlet that lies to the north of the Peninsula. Evidence from the cores indicates that channelised deposits underlying intertidal sediments, correlating with a drainage system north. Furthermore, the underlying channelised

deposits indicate the area has been subjected to uplift or sea level fall, with evidence suggesting uplift is a more likely explanation. Uplift in the middle section of the harbour could also correlate with a change in the drainage system, redirecting channels away from the middle section of the harbour towards the present day tidal inlets. Uplift of the middle section of the Tauranga Harbour is also consistent with the low sedimentation rates surrounding Omokoroa Peninsula.

Ota *et al*. (1992) report impacts of subduction earthquakes located east of New Zealand between approximately 900-1,200 yrs BP and 1,600-2,000 yrs BP. Goff (2002) and GeoEnvironmental (2000) found evidence of subsidence and tsunami deposits at Waihi during this period. The timeframe of the tsunami event correlated with ages of shells deposited within estuarine mud, dating at 1,652 ± 20 BP. I believe the emplacement of the shell layer was driven by a catastrophic tsunami event which would also lead to scour and reworking in the intertidal area particularly evident in cores. This implies that there has been land movement in the area, potentially driven by an earthquake or fault movement.

7.2 Evolution of the Omokoroa Domain

The upper sequence of cores on the eastern margin of Omokoroa Peninsula represent a sequence that changes from marine to terrestrial, documenting a transition from marine transgression to coastal progradation following the deceleration of sea level rise since the Last Glacial Maximum.

7.2.1 Sediment source

Based on present day geomorphology, three main landforms have been identified: a talus deposit, spit and lagoon. Sediment accumulation rates on the intertidal flats surrounding Omokoroa Peninsula are low, indicating that sediment is derived from local sources as opposed to sediment sourced from the harbour/catchment. Furthermore, the hydrodynamic results depict a low energy environment, one where transport is driven by intermittent wind-generated wave action. This evidence suggests accumulation of sediment was initiated by a large-scale sedimentation event that led to a significant volume of sediment being delivered to the coast.

Fluvial sediments do not appear to contribute a large proportion of sediment to Omokoroa. Active coastal cliffs, subject to intermittent marine erosion and landslide events are evident along the margins of the peninsular, and appear to provide a significant source of sediment. Geomorphic evidence shows a circular ridge on the slopes above the Domain, which is here interpreted as the headscarp of a large relic landslide. The location of the inferred landslide in relation to the talus deposit at the Omokoroa Domain led to the conclusion that the debris of a landslide provided a significant source of sediment, inundating the immediate coastal platform. Activation of the landslide occurred following 1,652 ± 20 BP and was likely caused by ground shaking, potentially associated with inferred vertical displacement reported in Section 7.1. The geomorphology of the landslide suggests that drainage though the centre caused continual erosion subsequent to the initial failure.

7.2.2 Sediment transport

The present geomorphology, based on the orientation of the spit, indicates that sediment transport reworked landslide debris towards the north. Mechanisms of sediment transport surrounding Omokoroa Peninsula involve interaction of residual tidal currents and locally generated wind waves. The residual tidal currents are north along the Omokoroa Domain and are consistent with the orientation of spit growth. The dominant mode of sediment transport operating at Omokoroa is the combination of wind induced waves entraining sediment further transported by currents. Further sedimentation from a smaller-scale landslide on the northern side of the Omokoroa Domain provided additional sediment to the system. The shoreline continued to prograde as the sediment budget, supplied by landslide debris, exceeded the accommodation space to form an enclosed lagoon (Figure 7.1).

Waves act on the landslide debris, eroding the material and reworking sediments, removing the finer sediments and forming laminated deposits of coarser and denser sediment, consistent with evidence of the underlying sediments adjacent to the landslide. Deposits show evidence of fluvial reworking, consistent with episodic drainage down the face of the landslide supplying small pulses of sediment. The absence of chaotic sediments in the marginal deposits sampled, normally associated

with landslide deposits, can be attributed to sufficient erosion and transportation to remove debris from the coastal platform over the past ~1,600 years.

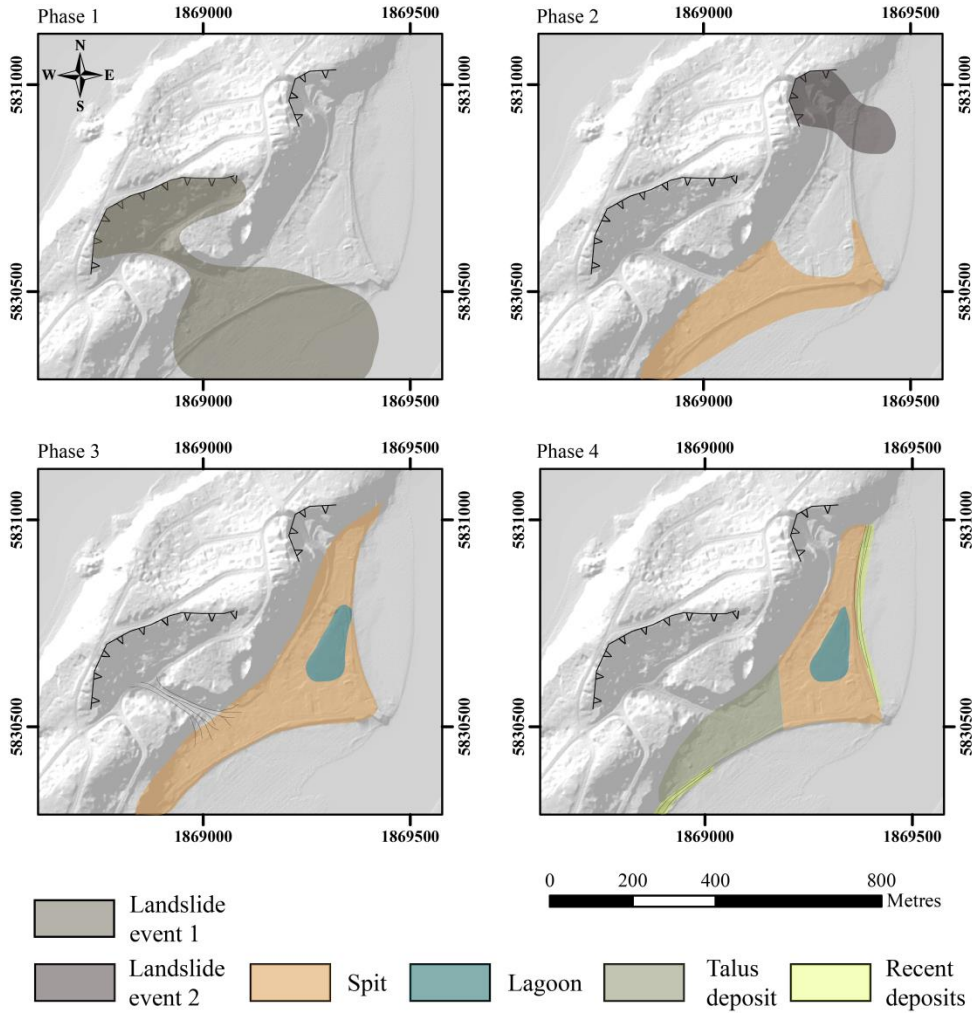

Figure 7.1: Schematic illustration of the evolution of the Omokoroa Domain. Phase 1: catastrophic landslide event supplying significant sediment to the coast. Phase 2: wave action and tidal currents rework sediment into a spit and additional sediment supplied from north. Phase 3: continued reworking and surface erosion enclosed a lagoon. Phase 4: present day landforms and accumulation of sediment on the northern side of the Domain.

Observations of a more recent smaller-scale landslide along the western margin of Omokoroa indicate that the landslide debris altered the shoreline, with wave action acting on the landslide debris to erode and redistribute sediments away from the site. The scale of the landslide at Omokoroa, and the large volume of sediment inundating the coastal platform in a relatively low energy environment, has led to significant shoreline progradation. The difference between the Domain and more

recent landslides such as at Bramley Drive, is the higher energy processes on the western side removes the sediment relatively quickly, whereas on the eastern side they are not strong enough to transport sediment away but rather largely rework material *in situ*.

7.3 Modern sedimentation at the Omokoroa Domain

7.3.1 Sedimentation

The evolution of estuarine environments is reflective of the long-term sediment supply and residual sediment transport patterns (Dronkers, 1986). The source of sediment accumulating at the Omokoroa Domain is derived predominately from erosion of the surrounding coastal cliffs with significant inputs through landslide events. Residual currents along the eastern margin of the Omokoroa Domain are north, illustrating the tidal data is consistent with hydrodynamic models of the Tauranga Harbour by McKenzie (2009) and Healy and Black (1985). However, the sediment transport regime operating around Omokoroa Peninsula suggests that the dominant transport direction is driven by locally generated wind waves which vary over a number of different time scales.

Wind patterns, and therefore wave climate in the Tauranga Harbour, are influenced by the Pacific Decadal Oscillation **(**PDO) (NIWA, 2006). The change in sediment transport direction along the eastern side of the Omokoroa Peninsula reflects the variation in wind direction driven by PDO. During the most recent El Niño dominated period, between 1976 and 1998, predominant south westerly winds drove sediment transport north. The southwesterlies are modified by the surrounding topography, hence the dominant wind direction at Omokoroa during El Niño periods are from the southern sector. Since 1998, La Niña patterns dominate and increased northeasterlies drive sediment transport south. Evidence suggests the effect of PDO on sediment transport is delayed as the effects of sediment transport are accumulative, therefore time is required to erode, transport and deposit sediments in the opposite direction.

The primary mechanism controlling sedimentation along the Omokoroa Peninsula is the action of the turbid fringe through interaction of waves and tidal currents.

Tidal currents surrounding the Omokoroa Peninsula are not strong enough to entrain sediment. The sediment threshold is a function of wave height and as Omokoroa is located in a relatively low energy environment, wave action only entrains sediment in a narrow near bed layer of 10-20 cm. The wave height at Omokoroa is primarily a function of wind, therefore sediment entrainment is switched on and off by wind generated wave activity. The extensive intertidal flats, exposed during the tidal cycle, significantly alters the available fetch and therefore action of the turbid fringe. Sediment transport of fine material is further transported by the tidal currents. Sediment data and analysis in this study suggest that fine sediment from the catchment is not concentrating in the upper harbour, but is transported out of the harbour entrance, contradicting the sediment transport model results reported by NIWA (2009), but consistent with the nutrient flux modelling of Tay (2011).

Historically, the long-term sediment transport pattern is north, contrasting with the present landform, suggesting the predominant sediment transport direction over the past 30 years is south. This could be a function of the location of the sediment source as the development of the spit was derived from the south, whereas currently the western margin of the peninsula is the main source of sediment.

7.3.2 Human modifications

The present feature evident at the Omokoroa Domain has been significantly altered by human modification which has resulted in disruption of the sediment transport regime. In particular, construction of hard engineering structures has modified the sediment budget and altered the recent development of the Omokoroa Domain. Construction of the ferry terminal (and boat ramp) interrupted wave energy, slowing the movement of sediment transport by wave action. South of the ferry terminal, construction has inhibited sediment transport to result in a negative sediment budget exacerbated by the construction of the seawall in an erosive environment. North of the boat ramp, construction has resulted in a positive sediment budget leading to continued shoreline progradation.

Sedimentation on the boat ramp is primarily a result of the location of the structure within the zone of sediment accumulation caused by the ferry terminal inhibiting sediment transport. The design of the boat ramp exacerbates the accumulation of

sediment. Constructing the boat ramp below the level of the bed, and enclosing the lower section of the boat ramp, creates a sheltered depression for fine sediment to accumulate. The sediment deposited is mostly fine organic rich sediment settling from the turbid fringe and derived from the intertidal flats.

7.3.3 Future evolution

In future, if the sediment transport processes behave the same as the recent past, sedimentation along the Omokoroa Domain will be driven by climatic shifts in the direction of sediment transport, reflecting the dominant phase of the PDO. In addition to the wind conditions, future evolution will depend on the sediment supply and the interference of human modification. If the current sediment supply from the western margin of the peninsula is reduced through the construction of seawalls, a sediment deficit will be created.

7.4 Summary

Reconstructing the evolution of the Omokoroa Domain illustrates five major phases of development and sedimentation:

- Pleistocene fluvial volcaniclastic deposits of the last glacial comprise the underlying geology at Omokoroa.
- Rapid sea level rise during the marine transgression deposited marine sediments in the valleys of the underlying fluvial surface.
- A phase of vertical movements resulted in potential faulting and tilting of the middle section of the Tauranga Harbour and has offset the sediments east and west of the Omokoroa Peninsula.
- Ground shaking and movements triggered large landslide events in the past ~1,600 years, providing a significant source of sediment since reworked into a cuspate spit and tidal lagoon.
- Construction of the ferry terminal (and boat ramp) has impacted the sedimentation patterns at the Omokoroa Domain. Current sedimentation processes are driven by locally generated wind waves influenced by PDO which sources sediment from the western margin of the Omokoroa Peninsula.

Chapter Eight

CONCLUSION

The following chapter summarises the main findings from this study in reference to the objectives and outlines recommendations for further research.

8.1 Summary of research findings

The main aim of this proposed research was to determine the geomorphic evolution of the Omokoroa Domain and assess the processes that contribute to the long-term stability and future evolution of the shoreline.

1. ***Collate information on the historical shoreline positions for the area to assess impacts of historical modifications.***

Significant changes in the shape of the shoreline occurred between 1943 and 1982 as a result of human modification including land reclamation and construction of the ferry terminal and seawalls. Construction of the ferry terminal inhibited sediment transport, indicating that present the net sediment transport is south along the eastern margin of Omokoroa Peninsula. There is also evidence of minor natural changes. These include accumulation of sediment on the northern side of the Omokoroa Domain, so that the seawall constructed along the shoreline is now mostly buried inland from the active beach. On the southern side of the domain, minor accumulation occurs around storm drains that act as groynes. The pattern of accumulations varied over time indicating switches between northward and southward directed longshore transport.

2. ***Establish the geological history and sedimentation patterns of the underlying sediments.***

Rapid sea level rise associated with the marine transgression after the Last Glacial Maximum deposited marine sediments in the valleys of the underlying Pleistocene fluvial surface. Significant relief is observed over the Pleistocene surface and

vertical displacement is identified between the western and eastern margin of the peninsula. Following the deceleration of sea level rise, shoreline progradation replaced marine sediment with terrestrial deposits. Episodes of ground shaking are evident and tilting of the terrestrial sediments suggest the Omokoroa Peninsula was uplifted/domed. Evidence for a tsunami event was also located, that correlates with a similar deposit described at Waihi Beach.

3. ***Examine the hydrodynamics, including tidal currents and waves in the vicinity of Omokoroa, used to evaluate sediment transport regime.***

Wave energy is low, with the maximum energy occurring on the western side of the Omokoroa Peninsula. While tidal currents are stronger in the deeper tidal channels, the tidal currents in shallow areas close to the shore are generally too weak to erode sediment. Storm surges and wind driven currents modify the wave and tidal regime. Continuous tidal action and episodic wind generated waves are the primary factors influencing sediment transport at Omokoroa. Sediment entrainment is mostly driven by waves and is confined to shallow depths (10-20 cm) on the rising and falling tides, defined as the turbid fringe. Current velocities do not have the ability to entrain sediment into suspension, however, once entrained, are capable of transporting sediment. The residual tidal currents along the Omokoroa Domain are north.

4. ***Identify potential sources of sediment and the pathways by which they contribute to sedimentation along the peninsula.***

Fluvial sediment sources were found to contribute little sediment to the beaches around Omokoroa. While sediment trend analysis indicated clear sediment transport pathways for Plummers Point and the western side of the Omokoroa Peninsula, the results were highly variable for the eastern side of the peninsula. Therefore, there was no convincing evidence of converging longshore transport creating either a cuspate foreland or cuspate spit. Overall, the sediment accumulation at Omokoroa Domain is derived from local sources, primarily through marine erosion and mass wasting of active cliffs along the western margin and the northern point of Omokoroa Peninsula. However, these sources appear

insufficient to provide sufficient sediment to develop the cuspate feature to the current extent. Therefore, it is likely that most of the sediment was provided by mass wasting of cliffs on the eastern side of Omokoroa Peninsula in close proximity to Omokoroa Domain.

5. ***Develop a conceptual model for the geomorphic evolution of Omokoroa Domain.***

Ground shaking and land movements triggered large landslide events along the eastern margin of the Omokoroa Peninsula in the past ~1,600 years, providing a significant source of sediment since reworked into a spit enclosed lagoon. The stages in the geomorphic evolution of the Omokoroa Domain are:

- Activation of a large-scale landslide occurred following 1,652 ± 20 BP, providing a significant source of sediment, inundating the immediate coastal platform.
- The combination of wave action and tidal currents redistributed sediments north, forming a spit.
- The shoreline continued to prograde as the sediment budget, sourced from continued surface erosion through the centre of the landslide and further sediment from a smaller-scale landslide on the northern side of the Omokoroa Domain exceeded the accommodation space to form an enclosed lagoon.
- Further progradation and infilling as a result of human modification has resulted in the present day geomorphology of which three geomorphic features can be identified: talus deposit, spit and lagoon.
- The sedimentation patterns today reflect the relative location of source material and climatic factors driven by PDO.

8.2 Management recommendations

The most simple, convenient and practical solution to mitigate the sedimentation on the boat ramp would be to reconstruct the existing boat ramp. The boat ramp and ferry terminal should be redesigned so that they act as a single structure. Currently,

the ferry terminal inhibits sediment transport resulting in accumulation of sediment on the boat ramp, produced by the turbid fringe migrating with the tides. In order to achieve this, the boat ramp will need to be at the same elevation and slope as the ferry terminal and extend an equal distance into the harbour. Furthermore, removing the raised lips bordering the lower section will allow water to flow freely over the boat ramp, making it less likely that sediment will accumulate. Furthermore, if the pile supported wharf could be replaced with floating pontoons or realigned to reduce the disruption to water flow, the entrainment of sediment by scour around the piles, and the settling of sediment in the sheltered lee of the structure, would be reduced.

8.3 Future research

This research addresses the paleogeographic coastal evolution of the eastern margin of the Omokoroa Peninsula. As a result of this study, a number of suspected structures/features have been identified and require confirmation via further assessment, including the following:

- Identify the internal structures associated with the three different geomorphic features: talus deposit, lagoon and spit.
- Map the underlying Pleistocene surface to determine vertical displacement and subsidence/uplift.

References

Abbiss, C. (2002). *Omokoroa Peninsula - Sea Walls Construction.* Tauranga, Opus International Consultants Ltd.

Ahrens, J. P. (2000). A fall-velocity equation. *Journal of waterway, port, coastal, and ocean engineering, 126*(2), 99-102.

Asselman, N. E. M. (1999). Grain-size trends used to assess the effective discharge for floodplain sedimentation, river waal, the netherlands. *Journal of Sedimentary Research, 69*(1), 51-61.

Barnett, A. G. (1985). *Tauranga Harbour Study. Part I Overview and Part III Hydrodynamics.* Report to the Bay of Plenty Harbour Board. 159p.

Bay of Plenty Regional Council. (2014). *Live Monitoring: TGA Hbr @ Omokoroa*. from http://monitoring.boprc.govt.nz/MonitoredSites/cgi-bin/hydwebserver.cgi/sites/details?site=9100

Bear, A. L. (2009). *Erosion and Sedimentation Processes at Northern Waihi Beach.* Unpublished MSc thesis. University of Waikato: Hamilton, New Zealand.

Bell, R., Goring, D., Gorman, R., Hicks, M., Hurran, H., & Ramsay, D. (2006). *Impacts of climate change on the coastal margins of the Bay of Plenty*. Unpublished Client Report HAM2006-031. Hamilton, NIWA.

Black, K. P. (1984). Sediment transport. Tauranga Harbour Study IV. *Report for the Bay of Plenty Harbour Board*, 150 p.

Boothroyd, I. K. G., Quinn, J. M., Langer, E. R., Costley, K. J., & Steward, G. (2004). Riparian buffers mitigate effects of pine plantation logging on New Zealand streams: 1. Riparian vegetation structure, stream geomorphology and periphyton. *Forest Ecology and Management, 194*(1–3), 199-213.

Briggs, R., Houghton, B., McWilliams, M., & Wilson, C. (2005). 40Ar/39Ar ages of silicic volcanic rocks in the Tauranga - Kaimai area, New Zealand: Dating the transition between volcanism in the Coromandel Arc and the Taupo Volcanic Zone. *New Zealand Journal of Geology and Geophysics, 48*(3), 459-469.

Briggs, R. M., Lowe, D. J., Esler, W. R., Smith, R. T., Henry, M. A. C., Wehrmann, H., & Manning, D. A. (2006). *Geology of the Maketu area, Bay of Plenty, North Island, New Zealand – Sheet V14 1:50 000.* Department of Earth Sciences, University of Waikato, Occassional Report 26.

Briggs, R. M., Hall, G. J., Harmsworth, G. R., Hollis, A. G., Houghton, B. F., Hughes, G. R., Morgan, M. D., & Whitbread-Edwards, A. R. (1996). *Geology of the Tauranga Area: Sheet U14 1: 50 000*: Department of Earth Sciences, University of Waikato Occasional Report 22.

Bronk Ramsey, C. (2001). Development of the radiocarbon calibration program OxCal. *Radiocarbon, 43*(2A), 355-364.

Brown, E., Wright, J., Colling, A., Park, D., & Open, U. (1999). *Waves, tides and shallow-water processes* Vol. 4 Oxford: Butterworth Heinemann.

Carling, P., Irvine, B., Hill, A., & Wood, M. (2001). Reducing sediment inputs to Scottish streams: a review of the efficacy of soil conservation practices in upland forestry. *Science of the total environment, 265*(1), 209-227.

Carter, D. (1982). Prediction of wave height and period for a constant wind velocity using the JONSWAP results. *Ocean Engineering, 9*(1), 17-33.

Chappell, P. R. (2013). *The Climate and Weather of Bay of Plenty* (3rd ed.) Wellington, New Zealand: NIWA.

Clement, A. J. H., Sloss, C. R., & Fuller, I. C. (2010). Late Quaternary geomorphology of the Manawatu coastal plain, North Island, New Zealand. *Quaternary International, 221*(1–2), 36-45.

Danišík, M., Shane, P., Schmitt, A. K., Hogg, A., Santos, G. M., Storm, S., Evans, N. J., Fifield, L. K., & Lindsay, J. M. (2012). Re-anchoring the late Pleistocene tephrochronology of New Zealand based on concordant radiocarbon ages and combined 238 U/230 Th disequilibrium and (U–Th)/He zircon ages. *Earth and Planetary Science Letters, 349*, 240-250.

Davies-Colley, R., & Healy, T. (1978). Sediment and hydrodynamics of the Tauranga Entrance to Tauranga Harbour. *New Zealand Journal of Marine and Freshwater Research, 12*(3), 225-236.

Davies-Colley, R. J. (1976). *Sediment dynamics of Tauranga Harbour and the Tauranga inlet.* Unpublished MSc thesis. University of Waikato: Hamilton, New Zealand.

Davies, R. A., & Healy, T. R. (1993). Holocene coastal depositional sequences on a tectonically active setting: southeastern Tauranga Harbour, New Zealand. *Sedimentary Geology, 84*(1), 57-69.

de Lange, W., & Healy, T. (1990a). Wave spectra for a shallow meso-tidal estuarine lagoon: Bay of Plenty, New Zealand. *Journal of Coastal Research*, 189-199.

de Lange, W. P. (1988). *Wave climate and sediment transport within the Tauranga Harbour, in the vicinity if Pilot Bay.* Unpublished PhD thesis. University of Waikato: Hamilton, New Zealand.

de Lange, W. P. (1996). Storm surges on the New Zealand coast. *Tephra*(15), 24-31.

de Lange, W. P., & Healy, T. R. (1990b). Renourishment of a Flood-Tidal Delta Adjacent Beach, Tauranga Harbour, New Zealand. *Journal of Coastal Research, 6*(3), 627-640.

de Lange, W. P., & Gibb, J. G. (2000). Seasonal, interannual, and decadal variability of storm surges at Tauranga, New Zealand. *New Zealand Journal of Marine and Freshwater Research, 34*(3), 419-434.

de Lange, W. P., Black, K. P., & Hatton, D. (1993). Programs for the reduction and analysis of tidal data (pp. 50). *Victorian Institute of Marine Sciences*.

Dolphin, T. J. (2003). *Wave-induced sediment transport on an estuarine intertidal flat.* Unpublished PhD thesis. University of Waikato Hamilton, New Zealand.

Dronkers, J. (1986). Tidal asymmetry and estuarine morphology. *Netherlands Journal of Sea Research, 20*(2), 117-131.

Elliott, S., Parshotam, A., & Wadhwa, S. (2009). *Tauranga harbour sediment study: catchment model results.* Unpublished Client Report HAM2009-046. Hamilton, NIWA.

Folk, R. L. (1968). *Petrology of sedimentary rocks* Austin, TX: Hemphills.

Folk, R. L., & Ward, W. C. (1957). Brazos River bar: a study in the significance of grain size parameters. *Journal of Sedimentary Research, 27*(1).

Friedman, G. M. (1961). Distinction between dune, beach, and river sands from their textural characteristics. *Journal of Sedimentary Research, 31*(4), 514-529.

Gao, S., & Collins, M. (1991). A Critique of the "McLaren method" for defining sediment transport paths — discussion. *Journal of Sedimentary Petrology, 61*(1), 143–146.

Gao, S., & Collins, M. (1992). Net sediment transport patterns inferred from grain-size trends, based upon definition of "transport vectors". *Sedimentary Geology, 81*(1–2), 47-60.

Garae, C. P. (2015). *Estimating patterns and rates of coastal cliff retreat around Tauranga Harbour.* Unpublished MSc thesis. University of Waikato: Hamilton, New Zealand.

GeoEnvironmental Consultants. (2000). *Tsunami Hazard for the Bay of Plenty and Eastern Coromandel Peninsula : Stage 1*. Unpublished Report prepared for Environment Bay of Plenty and Environmental Waikato. Hamilton, GeoEnvironmental Consultants.

Gibb, J. G. (1997). *Review of minimum sea flood levels for Tauranga Harbour.* Unpublished report prepared for Tauranga District Council and Western Bay of Plenty District Council.

Glade, T. (2003). Landslide occurrence as a response to land use change: a review of evidence from New Zealand. *CATENA, 51*(3–4), 297-314.

Goff, J. R. (2002). *Preliminary study of tsunami record on Coromandel East Coast.* GeoEnvironmental Client report: GEO2002/20024/6, Environmental Waikato, Environmental Bay of Plenty.

Goring, D. G. (1995). Short‐term variations in sea level (2–15 days) in the New Zealand region. *New Zealand Journal of Marine and Freshwater Research, 29*(1), 69-82.

Green, M. O. (2009). *Tauranga harbour sediment study: predictions of harbour sedimentation under future scenarios.* Unpublished Client Report HAM2009-078. Hamilton, NIWA.

Green, M. O., Black, K. P., & Amos, C. L. (1997). Control of estuarine sediment dynamics by interactions between currents and waves at several scales. *Marine Geology, 144*(1–3), 97-116.

Hancock, N., Hume, T., & Swales, A. (2009). *Tauranga harbour sediment study: harbour bed sediments.* Unpublished Client Report HAM2008-123, NIWA.

Harmsworth, G. R. (1983). *Quaternary stratigraphy of the Tauranga Basin.* Unpublished MSc Thesis. University of Waikato: Hamilton, New Zealand.

Harrison Grierson Consultants Limited. (1997). *Western Bay of Plenty District Council: Proposed Omokoroa Boat Ramp - Design Report - Revision 1.*

Hay, D. N., de Lange, W., & Healy, T. (1991). Storm and oceanographic databases for the Western Bay of Plenty. In R. G. Bell, T. M. Hume & T. R. Healy (Eds.), *Coastal Engineering: Climate for Change; Proceedings of 10th Australasian Conference on Coastal and Ocean Engineering, 1991* (pp. 139-143). Hamilton, New Zealand: Water Quality Centre, DSIR Marine and Freshwater: Water Quality Centre publication.

Healy, T. R., & Kirk, R. M. (1982). Landforms of New Zealand. In M. J. Soons & M. J. Selby (Eds.), *Coasts.* (pp. 81-180). Longman Paul: Auckland.

Herbst, P. H., Schuler, A. A., & Lawrie, A. (2002). *Erosion Protection Works Guidelines for Tauranga Harbour.* Tauranga, Environment Bay of Plenty.

Hicks, D. M., & Hume, T. M. (1996). Morphology and size of ebb tidal deltas at natural inlets on open-sea and pocket-bay coasts, North Island, New Zealand. *Journal of coastal research*, 47-63.

Hume, T., Bryan, K., Berkenbusch, K., & Swales, A. (2001). *Evidence for the effects of catchment sediment runoff preserved in estuarine sediments.* Unpublished Client Report ARC01272. Hamilton, NIWA.

Hume, T. M., & Herdendorf, C. E. (1988). A geomorphic classification of estuaries and its application to coastal resource management—A New Zealand example. *Ocean and Shoreline Management, 11*(3), 249-274.

Hume, T. M., Green, M. O., & Elliott, S. (2009). *Tauranga harbour sediment study: assessment of predictions for management.* Unpublished Client Report HAM2009-139. Hamilton, NIWA

InterOcean Systems. (1994). *S4 Current meter: User's manual* (4 ed.) San Diego: InterOcean Systems, inc.

Komar, P. D. (1996). *The Erosion of Wainui Beach, Gisborne – Causes and Mitigation.* Unpublished technical Report for Gisborne District Council.

Komar, P. D. (1998). *Beach processes and sedimentation* (2nd ed.) Upper Saddle River, NJ: Prentice-Hall.

Konert, M., & Vandenberghe, J. E. F. (1997). Comparison of laser grain size analysis with pipette and sieve analysis: a solution for the underestimation of the clay fraction. *Sedimentology, 44*(3), 523-535.

Kwoll, E. (2010). *Evaluation of the Tauranga Harbour numerical model.* Unpublished MSc thesis. University of Bremen: Gremany.

Larson, R., Morang, A., & Gorman, L. (1997). Monitoring the Coastal Environment; Part II: Sediment Sampling and Geotechnical Methods. *Journal of Coastal Research, 13*(2), 308-330.

Le Roux, J. P. (1994). Net sediment transport patterns inferred from grain-size trends, based upon definition of "transport vectors"—comment. *Sedimentary Geology, 90*(1–2), 153-156.

Le Roux, J. P., & Rojas, E. M. (2007). Sediment transport patterns determined from grain size parameters: Overview and state of the art. *Sedimentary Geology, 202*(3), 473-488.

Leonard, G. S., Begg, J. G., & Wilson, C. J. N. (2010). *Geology of the Rotorua Area.* Institute of Geological & Nuclear Sciences 1:250,000 geological map 5. 1 sheet + 102p. Lower Hutt, New Zealand. GNS Science.

LINZ (Land Information New Zealand). (2014). *Tidal predictions*. from www.linz.govt.nz/sea/tides/tide-predictions

Little, D. I., & Bullimore, B. (2015). Discussion of: McLaren, P., 2014. Sediment Trend Analysis (STA®): Kinematic vs. Dynamic Modeling. Journal of Coastal Research, 30(3), 429–437. *Journal of Coastal Research*, 224-232.

Lowe, D. J., Tippett, J. M., Kamp, P. J., Liddell, I. J., Briggs, R. M., & Horrocks, J. L. (2001). Ages on weathered Plio-Pleistocene tephra sequences, western north Island, New Zealand. *Les Dossiers de l'Archeo-Logis*, *1*, 45-60.

McCraw, J. (2011). *The wandering river: landforms and geological history of the Hamilton Basin* Guidebook No. 16. Lower Hutt, New Zealand: Geoscience Society of New Zealand.

McKenzie, J. S. (2014). *Predicted hydrodynamic and sediment transport impacts of breakwater construction in Tauranga Harbour, New Zealand.* Unpublished MSc thesis. University of Waikato Hamilton, New Zealand.

McLaren, P. (1981). An interpretation of trends in grain size measures. *Journal of Sedimentary Petrology, 51*(2), 611-624.

McLaren, P., & Bowles, D. (1985). The effects of sediment transport on grain-size distributions. *Journal of Sedimentary Petrology*, *55*(4), 457-470.

McLaren, P., & Teear, G. (2013). A Sediment Trend Analysis (STA®) in Support of Dredged Material Management in Lyttelton Harbour, Christchurch, New Zealand. *Journal of Coastal Research*, 438-447.

McLaren, P., Hill, S. H., & Bowles, D. (2007). Deriving transport pathways in a sediment trend analysis (STA). *Sedimentary Geology*, *202*(3), 489-498.

McLaren, P., Collins, M. B., Gao, S., & Powys, R. I. L. (1993). Sediment dynamics of the Severn Estuary and inner Bristol Channel. *Journal of the Geological Society*, *150*(3), 589-603.

Mead, S. T., & Moores, A. (2005). Estuary Sedimentation: a review of estuarine sedimentation in the Waikato region. *Environment Waikato*.

Nautilis Contracting Ltd. (2011). *Omokora escarpment stabilisation - a proposed action plan interating hard and soft engineering.* Unpublished report prepared for Western Bay of Plenty District Council. Tauranga, Nautilis Contracting Ltd.

Neil, P. (2012). *Omokoroa Boat Club History*. Omokoroa Boat Club Incorporation. from http://www.omokoroaboatclub.co.nz/about.html

New Zealand Geotechnical Society (NZGS). (2005). *Field description of soil and rock: Guideline for the field classification and description of soil and rock for engineering purposes*: NZ Geotechnical Society Inc.

NIWA. (2014). *Tide envelopes*. from https://www.niwa.co.nz/our-science/coasts/tools-and-resources/tides/tide-envelopes

Nordstrom, K. F., & Roman, C. T. (1996). Estuarine shores: evolution, environments and human alterations. In. West Sussex, England: John Wiley and Sons Ltd.

Opus International Consultants Ltd (OPUS). (2000). *Omokoroa Point Groundwater, Stormwater and Erosion Control.* Unpublished Report 2136. Tauranga, Opus International Consultants Ltd.

Opus International Consultants Ltd (OPUS). (2009). *Omokoroa Coastal Erosion Sites.* Unpublished Report: Project Number 2-9C074.01-001TC. Tauranga, Opus International Consultants Ltd.

Ota, Y., Hull, A. G., Iso, N., Ikeda, Y., Moriya, I., & Yoshikawa, T. (1992). Holocene marine terraces on the northeast coast of North Island, New Zealand, and their tectonic significance. *New Zealand Journal of Geology and Geophysics, 35*(3), 273-288.

Park, S. G. (1999). *Changes in Abundance of Seagrass (Zostera spp.) in Tauranga Harbour from 1959-96.* Environmental Report 99/30. Whakatane, Environment B.O.P.

Pawlowicz, R., Beardsley, R., & Lentz, S. (2010). Tidal Analysis Toolbox. *Version 1.3b*.

Perano, K. M. (2000). *Sediment transport on intertidal flats in a tide-dominated environment, Wairoa estuary, Tauranga, New Zealand.* Unpublished MSc thesis. University of Waikato: Hamilton, New Zealand.

Phizacklea, D. J. D. (1993). *Littoral Sediment Budget and Beach Morphodynamics, Pukehina Beach to Matata, Bay of Plenty*. Unpublished MSc thesis. University of Waikato: Hamilton, New Zealand.

Poizot, E., & Méar, Y. (2010). Using a GIS to enhance grain size trend analysis. *Environmental Modelling & Software, 25*(4), 513-525.

Poizot, E., Mear, Y., Thomas, M., & Garnaud, S. (2006). The application of geostatistics in defining the characteristic distance for grain size trend analysis. *Computers & Geosciences, 32*(3), 360-370.

Pritchard, M., Gorman, R., & Hume, T. (2009). *Tauranga harbour sediment study: hydrodynamic and sediment transport modelling.* Unpublished Client Report HAM2009-032. Hamilton, NIWA

Pugh, D., & Woodworth, P. (2014). *Sea-level Science: Understanding Tides, Surges, Tsunamis and Mean Sea-level Changes*: Cambridge University Press.

RBR Ltd. (2007). *Submersible data logger: User's manual* Canada: RBR Ltd.

Saunders, H. A. (1999). *Coastal processes influencing beach erosion at West End Ohope.* Unpublished MSc thesis. University of Waikato: Hamilton, New Zealand.

Schofield, J. C. (1985). Coastal change at Omaha and Great Barrier Island. *New Zealand Journal of Geology and Geophysics, 28*(2), 313-322.

Shepherd, M. J. (1997). *Formation, landforms and palaeoenvironment of Matakana Island and implications for archaeology*: Department of Conservation.

Shepherd, M. J., Betts, H. D., McFadgen, B. G., & Sutton, D. G. (2000). Geomorphological evidence for a Pleistocene barrier at Matakana Island, Bay of Plenty, New Zealand. *New Zealand Journal of Geology and Geophysics, 43*(4), 579-586.

Shrimpton & Lipinski Ltd. (1998). *Report on Landslips at Omokoroa.* Unpublished Report 14010. Tauranga, Shrimpton and Lipinski Ltd.

Spiers, K. C., Healy, T. R., & Winter, C. (2009). Ebb-Jet Dynamics and Transient Eddy Formation at Tauranga Harbour: Implications for Entrance Channel Shoaling. *Journal of Coastal Research*, 234-247.

Swales, A., Bentley, S., McGlone, M., Ovenden, R., Hermanspann, N., Budd, R., Hill, A., Pickmere, S., Haskew, R., & Okey, M. J. (2005). *Pauatahanui Inlet: effects of historical catchment land cover changes on inlet sedimentation.* Unpublished Client Report HAM2004-149. Hamilton, NIWA

Syvitski, J. P. (2003). Supply and flux of sediment along hydrological pathways: research for the 21st century. *Global and Planetary Change, 39*(1), 1-11.

Tay, H. W. (2011). *Nutrient dynamics in shallow tidally-dominated estuaries.* Unpublished PhD thesis. University of Waikato: Hamilton, New Zealand.

Taylor, T. (2014). *Bramley Drive Landslip Hazard Assessment.* Unpublished Report prepared for Western Bay of Plenty District Council. Tauranga, Tonkin and Taylor.

Tonkin & Taylor. (1980). *Omokoroa point land stability investigation.* Unpublished Report 4487/2. Tauranga, Tonkin and Taylor.

Tonkin & Taylor. (1981). *Stability assessment of coastal land in Tauranga country.* Unpublished Report 4879. Tauranga, Tonkin and Taylor.

Tonkin & Taylor. (1999). *Storm Surge Inundation Study for Tauranga Harbour.* Unpublished Report prepared for Tauranga District Council. Tauranga, Tonkin and Taylor.

Tonkin & Taylor. (2010). *Matahui Road, Katikati.* Unpublished Coastal Erosion Report prepared for the Western Bay of Plenty District Council. Tauranga, Tonkin and Taylor.

Tonkin & Taylor. (2011). *Bramley Drive Landslip Hazard Assessment.* Unpublished Report 851378.150. Tauranga, Tonkin and Taylor.

Udden, J. A. (1914). Mechanical composition of clastic sediments. *Bulletin of the Geological Society of America, 25*, 655-744.

USACE. (1984). *Shore Protection Manual* Vol. 2 Army Engineer Waterways Experiment Station, Coastal Engineering Reseach Center: U.S Government Printing Office, Washington D.C.

Walling, D. (2006). Human impact on land–ocean sediment transfer by the world's rivers. *Geomorphology, 79*(3), 192-216.

Wang, Q., Li, Y., & Wang, Y. (2011). Optimizing the weight loss-on-ignition methodology to quantify organic and carbonate carbon of sediments from

diverse sources. *Environmental monitoring and assessment, 174*(1-4), 241-257.

Watson, G. S. (1966). The statistics of orientation data. *Journal of Geology, 74*, 786-797.

Wentworth, C. K. (1922). A Scale of Grade and Class Terms for Clastic Sediments. *The Journal of Geology, 30*(5), 377-392.

Western Bay of Plenty District Council. (2010a). *Omokoroa community development plan.* Tauranga, Western Bay of Plenty District Council.

Western Bay of Plenty District Council. (2010b). *Community Development Plan: Omokoroa* Tauranga: Western Bay of Plenty District Council.

Western Bay of Plenty District Council. (2014). *Long Term Plan 2012-2022 - Stormwater.* Unpublished community plan. Tauranga, Western Bay of Plenty District Council.

Whites Aviation Ltd :Photographs. (1954a). *Omokoroa, Tauranga*. Ref: WA-35190-F. Alexander Turnbull Library, Wellington, New Zealand. from http://natlib.govt.nz/records/23529618

Whites Aviation Ltd :Photographs. (1954b). *The Esplanade, Omokoroa, Tauranga*. Ref: WA-35191-F. Alexander Turnbull Library, Wellington, New Zealand. from http://natlib.govt.nz/records/23527131

Whites Aviation Ltd :Photographs. (1954c). *Omokoroa, Tauranga, including Mount Maunganui in the background*. Ref: WA-35191-F. Alexander Turnbull Library, Wellington, New Zealand. from http://natlib.govt.nz/records/23524779

Whitton, J. S., & Churchman, G. J. (1987). *Standard methods for mineral analysis of soil survey samples for characterisation and classification.* New Zealand Soil Bureau Scientific Report 79.

Wilson, C., Rhoades, D., Lanphere, M., Calvert, A., Houghton, B., Weaver, S., & Cole, J. (2007). A multiple-approach radiometric age estimate for the Rotoiti and Earthquake Flat eruptions, New Zealand, with implications for the MIS 4/3 boundary. *Quaternary Science Reviews, 26*(13), 1861-1870.